REVISTA

DE PIELĂRIE ÎNCĂLŢĂMINTE

Leather and Footwear Journal

September / Septembrie 2026
Volume / Volumul 26
Issue / Ediția 3

INCDTP - SUCURSALA INSTITUTUL DE CERCETĂRI PIELĂRIE ÎNCĂLŢĂMINTE
INCDTP - DIVISION: LEATHER AND FOOTWEAR RESEARCH INSTITUTE



PIELĂRIE/LEATHER ÎNCĂLŢĂMINTE/FOOTWEAR BUNURI DE CONSUM DIN CAUCIUC/RUBBER GOODS

AIMS AND SCOPE

Revista de Pielărie Încălţăminte / Leather and Footwear Journal (Print ISSN 1583-4433) is published 4 times a year, by Leather and Footwear Research Institute (ICPI) Bucharest, Romania, Division of The National Research and Development Institute for Textiles and Leather (INCDTP), CERTEX Press.

Revista de Pielărie Încălţăminte / Leather and Footwear Journal aims to present current science and technology developments as well as initiatives in Romania and South Eastern Europe region. The Journal publishes original research papers of experimental and theoretical nature, followed by scientific, technical, economic and statistic information, reviews of local and foreign conferences, congresses, symposia, with the purpose of stimulating the dissemination of research results.

Revista de Pielărie Încălţăminte / Leather and Footwear Journal focuses particular attention on the key areas of new systems and technologies applied in leather, footwear and rubber goods sectors; biomaterials, collagen-based medical devices, biochemistry of collagen; environment; innovation; leather and parchment cultural heritage; management and marketing, quality control; applications of IT field in these sectors, and other related fields.

OPEN ACCESS STATEMENT

Revista de Pielărie Încălţăminte / Leather and Footwear Journal is a peer reviewed, open access journal. All articles published open access will be immediately and permanently free for everyone to read, download, copy and distribute, under the provisions of a Creative Commons Attribution (CC BY) which lets others distribute and copy the article, create extracts, abstracts, and other revised versions, adaptations or derivative works of or from an article (such as a translation), include in a collective work (such as an anthology), text or data mine the article, even for commercial purposes, as long as they credit the author(s), do not represent the author as endorsing their adaptation of the article, and do not modify the article in such a way as to damage the author's honor or reputation.

PEER-REVIEW PROCEDURE

Submission of a manuscript to *Revista de Pielărie Încălţăminte* implies that the work described has not been published before (except in the form of an abstract or as part of a published lecture, review, or thesis); that it is not under consideration for publication elsewhere; that its publication has been approved by all coauthors, if any.

Submitted manuscripts are double-blind peer-reviewed by two qualified reviewers selected by the Editorial Board. The manuscript will be accepted for publication provided reviews are favorable. In case of diversified opinions of the reviewers, the Editorial board will make the final decision. The authors will be notified as soon as possible of the result of the paper evaluation (accepted as such, accepted after revision, rejected).

PLAGIARISM POLICY

Authors submitting manuscripts to the Leather and Footwear Journal shall ensure that their work is original and not for consideration elsewhere. Plagiarism in its varied forms is not tolerated. The editors verify the originality of manuscripts submitted to Leather and Footwear Journal using dedicated software Sistemantiplagiat.ro to check for similarities with previous publications. If plagiarism is detected, the manuscript in question will be rejected.

COPYRIGHT

The copyright for all articles published in *Revista de Pielărie Încălţăminte / Leather and Footwear Journal* shall remain the property of the author(s). The copyright on the layout and final design of the articles published in *Revista de Pielărie Încălţăminte / Leather and Footwear Journal* belongs to INCDTP – Division: Leather and Footwear Research Institute and cannot be used in other publications.

ABSTRACTING AND INDEXING

Revista de Pielărie Încălţăminte / Leather and Footwear Journal is acknowledged in Romania by the National University Research Council (CNCSIS) in B+ Category (code 565), and is indexed in Chemical Abstracts Service (CAS) Database, USA, CAB Database (CAB International, UK), Elsevier's Compendex and SCOPUS, CrossRef, EBSCO, ProQuest, Index Copernicus, CiteFactor, Research Bible, and listed in Matrix for the Analysis of Journals (MIAR), Electronic Journals Library (EZB), Journal TOCs, Root Indexing, Scilit, and SCIPIO.

INCDTP-ICPI is a member of The Publishers International Linking Association, Inc. (PILA), a nonprofit corporation doing business as Crossref. As a PILA member, we have the right to assign Digital Object Identifiers (DOIs) to journal content. DOIs are persistent links to an object/entity and can be used to cite and link to any article existing online, even if full citation information is not yet available. We strongly recommend that authors cite references using DOIs where possible. For details regarding citation format and examples, please visit the Instructions for Authors section on *Revista de Pielărie Încălţăminte / Leather and Footwear Journal*'s website, http://www.revistapielarieincaltaminte.ro

FEES AND SUBSCRIPTIONS

Revista de Pielărie Încălţăminte / Leather and Footwear Journal requires article processing charges of 200 EURO per article, for accepted manuscripts, payable by the author to cover the costs associated with publication. There are no submission charges.

Hard copies of journal issues are available for purchase at subscription rates of 160 EURO for companies and 100 EURO for individual subscribers, while the rate for a single issue is 40 EURO. Subscriptions (include mailing costs) can be made at the editorial office, to the following address:

INCDTP – DIVISION: LEATHER AND FOOTWEAR RESEARCH INSTITUTE, 93 Ion Minulescu Street, postal code 031215, sector 3, Bucharest, Romania, Europe.

Both article processing charges and subscription fees are to be paid in the following account:

Account holder: INCDTP – Division: Leather and Footwear Research Institute; Address of the account holder: 93 Ion Minulescu Street, postal code 031215, sector 3, Bucharest, Romania, Europe
IBAN Code: RO25 RNCB 0074029208380005
Bank code: 300413024
Swift bank address: RNCBROBU; Bank: BCR sector 3 (ROMANIAN COMMERCIAL BANK – SECTOR 3); Bank address: 11 Decebal Blvd., Bl. S14, sector 3, Bucharest, Romania.

CORRESPONDENCE

Editor-in-Chief – Dana Gurău
INCDTP – Division: Leather and Footwear Research Institute (ICPI), 93, Ion Minulescu Street, Bucharest, sector 3, postal code 031215, Romania, Europe; tel./fax: + 40 21 323 52 80, e-mail: jlfjournal@gmail.com

CERTEX Publishing House – Bucharest, 16 Lucreţiu Pătrăşcanu St., sector 3; Tel./ Fax: (0040) 21 340.55.15; office@incdtp.ro

Website: http://www.revistapielarieincaltaminte.ro
Facebook: http://www.facebook.com/LeatherFootwearJournal
Title DOI: https://doi.org/10.24264/lfj

EDITOR IN CHIEF
Dana GURĂU

EDITOR
Dr. Laurenţia ALEXANDRESCU
Scientific Secretary of INCDTP-ICPI

EDITOR
Dr. Carmen GAIDĂU
Coordinator of Materials Research and Investigations Department, INCDTP

INCDTP - Division: Leather and Footwear Research Institute, Bucharest

EDITORIAL ADVISORY BOARD

Prof. Dr. Aurel ARDELEAN
Western University "Vasile Goldis" Arad
94-96 Revolutiei Blvd., 310025, Arad, Romania
Member of the Romanian Academy of Medical Sciences,
Member of Academy of Science, New York
Tel./Fax: +40 257 28 03 35
e-mail: rectorat@uvvg.ro

Prof. Dr. Anton FICAI
University "Politehnica" of Bucharest
Faculty of Applied Chemistry and Materials Science
1-7 Polizu, sector 1, 011061, Bucharest, Romania 35100,
Phone/Fax: 004021 402 3852
e-mail: anton.ficai@upb.ro

Prof. Dr. Behzat Oral BITLISLI
Ege University Faculty of Engineering
Head of Leather Engineering Department
35100, Bornova, Izmir, Turkey
Tel: + 90 232-311 26 44; Fax: +90 232 342 53 76
e-mail: oral.bitlisli@ege.edu.tr

Prof. Dr. Viaceslav BARSUKOV
National University of Technology & Design
2, Nemyrovych-Danchenko Str., Kiev, Ukraine
Tel./Fax: +380 (44) 290-05-12
e-mail: keeh@knutd.com.ua

Prof. Dr. Mehmet Mete MUTLU
Ege University, Faculty of Engineering
Leather Engineering Department,
35100 Bornova, Izmir, Turkey
Tel.: +90 232 3880110 – 2644; Fax: + 90 232 342 53 76
e-mail: mete.mutlu@ege.edu.tr

Prof. Dr. Todorka Gancheva VLADKOVA
University of Chemical Technology and Metallurgy,
Bld. Kliment Ohridsky 8, Sofia, 1756, Bulgaria
e-mail: tgv@uctm.edu

Prof. Dr. Margareta FLORESCU
The Bucharest Academy of Economic Studies
6 Piata Romana, 010374, Bucharest, Romania
Tel.: +40 21 319 1900; +40 21 319 1901; Fax: +40 21 319 1899
e-mail: icefaceus@yahoo.com

Assoc. Prof. Dr. Dana Corina DESELNICU
University "Politehnica" of Bucharest
1-7 Polizu, sector 1, 011061, Bucharest, Romania
Tel.: +40 021 212 99 52
e-mail: dana.deselnicu@upb.ro

Prof. Dr. Hüseyin Ata KARAVANA
Ege University, Faculty of Engineering
Leather Engineering Department,
35100 Bornova, Izmir, Turkey
Tel.: +90 232 3880110 – 2644; Fax: + 90 232 342 53 76
e-mail: huseyin.ata.karavana@ege.edu.tr

Prof. Dr. Wuyong CHEN
National Engineering Laboratory for Clean Technology of Leather Manufacture, Sichuan University,
Chengdu 610065, Sichuan, P. R. China
Tel: +86-(0)28-85404462; +86-28-85405840
Fax: +86-28-85405237
e-mail: wuyong.chen@163.com

Dr. Ding ZHIWEN
China Leather & Footwear Industry Research Institute
18 Jiangtaixi Road, Chaoyang District,
Beijing, P. R. China, 100015
Tel: +86-10-13701315570
e-mail: ding-zhiwen@263.net

Assoc. Prof. Dr. Alina IOVAN-DRAGOMIR
"Gh. Asachi" Technical University of Iasi
28 Dimitrie Mangeron Blvd., Iaşi, Romania
Tel.: +40 232 21 23 22; Fax: +40 232-21 16 67
e-mail: adragomir@tex.tuiasi.ro

Assoc. Prof. Dr. Sergiu Stelian MAIER
"Gh. Asachi" Technical University of Iasi
28 Dimitrie Mangeron Blvd., Iaşi, Romania
Tel.: +40 232 21 23 22; Fax: +40 232-21 16 67
e-mail: smaier@ch.tuiasi.ro

Assoc. Prof. Dr. Zenovia MOLDOVAN
University of Bucharest
90-92 Şos. Panduri, 050663, sector 5, Bucharest, Romania
Tel.: +40 21 4103178/125
e-mail: z_moldovan@yahoo.com

Prof. Dr. Aura MIHAI
"Gh. Asachi" Technical University of Iasi
28 Dimitrie Mangeron Blvd., Iaşi, Romania
Tel.: +40 232 21 23 22; Fax: +40 232-21 16 67
e-mail: amihai@tex.tuiasi.ro

ISSN: 1583-4433
Volume 26, No. 3, September 2026
https://doi.org/10.24264/lfj.26.3

	CONTENTS	*CUPRINS*	*SOMMAIRE*	
Merab SHALAMBERIDZE **Malvina TATVIDZE**	Dynamic Study of the Feet in Patients with Type 2 Diabetes Mellitus and the Design of Individual Orthopedic Insoles Considering Locally Over-Pressure Areas	Studiu dinamic al picioarelor la pacienții cu diabet zaharat de tip 2 și proiectarea branțurilor ortopedice personalizate, ținând cont de zonele de suprapresiune locală	Etude dynamique des pieds chez les patients atteints de diabète de type 2 et conception de semelles orthopédiques sur mesure tenant compte des zones de surpression locale	**139**
Pinar ARSLAN **Ozge OZTURK**	A Systematic Approach to Textile Design: An Experimental Study	O abordare sistematică a designului textil: studiu experimental	Une approche systématique du design textile : étude expérimental	**155**
Ali YORGANCIOGLU	Influence of Fatliquor Chemistry on Fogging and Odour Characteristics of Automotive Leather: A Comparative Study of Commercial Fatliquor	Influența compoziției chimice a agenților de ungere asupra caracteristicilor de condensare și cele olfactive ale pielii pentru tapițerie auto: un studiu comparativ al agenților de ungere comerciali	Influence de la composition chimique des produits de nourrissage sur les caractéristiques de condensation et olfactives des cuirs automobiles : une étude comparative de produits commerciaux	**177**
Megabi Adane YIZENGAW	Deodorization of Leather Tannery Waste Water Toxic Gases Using Spent Coffee Grounds: A Comprehensive Review	Dezodorizarea gazelor toxice rezultate din apele uzate ale tăbăcăriilor folosind zațul de cafea: o analiză cuprinzătoare	Désodorisation des gaz toxiques issus des eaux usées de tannerie à l'aide de marc de café : une synthèse approfondie	**189**
Fatih Furkan YILDIZ **Fatih YALÇIN** **Nilay ORK EFENDIOGLU** **Hüseyin Ata KARAVANA**	Mechanical Behavior of Belt Leathers Produced with Different Tanning Systems	Comportamentul mecanic al pieilor pentru curele obținute prin diferite sisteme de tăbăcire	Le comportement mécanique des cuirs de ceinture produits avec différents systèmes de tannage	**207**
Cornel Adrian MARIN **Raluca Maria AILENI**	Conductive Textiles for Electromagnetic Shielding: A Short Review	Textile conductoare pentru ecranare electromagnetică: o scurtă analiză	Textiles conducteurs pour le blindage électromagnétique : une brève synthèse	**217**
Laurenția ALEXANDRESCU **Mihai GEORGESCU** **Maria SÖNMEZ**	Compact Thermoplastic Polymer Biocomposite Based on PE/PE-g-MA/EPDM/CF and Dynamically Vulcanized with Dicumyl Peroxide	Biocompozit polimeric termoplast compact, pe bază de PE/PE-g-MA/EPDM/CF, vulcanizat dinamic cu peroxid de dicumil	Biocomposite polymère thermoplastique compact, à base de PE/PE-g-MA/EPDM/CF, à vulcanisation dynamique avec peroxyde de dicumyle	**229**
	European Research Area	Spațiul european al cercetării	Espace Européen de la Recherche	**237**

DYNAMIC STUDY OF THE FEET IN PATIENTS WITH TYPE 2 DIABETES MELLITUS AND THE DESIGN OF INDIVIDUAL ORTHOPEDIC INSOLES CONSIDERING LOCALLY OVER-PRESSURE AREAS

Merab SHALAMBERIDZE[1*], Malvina TATVIDZE[2]

[1]Department of Design and Technology, Akaki Tsereteli State University, 59 Tamar Mepe Str., Kutaisi 4600, Georgia, merab.sh@hotmail.com

[2]Department of Chemical and Environmental Engineering, Akaki Tsereteli State University, 59 Tamar Mepe Str., Kutaisi, 4600, Georgia, m.tatvidze@yahoo.com

Received: 01.02.2026 Accepted: 21.09.2026 https://doi.org/10.24264/lfj.26.3.1

DYNAMIC STUDY OF THE FEET IN PATIENTS WITH TYPE 2 DIABETES MELLITUS AND THE DESIGN OF INDIVIDUAL ORTHOPEDIC INSOLES CONSIDERING LOCALLY OVER-PRESSURE AREAS

ABSTRACT. This paper presents a dynamic study of the feet of patients with type 2 diabetes mellitus, as well as the design and manufacture of individual orthopedic insoles, taking into account locally overpressure areas. As a result of pedographic investigation, overpressure areas in the plantar side of the diabetic foot were identified. These locally overpressure areas were marked on the pedogram by curves when the pressure exceeded 150 kPa. A mathematical approach based on integral curves derived from the solution to Dirichlet singular boundary problem was applied to describe the overpressure areas with high precision. Based on the proposed mathematical algorithm, the software package was developed. Individualized orthopedic insoles were manufactured using silicone polymers and ethylene-vinyl acetate polymers of varying degrees of hardness. Soft polymer composites were used for locally overpressure areas, while relatively rigid material for the insole frame providing stability. Individual orthopedic insoles were produced on a computer numerical control milling machine taking into account locally overpressure areas. Individual orthopedic insoles manufactured using these technologies effectively reduce locally overloaded areas on the plantar surface of the foot and protect the foot from mechanical damage. The production and practical use of individual orthopedic insoles, developed on the basis of the research findings, contribute to the effective treatment and prevention of complications in patients with diabetic foot.
KEYWORDS: diabetic foot, foot plantar pressure area, pedograph method, individual orthopedic insoles.

STUDIU DINAMIC AL PICIOARELOR LA PACIENȚII CU DIABET ZAHARAT DE TIP 2 ȘI PROIECTAREA BRANȚURILOR ORTOPEDICE PERSONALIZATE, ȚINÂND CONT DE ZONELE DE SUPRAPRESIUNE LOCALĂ

REZUMAT. Lucrarea de față prezintă un studiu dinamic al picioarelor pacienților cu diabet zaharat de tip 2, precum și proiectarea și fabricarea unor branțuri ortopedice personalizate, ținând cont de zonele de suprapresiune locală. În urma investigației pedografice, au fost identificate zone de suprapresiune în zona plantară a piciorului diabetic. Aceste zone de suprapresiune locală au fost marcate pe pedogramă prin curbe atunci când presiunea depășea 150 kPa. Pentru a descrie zonele de suprapresiune cu o precizie ridicată, s-a aplicat o abordare matematică bazată pe curbe integrale derivate din soluția la problema Dirichlet. Pe baza algoritmului matematic propus, s-a dezvoltat un pachet software. Branțurile ortopedice personalizate au fost fabricate utilizând polimeri pe bază de silicon și polimeri de etilen-acetat de vinil cu grade variabile de duritate. Pentru zonele cu suprapresiune locală s-au utilizat compozite polimerice moi, în timp ce pentru structura branțului s-a folosit un material relativ rigid care să asigure stabilitate. Branțurile ortopedice personalizate au fost realizate pe o mașină de frezat cu comandă numerică computerizată, ținând cont de zonele cu suprapresiune locală. Branțurile ortopedice personalizate fabricate cu ajutorul acestor tehnologii reduc în mod eficient zonele suprasolicitate local de pe suprafața plantară a piciorului și protejează piciorul de leziuni mecanice. Fabricarea și utilizarea practică a branțurilor ortopedice personalizate, dezvoltate pe baza rezultatelor cercetării, contribuie la tratarea eficientă și la prevenirea complicațiilor la pacienții cu picior diabetic.
CUVINTE CHEIE: picior diabetic, zona de presiune plantară a piciorului, metoda pedografică, branțuri ortopedice personalizate.

ÉTUDE DYNAMIQUE DES PIEDS CHEZ LES PATIENTS ATTEINTS DE DIABÈTE DE TYPE 2 ET CONCEPTION DE SEMELLES ORTHOPÉDIQUES SUR MESURE TENANT COMPTE DES ZONES DE SURPRESSION LOCALE

RÉSUMÉ. Cet article présente une étude dynamique des pieds de patients atteints de diabète de type 2, ainsi que la conception et la fabrication de semelles orthopédiques sur mesure, en tenant compte des zones de surpression locale. Une analyse podographique a permis d'identifier des zones de surpression sur la face plantaire du pied diabétique. Ces zones de surpression locale ont été marquées sur le pédogramme par des courbes lorsque la pression dépassait 150 kPa. Une approche mathématique basée sur des courbes intégrales dérivées de la solution du problème aux limites singulières de Dirichlet a été appliquée pour décrire les zones de surpression avec une grande précision. Un logiciel a été développé à partir de l'algorithme mathématique proposé. Des semelles orthopédiques sur mesure ont été fabriquées à partir de polymères de silicone et de polymères d'éthylène-acétate de vinyle présentant différents degrés de dureté. Des composites polymères souples ont été utilisés pour les zones de surpression locale, tandis qu'un matériau relativement rigide a été employé pour la structure de la semelle intérieure afin d'assurer sa stabilité. Les semelles orthopédiques sur mesure ont été fabriquées sur une fraiseuse à commande numérique, en tenant compte des zones de surpression locale. Grâce à ces technologies, ces semelles orthopédiques sur mesure réduisent efficacement les zones de surpression locale sur la plante du pied et le protègent des traumatismes mécaniques. La fabrication et l'utilisation pratique de semelles orthopédiques sur mesure, mises au point à partir des résultats de la recherche, contribuent au traitement efficace et à la prévention des complications chez les patients atteints de pied diabétique.
MOTS-CLÉS : pied diabétique, zone de pression plantaire, méthode pédographique, semelles orthopédiques sur mesure.

* *Correspondence to: Merab SHALAMBERIDZE, Department of Design and Technology, Akaki Tsereteli State University, 59 Tamar Mepe Str., Kutaisi 4600, Georgia, merab.sh@hotmail.com*

INTRODUCTION

Diabetes mellitus (DM) is one of the most prevalent diseases worldwide. According to the International Diabetes Federation (IDF), diabetes currently affects over 9.3% of the global population. This figure is expected to rise from 10.2% to 10.9% between 2030 and 2045, respectively [1]. One of the most severe, destructive, and irreversible complications of diabetes is the development of diabetic foot ulcer (DFU). Up to 25% of individuals with diabetes mellitus may develop diabetic foot syndrome [2, 3]. Approximately within a year after the diagnosis of DFU, patients undergo major (10%) and minor (19%) lower-limb amputations due to unsatisfactory treatment outcomes [4].

Based on the dynamics of human movement during walking and running relatively less load falls on the medial part of the foot. However, in patients with DM, ulcers more frequently develop in the anterior and medial areas of the foot than in the heel. At the same time, when ulcers develop in the heel area, the survival rate of the lower limb is 2-3 times lower [5, 6].

Considering the biomechanics of human motion, the heel initially contacts the supporting surface, then the midfoot, and finally toe joints and toes. The foot acts as an effective shock absorber to reduce the load on the skeletal system of the lower limb [7-9]. Histologically, the plantar fat pads consist of microglobules embedded within the fibroelastic septa. The plantar fat cells and the configuration of the surrounding fibrous membrane are essential for the foot to resist the external compressive loads during the stance phase and gait [10, 11].

In patients with diabetic foot, the histomorphology of the plantar fascia undergoes significant changes. Specifically, the collagen network loses its integrity, elastin fibers become degraded and fragmented, and the number of adipocytes is reduced. These changes are directly related to the widespread damage of the soft tissues of the foot and increased vulnerability [12-14].

To prevent the formation of soft tissue ulcers on the plantar part of the foot and related complications in patients with diabetes, various designs of orthopedic shoes and individual orthopedic insoles have been developed. These designs are primarily aimed at reducing peak loads on the plantar part of the foot.

The effect of reduction of overpressure on localized areas of the plantar part of the diabetic foot is widely recognized as a key indicator for assessing the treatment effectiveness [15-18]. According to the literature [19], more than 42% of diabetic foot amputations are caused by wearing ill-fitting footwear and improperly designed insoles. Consequently, peak loads in ulcer-risk areas can be substantially reduced through the use of properly designed individual orthopedic insoles.

In the treatment of patients with diabetic foot, orthopedic insoles manufactured from homogeneous material often fail to achieve the desired therapeutic effect. For effective treatment, individual orthopedic insoles fabricated from a combination of materials with various degree of hardness are necessary. In particular, soft polymeric materials should be used in overpressure areas of the plantar surface to provide pressure relief, whereas relatively rigid polymeric materials should be used for the main frame of the insoles.

The purpose of this work is to study the diabetic foot under dynamic conditions and to design and manufacture individual orthopedic insoles composed of materials with different hardness, with account of the peak loads on the plantar part of the foot. To achieve this goal, the following objectives were set:

- to study the diabetic foot using the pedograph method;
- to identify the overpressure areas on the pedograms using curved lines, where the pressure exceeds 150 kPa;
- to describe complex geometric shapes of curves defining overpressure areas using mathematical research methods;
- to develop software packages based on the proposed mathematical algorithms;

- to select suitable combinations of polymer materials with varying hardness for manufacturing orthopedic insoles;
- to produce individual orthopedic insoles from a package of polymer materials on a CNC milling machine.

RESEARCH METHODS AND MATERIALS

Study Population

The study population included 15 male patients aged 45–60 years with diagnosed diabetic foot syndrome and a disease duration exceeding 10 years. Inclusion criteria comprised the presence of plantar hyperkeratosis and diabetic foot ulcers. All patients were overweight, with body weight ranging from 100 to 140 kg. All participants provided informed consent to participate in the study.

The proposed methodology was applied to all patients included in the study.

Foot Anthropometric Research Method

At the first stage of the study, we established the clinical diagnoses, body mass index BMI and foot pathologies of the patient group. In the subsequent stage, a foot anthropometric examination was performed according to the scheme presented in Fig. 1.

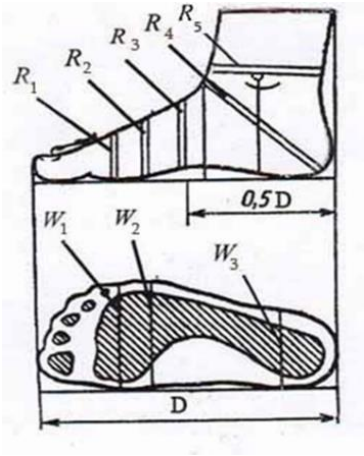


Figure 1. Anthropometric measurement scheme of the foot

Based on this examination, the following parameters were determined: foot size D, midfoot size 5D, foot width at the medial ball region W_1, foot width at the lateral ball region W_2, heel width W_3, foot girth at the medial ball region R_1, foot girth at the lateral ball region R_2, midfoot girth R_3, oblique foot girth R_4, and foot girth at the malleolus center R_5.

Mathematical Research Method

The significant novelty of this research consists in the fact that complex geometric shapes of locally overpressure areas were described on patients' pedograms by integral curves of the solutions to Dirichlet singular boundary problem [20-22].

The overloaded zones of the plantar part of the foot (hyperkeratosis/ulcer areas) have very complex, non-standard, and curvilinear geometric shapes, the description of which is impossible using conventional geometric figures (circles or ellipses). To describe the geometric curves of complex shapes, we considered various types of integral curves of solutions to first- and second-order differential equations, including the integral curves of solutions to the Dirichlet singular boundary value problem. To describe the complex geometric shapes of the curvilinear contours of locally overloaded areas of the plantar part of the foot, the integral curves of solutions to the Dirichlet singular boundary value problem were chosen, as they allow us to describe geometric contours of complex shapes with high precision. By varying the coefficient c (c = 0, 1, 2, 3, 4, 5) in the solution of the Dirichlet singular boundary value problem, a set of curvilinear curves of varying complexity is obtained.

The Dirichlet singular boundary problem is presented below:

$$u''(t) + \frac{a}{t}u'(t) - \frac{a}{t^2}u(t) = f\big(t, u(t), u'(t)\big) \quad (1)$$

$$u(t) = 0, \quad u'^{(t)} = 0, \quad (2)$$

where $a \in (-\infty; 1), f$ satisfies the local Carathéodory condition for a set $[0, t] \times D$, $\mathrm{D} = (0; +\infty) \times \mathrm{R}$.

The solution to problems (1) - (2) is expressed in the form of functions (3) and (4):

$$u(t) = \frac{t^3}{2} - \frac{1}{3}ct^{-2} - \left(1 - \frac{1}{3}c\right)t + \frac{1}{2}, \quad (3)$$

$$u(t) = \left(-\frac{1}{3} - \frac{1}{3}c\right)t + \frac{1}{3}c\frac{1}{t^2} + \frac{2}{3}t - \frac{t^2}{2} + \frac{t^4}{6}, \quad (4)$$

The corresponding integral curves of functions (3) and (4) are presented in Figure 2 and Figure 3.

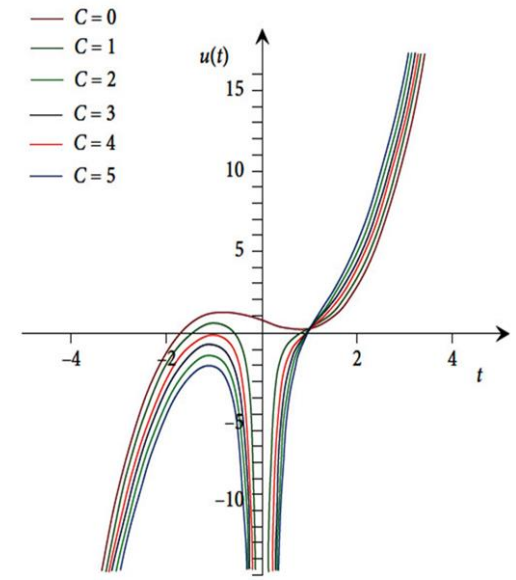


Figure 2. Integral curves of the solution to problem (3), when c=0; 1; 2; 3; 4; 5

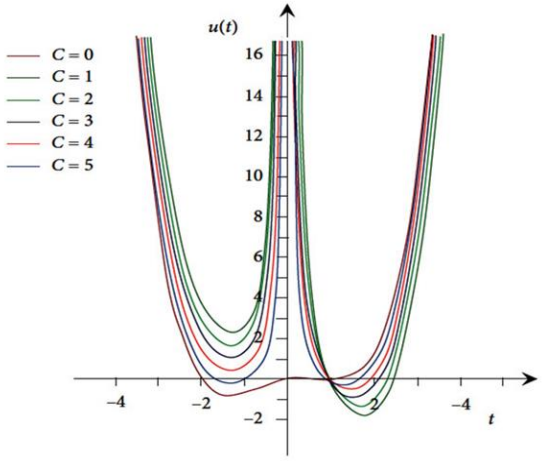


Figure 3. (4) Integral curves of the solution to problem (4), when c=0; 1; 2; 3; 4; 5

Using the above curves, we described geometric shapes of the curves of locally overpressure areas on the pedograms.

Research novelty lies in the use of a mathematical algorithm based on integral circles for solving the Dirichlet singular boundary-value problem. This approach allows highly accurate modeling of the complex geometric shapes of overloaded plantar pressure zones. Unlike existing software, which primarily visualizes pressure distribution, this method enables precise computer-aided design of these overload zones and their direct integration into the manufacturing of individualized orthopedic insoles, ensuring that material hardness are optimized for each patient.

Pedograph Research Method

The pedograph method provides important information on dynamic pressure of the plantar side of the foot. It is used to determine and record the following parameters: pressure distribution on the foot plantar surface during locomotion, peak pressure, arch index, time of contact of the foot with pedograph surface and pressure-time integral. All these parameters are calculated automatically. Information is reflected as an image of the foot with different color spectra. Pedographic examination of patients with diabetic foot was performed using the Emed-25 pedograph at/D manufactures by the Novel company (Germany).

Materials

Manufacturing individual orthopedic insoles for patients with diabetic foot using only homogeneous polymer material does not yield the desired result. For local pressures on the plantar side of the foot, soft polymer materials should be used, while relatively rigid materials are required to ensure stability of the main frame of the insole. In areas affected by diabetic foot ulcers, the use of ultra-soft polymer materials is recommended. This combination of composite polymer materials reduces the risk of ulcer development and provides fairly effective outcomes in diabetic foot treatment.

During the production of individual orthopedic insoles for overpressure areas of the diabetic foot, we used EVA polymers of various degrees of hardness from 15 to 20 Shore A. EVA polymer with a hardness of 40-45 Shore A was used for the main frame of the insoles, and ultra-soft leather-like silicone-based materials with a hardness of 5-10 Shore A were used in areas affected by diabetic foot ulcers.

The selection of material hardness was performed individually for each patient. The

choice was based on peak plantar pressure values, anatomical location of overpressure zones, condition of soft tissues, and patient-reported comfort. This approach combines quantitative pedographic data with clinical judgment.

RESEARCH RESULTS

A total of 15 patients (males, aged 45-60 years) diagnosed with diabetic foot syndrome and with a disease duration of 10 years or more, were enrolled in this study. All of them had hyperkeratosis and diabetic foot ulcers on the plantar part of the foot. All patients were overweight, with an average weight ranging from 100 to 140 kg. The clinical diagnosis, type of foot deformity, foot pathology, location, peak pressure, and body mass index (BMI) were assessed for 15 patients participating in the study. The data are presented in Table 1.

Table 1: Clinical data of the patients

Patient №	Diagnosis	Type of foot deformity		Plantar Pathology, Location, Peak Pressure		Body mass index BMI
		Left foot	Right foot	Left foot	Right foot	
1	2	5	6	7	8	9
1	Type 2 diabetes mellitus; diabetic peripheral neuropathy; neuroischemic diabetic foot	Stage 3 flat foot	Stage 2 flat foot	Hyperkeratosis of the MTP joints Peak pressure 650 Kpa. Diabetic foot ulcer of the midfoot Peak pressure 380 Kpa.	Hyperkeratosis of the MTP joints Peak pressure 310 Kpa. Hyperkeratosis of the heel Peak pressure 340 Kpa.	41.4
2	Type 2 diabetes mellitus; diabetic peripheral neuropathy; neuroischemic diabetic foot	Stage 2 flat foot	Stage 2 flat foot	Diabetic foot ulcer of the MTP joints Peak pressure 420 Kpa. Hyperkeratosis of the heel Peak pressure 385 Kpa.	Hyperkeratosis of the MTP joints Peak pressure 310 Kpa. Hyperkeratosis of the heel Peak pressure 410 Kpa.	38.5
3	Type 2 diabetes mellitus; diabetic peripheral neuropathy; neuroischemic diabetic foot	Stage 3 flat foot	Stage 3 flat foot	Diabetic foot ulcer of the MTP joints Peak pressure 635 Kpa. Hyperkeratosis of the heel Peak pressure 735 Kpa.	Diabetic foot ulcer of the MTP joints Peak pressure 640 Kpa. Hyperkeratosis of the heel Peak pressure 765 Kpa.	44.2
4	Type 2 diabetes mellitus; diabetic peripheral neuropathy; neuroischemic diabetic foot	Stage 1 flat foot	Stage 1 flat foot	Hyperkeratosis of the MTP joints Peak pressure 335 Kpa. Hyperkeratosis of the heel Peak pressure 370 Kpa.	Diabetic foot ulcer of the MTP joints Peak pressure 360 Kpa. Hyperkeratosis of the heel Peak pressure 395 Kpa.	37.8
5	Type 2 diabetes mellitus; diabetic peripheral neuropathy; neuroischemic diabetic foot	Stage 2 flat foot	Stage 2 flat foot	Diabetic foot ulcer of the MTP joints Peak pressure 520 Kpa. Hyperkeratosis of the heel Peak pressure 670 Kpa.	Hyperkeratosis of the MTP joints Peak pressure 570 Kpa. Hyperkeratosis of the heel Peak pressure 685 Kpa.	43.4

Patient №	Diagnosis	Type of foot deformity		Plantar Pathology, Location, Peak Pressure		Body mass index BMI
		Left foot	Right foot	Left foot	Right foot	
1	2	5	6	7	8	9
6	Type 2 diabetes mellitus; diabetic peripheral neuropathy; neuroischemic diabetic foot	Stage 3 flat foot	Stage 3 flat foot	Diabetic foot ulcer of the MTP joints Peak pressure 580 Kpa. Hyperkeratosis of the heel Peak pressure 620 Kpa.	Diabetic foot ulcer of the MTP joints Peak pressure 610 Kpa. Hyperkeratosis of the heel Peak pressure 655 Kpa.	43.8
7	Type 2 diabetes mellitus; diabetic peripheral neuropathy; neuroischemic diabetic foot	Stage 3 flat foot	Stage 3 flat foot	Diabetic foot ulcer of the MTP joints Peak pressure 310 Kpa. Hyperkeratosis of the heel Peak pressure 350 Kpa.	Diabetic foot ulcer of the MTP joints Peak pressure 340 Kpa. Hyperkeratosis of the heel Peak pressure 380 Kpa.	39.2
8	Type 2 diabetes mellitus; diabetic peripheral neuropathy; neuroischemic diabetic foot	Stage 3 flat foot	Stage 3 flat foot	Diabetic foot ulcer of the MTP joints Peak pressure 410 Kpa. Hyperkeratosis of the heel Peak pressure 455 Kpa.	Diabetic foot ulcer of the MTP joints Peak pressure 4250 Kpa. Diabetic foot ulcer of the heel Peak pressure 510 Kpa.	42.5
9	Type 2 diabetes mellitus; diabetic peripheral neuropathy; neuroischemic diabetic foot	Stage 2 flat foot	Stage 3 flat foot	Diabetic foot ulcer of the MTP joints Peak pressure 430 Kpa. Hyperkeratosis of the heel Peak pressure 490 Kpa.	Hyperkeratosis of the MTP joints Peak pressure 405 Kpa. Hyperkeratosis of the heel Peak pressure 395 Kpa. Diabetic foot ulcer of the midfoot Peak pressure 465 Kpa.	43.9
10	Type 2 diabetes mellitus; diabetic peripheral neuropathy; neuroischemic diabetic foot	Stage 2 flat foot	Stage 2 flat foot	Hyperkeratosis of the MTP joints Peak pressure 330 Kpa. Hyperkeratosis of the heel Peak pressure 370 Kpa.	Diabetic foot ulcer of the MTP joints Peak pressure 360 Kpa. Hyperkeratosis of the heel Peak pressure 385 Kpa.	42.7
11	Type 2 diabetes mellitus; diabetic peripheral neuropathy; neuroischemic diabetic foot	Stage 1 flat foot	Stage 2 flat foot	Diabetic foot ulcer of the MTP joints Peak pressure 340 Kpa. Hyperkeratosis of the heel Peak pressure 380 Kpa.	Diabetic foot ulcer of the MTP joints Peak pressure 360 Kpa. Hyperkeratosis of the heel Peak pressure 390 Kpa.	38.1
12	Type 2 diabetes mellitus; diabetic peripheral neuropathy;	Stage 3 flat foot	Stage 3 flat foot	Diabetic foot ulcer of the MTP joints Peak pressure 680 Kpa.	Diabetic foot ulcer of the MTP joints Peak pressure 695 Kpa.	44.2

Patient №	Diagnosis	Type of foot deformity		Plantar Pathology, Location, Peak Pressure		Body mass index BMI
		Left foot	Right foot	Left foot	Right foot	
1	2	5	6	7	8	9
	neuroischemic diabetic foot			Hyperkeratosis of the heel Peak pressure 710 Kpa.	Diabetic foot ulcer of the heel Peak pressure 745 Kpa.	
13	Type 2 diabetes mellitus; diabetic peripheral neuropathy; neuroischemic diabetic foot	Stage 3 flat foot	Stage 3 flat foot	Hyperkeratosis of the MTP joints Peak pressure 845 Kpa. Diabetic foot ulcer of the midfoot Peak pressure 880 Kpa.	Diabetic foot ulcer of the MTP joints Peak pressure 835 Kpa. Hyperkeratosis of the heel Peak pressure 790 Kpa.	44.7
14	Type 2 diabetes mellitus; diabetic peripheral neuropathy; neuroischemic diabetic foot	Stage 2 flat foot	Stage 2 flat foot	Hyperkeratosis of the MTP joints Peak pressure 410 Kpa. Hyperkeratosis of the heel Peak pressure 470 Kpa.	Hyperkeratosis of the MTP joints Peak pressure 425 Kpa. Diabetic foot ulcer of the heel Peak pressure 485 Kpa.	38.4
15	Type 2 diabetes mellitus; diabetic peripheral neuropathy; neuroischemic diabetic foot	Stage 3 flat foot	Stage 2 flat foot	Diabetic foot ulcer of the MTP joints Peak pressure 450 Kpa. Hyperkeratosis of the heel Peak pressure 510 Kpa.	Hyperkeratosis of the MTP joints Peak pressure 490 Kpa. Hyperkeratosis of the heel Peak pressure 530 Kpa.	41.5

The table presents the clinical data of 15 patients, whose main characteristics are as follows: all patients present with type 2 diabetes mellitus, diabetic peripheral neuropathy, and neuroischemic diabetic foot. The patients predominantly exhibit second- and third-stage flat foot on both feet, with first-stage flat foot occurring only in rare cases. Foot pathologies (ulcers, hyperkeratosis) are mainly localized in the metatarsophalangeal joint region and the heel region, and rarely in the midfoot area. As seen from the table, the peak plantar pressure values are extremely high in all cases, representing risk zones for the pathology. The body mass index (BMI) of the patients is high, ranging from 37.8 to 44.7, which reflects overweight or class 3 obesity.

At the next stage of the study, the patients' anthropometric data were evaluated. The results are presented in Table 2.

Table 2: Anthropometric data of the patients with diabetic foot

Patient №	D Foot size	W_1 Foot width at the medial ball region, mm	W_2 Foot width at the lateral ball region, mm	W_3 Heel width, mm	R_1 Foot girth at the medial ball region, mm	R_2 Foot girth at the lateral ball region, mm	R_3 Midfoot girth, mm	R_4 oblique foot girth, mm	R_5 Foot girth at the malleolus center, mm
1	2	3	4	5	6	7	8	9	10
1	44	118	127	94	289	291	315	398	315
2	42	112	119	82	279	285	301	378	308
3	45	121	129	102	298	304	315	421	401
4	41	108	113	78	268	275	287	354	291
5	43	117	122	99	285	287	314	385	297

Patient №	D Foot size	W_1 Foot width at the medial ball region, mm	W_2 Foot width at the lateral ball region, mm	W_3 Heel width, mm	R_1 Foot girth at the medial ball region, mm	R_2 Foot girth at the lateral ball region, mm	R_3 Midfoot girth, mm	R_4 oblique foot girth, mm	R_5 Foot girth at the malleolus center, mm
1	2	3	4	5	6	7	8	9	10
6	43	119	125	101	286	288	316	387	296
7	42	114	121	86	285	288	304	382	312
8	44	121	129	97	293	297	318	401	319
9	44	118	127	94	289	291	315	398	315
10	43	121	128	110	288	293	318	395	311
11	42	112	119	84	276	287	301	379	305
12	45	124	133	109	303	312	318	428	406
13	46	128	138	128	316	324	336	425	437
14	42	110	116	81	273	281	299	374	302
15	43	118	126	108	286	289	314	387	308

The majority of patients have medium to large foot sizes (predominantly ranging from 42 to 44), which demonstrates a normal distribution of sizes within the study group. The foot width at the medial ball region ranges from 108 mm to 128 mm, at the lateral ball region from 113 mm to 138 mm, and at the heel from 78 mm to 128 mm; these values exceed standard measurements in all cases. The foot girths at the medial and lateral regions are 268–316 mm and 275–324 mm, respectively. In diabetic foot conditions, these zones are particularly sensitive to pressure and ulcer formation. The oblique foot girth ranges from 354 mm to 428 mm, characterized by the highest numerical values, which reflect the volumetric dimensions of the foot in an oblique direction. The foot girth at the malleolus center ranges from 291 mm to 437 mm, indicating the volume of the ankle and lower leg region.

This paper considers the results of a detailed examination of the foot of Patient 1 presented in Table 1, along with the process of design and manufacturing of individual orthopedic insoles. The patient was diagnosed with Type 2 diabetes mellitus, diabetic peripheral neuropathy, and neuroischemic diabetic foot. The patient was 58 years old, weighing 137 kg, with a height of 182 cm, a body mass index of 41.4, a foot size of 44, and was classified as third-degree obesity. Figure 4 presents the pedogram of this patient.

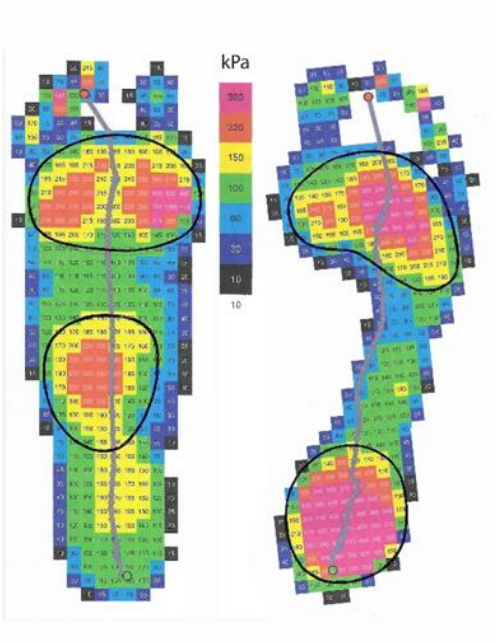


Figure 4. The pedogram of a patient with diabetic foot

The patient's clinical data and the analysis of pedogram shown in Figure 4 indicate third degree flatfoot of the left foot. Hyperkeratosis is observed in metatarso-phalangeal (MTP) joint area of the plantar part of the foot. The highlighted area on the pedogram indicates overpressure areas, marked in red and yellow, with pressures ranging from 180 to 650 Kpa. This area is at risk of disease complications and ulceration. The pressure in the mid-plantar region of the left foot ranges from 180 to 380 Kpa (overpressure area) indicating a diabetic foot ulcer. This area is also marked in red and yellow on the pedogram.

The analysis of the right foot revealed that the patient had second-degree flatfoot. Hyperkeratosis was observed in the metatarsophalangeal (MTP) joints of the plantar part of the foot and in the heel area. The region marked in red and yellow on the pedogram indicate overpressure area, where the pressures per unit area is 170-340 Kpa, representing a high risk for complications and ulcer development.

The locally overpressure areas are marked with curves, which showed the pressure of 150 Kpa and over (Figure 4). The description of the presented curves was carried out by means of integral curves of the solutions to Dirichlet singular boundary problem.

Since the contour of the overloaded zone of the plantar part of the foot is complex and non-uniform, a single mathematical function and a single integral curve of its solution cannot fit the entire figure. Therefore, the contour of each overloaded zone is divided into individual segments depending on the sharpness of the contour curvature in different areas. The corresponding integral curves were fitted to each segment individually by varying the coefficients c.

Existing software simply visualizes the overpressure areas through a color spectrum on a pedogram, but does not provide their exact geometric model or the ability to transfer them to a CNC machine. In contrast, this method provides millimeter-precision of the overloaded zones through their computer-aided design and direct integration into the CNC milling process.

Figure 5 the geometric shape of the curve of a locally overpressure area of the MTP of the plantar part of the left foot, which was taken from the pedogram (Figure 4).

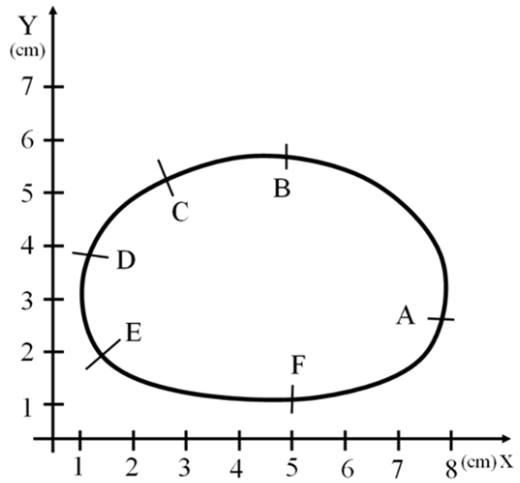


Figure 5. Geometric shape of the curve of the overpressure area of the MTP joints of the plantar part of the left foot

The curve illustrated in Figure 5 was preliminarily divided into six parts. Each numbered region was described using the integral curves of the functions given below. Six parts of the integral curves identically corresponding to the geometric shapes of the curve on the overpressure area of the plantar side of the MTP of the left foot were chosen, namely the following:

1. AB - curve corresponds to that part of the solution to equation

$$u(t)=\frac{t^3}{2}-\frac{1}{3}ct^{-2}-\left(1-\frac{1}{3}c\right)t+\frac{1}{2}, \quad (5)$$

for which c = 0 and corresponds to a set [0,1;0,7] × [-2,5; -5,0]

2. BC - curve corresponds to that part of the solution to equation

$$u(t)=\frac{t^3}{2}-\frac{1}{3}ct^{-2}-\left(1-\frac{1}{3}c\right)t+\frac{1}{2}, \quad (6)$$

for which c = 5 and corresponds to a set [-1,5; -1,5] × [-7,0; -2.2]

3. BC - curve corresponds to that part of the solution to equation

$$u(t)=\frac{t^3}{2}-\frac{1}{3}ct^{-2}-\left(1-\frac{1}{3}c\right)t+\frac{1}{2}, \quad (7)$$

for which c = 0 and corresponds to a set [-1,2; 2; 1,0] × [-2,1; -2,0]

4. DE - curve corresponds to that part of the solution to equation

$$u(t) = (-\frac{1}{3} - \frac{1}{3}c)t + \frac{1}{3}c\frac{1}{t^2} + \frac{2}{3}t - \frac{t^2}{2} + \frac{t^4}{6}, \quad (8)$$

for which *c* = 1 and corresponds to a set [-1,0; -0,1] × [-0.4; 2.2]

5. EF – curve corresponds to that part of the solution to equation

$$u(t) = (-\frac{1}{3} - \frac{1}{3}c)t + \frac{1}{3}c\frac{1}{t^2} + \frac{2}{3}t - \frac{t^2}{2} + \frac{t^4}{6}, \quad (9)$$

for which *c* = 0 and corresponds to a set [1,6; 0,3] × [2,5; 5,5]

6. FA – curve corresponds to that part of the solution to equation

$$u(t) = (-\frac{1}{3} - \frac{1}{3}c)t + \frac{1}{3}c\frac{1}{t^2} + \frac{2}{3}t - \frac{t^2}{2} + \frac{t^4}{6}, \quad (10)$$

for which *c* = 5 and corresponds to a set [-11,9; 5,0] × [-2.3; 6,0].

Based on the above-mentioned mathematical algorithm, the software was developed to describe the curve segments. By rotating and translating these curves, an exact geometric shape of the curve was obtained to represent the locally overpressure areas in MTP region of the plantar surface of the left foot.

Figure 6 shows the geometric shape of the curve of the locally overpressure area of the middle of the plantar part of the left foot, taken from the pedogram (Figure 4).

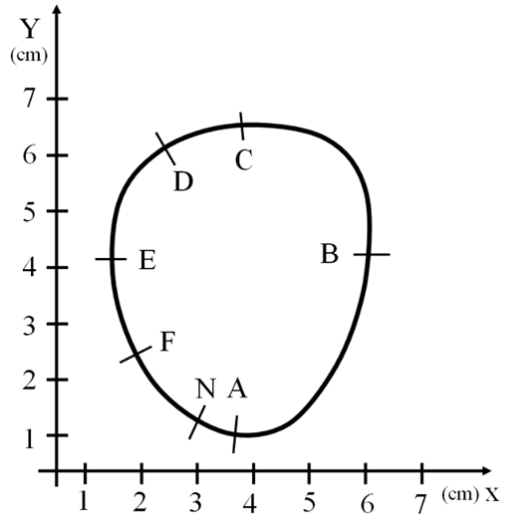


Figure 6. The shape of the curve of the locally overpressure area of the middle of the plantar part of the left foot

The curve shown in Figure 6 was preliminarily divided into 7 parts. Each numbered section was described using the integral curves of the functions given below. From these integral curves, 7 parts identically corresponding to the geometric shapes of the curve of overpressure area in the middle of the plantar part of the left foot were chosen, namely:

1. AB - curve corresponds to that part of the solution to equation

$$u(t) = \frac{t^3}{2} - \frac{1}{3}ct^{-2} - \left(1 - \frac{1}{3}c\right)t + \frac{1}{2}, \quad (11)$$

for which *c* = 0 and corresponds to a set [0.9; -0.5] × [-2,5; -5,0]

2. BC - curve corresponds to that part of the solution to equation

$$u(t) = (-\frac{1}{3} - \frac{1}{3}c)t + \frac{1}{3}c\frac{1}{t^2} + \frac{2}{3}t - \frac{t^2}{2} + \frac{t^4}{6}, \quad (12)$$

for which *c* = 0 and corresponds to a set [-0,2; -0,1] × [1,5; -2,4]

3. CD - curve corresponds to that part of the solution to equation

$$u(t) = \frac{t^3}{2} - \frac{1}{3}ct^{-2} - \left(1 - \frac{1}{3}c\right)t + \frac{1}{2}, \quad (13)$$

for which *c* = 5 and corresponds to a set [-1,4; -2,4] × [-2,0; -4,9]

4. DE - curve corresponds to that part of the solution to equation

$$u(t) = (-\frac{1}{3} - \frac{1}{3}c)t + \frac{1}{3}c\frac{1}{t^2} + \frac{2}{3}t - \frac{t^2}{2} + \frac{t^4}{6}, \quad (14)$$

for which *c* = 1 and corresponds to a set [-1,2; -0,1] × [-0,4; -1,1]

5. EF - curve corresponds to that part of the solution to equation

$$u(t) = (-\frac{1}{3} - \frac{1}{3}c)t + \frac{1}{3}c\frac{1}{t^2} + \frac{2}{3}t - \frac{t^2}{2} + \frac{t^4}{6}, \quad (15)$$

for which *c* = 5 and corresponds to a set [-1,1; 2,1] × [2,5;1,1]

6. FN – curve corresponds to that part of the solution to equation

$$u(t) = (-\frac{1}{3} - \frac{1}{3}c)t + \frac{1}{3}c\frac{1}{t^2} + \frac{2}{3}t - \frac{t^2}{2} + \frac{t^4}{6}, \quad (16)$$

for which c = 0 and corresponds to a set [1,4; 0,1] × [2,1; 1,9]

7. NA - curve corresponds to that part of the solution to equation

$$u(t)=\frac{t^3}{2}-\frac{1}{3}ct^{-2}-\left(1-\frac{1}{3}c\right)t+\frac{1}{2}, \quad (17)$$

for which c = 0 and corresponds to a set [-1,6; 0,1] × [-1,0; -1,8]

Based on the mathematical algorithm, computer programs describing curves were developed. By rotating and translating the curves, a precise geometric shape was obtained to represent the locally overpressure area in the middle part of the left foot.

Similarly, we constructed complex geometric shapes for the overpressure area of the plantar part of the right foot and the heel.

Figure 7 shows a complex geometric shape of the overpressure area in the plantar part of the MTP joints of the right foot taken from the pedogram (Figure 4).

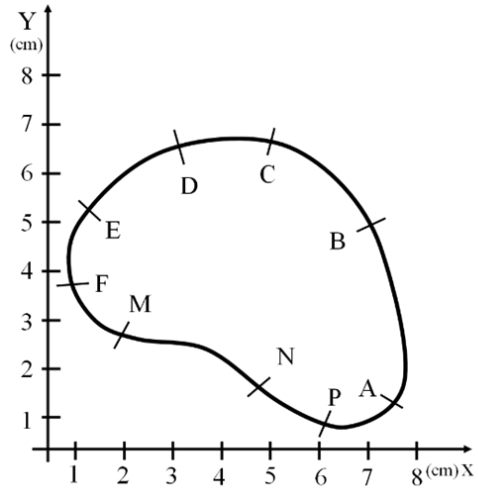


Figure 7. Geometric shape of the curve of the overpressure area of the MTP joints of the plantar part of the right foot

The curve shown in Figure 7 was preliminarily divided into nine segments. Each section was described using the integral circles of the functions listed below. From the integral curves, nine sections of the integral curves identically corresponding to the complex geometric shapes of the curve of the overpressure area at the point of MTP joints of the plantar part of the right foot were chosen, namely the following:

1. AB - curve corresponds to that part of the solution to equation

$$u(t)=\frac{t^3}{2}-\frac{1}{3}ct^{-2}-\left(1-\frac{1}{3}c\right)t+\frac{1}{2}, \quad (18)$$

for which c = 0 and corresponds to a set [1,0; -1,1] × [-2,5; -5,1]

2. BC - curve corresponds to that part of the solution to equation

$$u(t)=\frac{t^3}{2}-\frac{1}{3}ct^{-2}-\left(1-\frac{1}{3}c\right)t+\frac{1}{2}, \quad (19)$$

for which c = 5 and corresponds to a set [-1,4; -2,9] × [-2,0; -5,1]

3. CD - curve corresponds to that part of the solution to equation

$$u(t)=(-\frac{1}{3}-\frac{1}{3}c)t+\frac{1}{3}c\frac{1}{t^2}+\frac{2}{3}t-\frac{t^2}{2}+\frac{t^4}{6} \quad (20)$$

for which c = 5 and corresponds to a set [-1,0; 2,5] × [-0,5; 5,5]

4. DE – curve corresponds to that part of the solution to equation

$$u(t)=(-\frac{1}{3}-\frac{1}{3}c)t+\frac{1}{3}c\frac{1}{t^2}+\frac{2}{3}t-\frac{t^2}{2}+\frac{t^4}{6}, \quad (21)$$

for which c = 0 and corresponds to a set [1,5; 0,2] × [2,2; 3,1]

5. EF – curve corresponds to that part of the solution to equation

$$u(t)=(-\frac{1}{3}-\frac{1}{3}c)t+\frac{1}{3}c\frac{1}{t^2}+\frac{2}{3}t-\frac{t^2}{2}+\frac{t^4}{6}, \quad (22)$$

for which c = 1 and corresponds to a set [-1,1; -0,1] × [-0,5; 1,9]

6. FM – curve corresponds to that part of the solution to equation

$$u(t)=\frac{t^3}{2}-\frac{1}{3}ct^{-2}-\left(1-\frac{1}{3}c\right)t+\frac{1}{2}, \quad (23)$$

for which c = 1 and corresponds to a set [-1,2; 0,1] × [-1.8; 0,1]

7. MN – curve corresponds to that part of the solution to equation

$$u(t)=(-\frac{1}{3}-\frac{1}{3}c)t+\frac{1}{3}c\frac{1}{t^2}+\frac{2}{3}t-\frac{t^2}{2}+\frac{t^4}{6}, \quad (24)$$

for which c = 0 and corresponds to a set [-0,8; -1,1] × [1,0; 0,1]

8. NP – curve corresponds to that part of the solution to equation

$$u(t)=(-\frac{1}{3}-\frac{1}{3}c)t+\frac{1}{3}c\frac{1}{t^2}+\frac{2}{3}t-\frac{t^2}{2}+\frac{t^4}{6}, \quad (25)$$

for which c = 5 and corresponds to a set [-1,2; 2,1] × [2,5; 1,0]

9. PA – curve corresponds to that part of the solution to equation

$$u(t)=\frac{t^3}{2}-\frac{1}{3}ct^{-2}-\left(1-\frac{1}{3}c\right)t+\frac{1}{2}, \quad (26)$$

for which c = 4 and corresponds to a set [-5,8; -0,5] × [-1,8; -1,0].

Based on the mathematical algorithm, computer programs were developed to describe the curves. By rotating and translating these curves, we got complex geometric shape of the curve of the locally overpressure area on the MTP of the right foot's plantar surface, which is an exact analogue of the complex geometric curved line shown on the pedogram.

Similarly, we constructed complex geometric shapes for the overpressure area of the plantar part of the heel of the right foot.

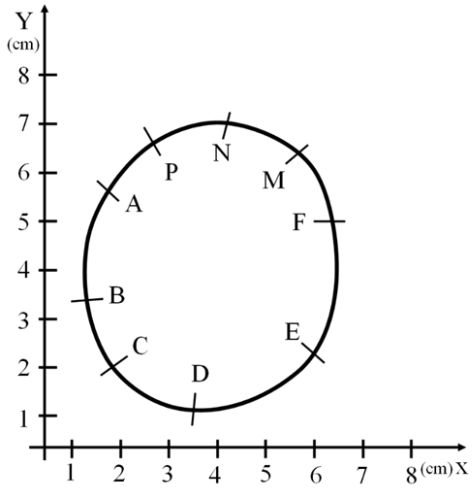


Figure 8. Geometric shape of the curve of the locally overpressure area in the heel area of the plantar part of the right foot

Figure 8 shows the curve of a complex geometric shape of the overpressure area in the heel area of the plantar part of the right foot, taken from the pedogram (Figure 4). This curve was preliminary divided into nine parts and the description of each section using the integral curves of the functions given below.

From the integral curves, nine sections of curves were selected that identically correspond to the complex geometric shapes of the curves of the overpressure area in the heel area of the plantar part of the right foot, namely:

1. AB - curve corresponds to that part of the solution to equation

$$u(t)=(-\frac{1}{3}-\frac{1}{3}c)t+\frac{1}{3}c\frac{1}{t^2}+\frac{2}{3}t-\frac{t^2}{2}+\frac{t^4}{6}, \quad (27)$$

for which c = 5 and corresponds to a set [-1,9; 2,0][2,5; 1,1]

2. BC - curve corresponds to that part of the solution to equation

$$u(t)=\frac{t^3}{2}-\frac{1}{3}ct^{-2}-\left(1-\frac{1}{3}c\right)t+\frac{1}{2}, \quad (28)$$

for which c = 5 and corresponds to a set [-2,5;-1,4][-4,9; -1,9]

3. CD – curve corresponds to that part of the solution to equation

$$u(t)=(-\frac{1}{3}-\frac{1}{3}c)t+\frac{1}{3}c\frac{1}{t^2}+\frac{2}{3}t-\frac{t^2}{2}+\frac{t^4}{6}, \quad (29)$$

for which c = 0 and corresponds to a set [-2,3; 1,1][-1,8; -1,6]

4. DE – curve corresponds to that part of the solution to equation

$$u(t)=\frac{t^3}{2}-\frac{1}{3}ct^{-2}-\left(1-\frac{1}{3}c\right)t+\frac{1}{2}, \quad (30)$$

for which c = 0 and corresponds to a set [-1,8; 1,0][-2,5; -2,1]

5. EF – curve corresponds to that part of the solution to equation

$$u(t)=\frac{t^3}{2}-\frac{1}{3}ct^{-2}-\left(1-\frac{1}{3}c\right)t+\frac{1}{2}, \quad (31)$$

for which c = 0 and corresponds to a set [-1,2; 1,8][-2,1; -4,0]

6. FM – curve corresponds to that part of the solution to equation

$$u(t)=(-\frac{1}{3}-\frac{1}{3}c)t+\frac{1}{3}c\frac{1}{t^2}+\frac{2}{3}t-\frac{t^2}{2}+\frac{t^4}{6}, \quad (32)$$

for which c = 0 and corresponds to a set [1,6; 0,2][2,1; 2,1]

7. MN – curve corresponds to that part of the solution to equation

$$u(t) = (-\frac{1}{3} - \frac{1}{3}c)t + \frac{1}{3}c\frac{1}{t^2} + \frac{2}{3}t - \frac{t^2}{2} + \frac{t^4}{6}, \quad (33)$$

for which *c* = 1 and corresponds to a set [-1,9; 0,1][-0,5; 2,1]

8. NP – curve corresponds to that part of the solution to equation

$$u(t) = (-\frac{1}{3} - \frac{1}{3}c)t + \frac{1}{3}c\frac{1}{t^2} + \frac{2}{3}t - \frac{t^2}{2} + \frac{t^4}{6}, \quad (34)$$

for which *c* = 2 and corresponds to a set [-1,8; 0,8][-0.6; 2,2]

9. PA – curve corresponds to that part of the solution to equation

$$u(t) = (-\frac{1}{3} - \frac{1}{3}c)t + \frac{1}{3}c\frac{1}{t^2} + \frac{2}{3}t - \frac{t^2}{2} + \frac{t^4}{6}, \quad (35)$$

for which *c* = 5 and corresponds to a set [-1,0; 2,8][-0,7; 3,3].

Here, computer programs describing curves were also constructed using a mathematical algorithm. By rotating and translating these curves, we got a precise curve of the complex geometric shape of the overpressure area in the heel of the plantar part of the right foot.

Thus, through the use of integral curves of the solutions to Dirichlet singular boundary problem, it is possible to describe complex the geometric shape of a curve of any complexity with high precision. The proposed study was applied to all patients included in the group.

DISCUSSION

The process of design and manufacturing of individual orthopedic insoles is quite complicated and sequential. The curves with complex geometric shape of the locally overpressure areas taken from the pedogram are described through the integral curves of the solutions to the Dirichlet singular boundary problem. Based on the mathematical algorithm, the complete software packages were developed for the production of complex geometric shapes of overpressure areas of the plantar part of the foot.

Using the CNC milling machine, we pre-milled the overpressure areas from relatively soft materials. Specifically, for the plantar area of the left foot, where the peak pressure ranged from 180 to 650 Kpa, we chose an EVA polymer with a hardness of 15 Shore A. In the midfoot area (location of the diabetic foot ulcer, with the peak pressure 170-380 Kpa, we used a combination of polymer materials: a silicone-based, leather-like polymer with a hardness of 5 Shore A and an EVA polymer with a hardness of 15 Shore A. For the plantar area of the right foot, where the pressure is 180-340 Kpa, we chose an EVA polymer with a hardness of 40 Shore A. When selecting materials, we took into account the patient's subjective factors as much as possible.

The shapes of the overloaded areas were first milled from soft materials using a CNC milling machine. The corresponding shapes were then cut from the frame of insole using a CNC milling machine. At the next stage, the shapes of the overloaded areas were embedded into the frame of insole, resulting in the final material for manufacturing the orthotic insole.

Using the developed computer programs and a CNC machine, custom orthotic insoles were manufactured, taking into account localized overloaded areas of the plantar surfaces. The resulting insoles are shown in Figure 9.

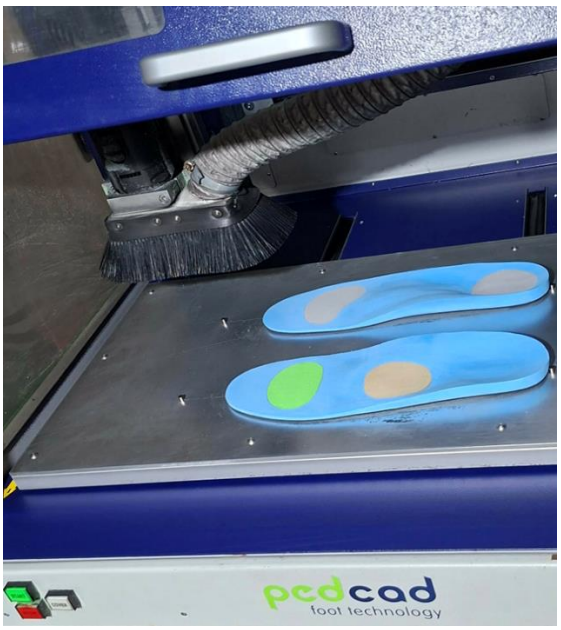


Figure 9. Individual orthopedic insoles, designed to account for the locally overpressured areas on the plantar surfaces of the feet

Figures 10 and 11 show images of individual orthopedic insoles in various projections.

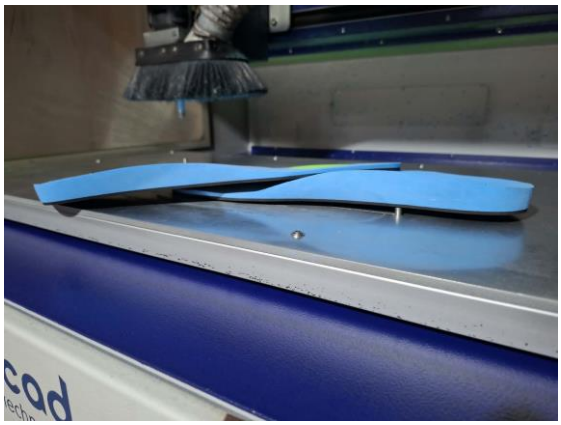


Figure 10. Insole arch parts

Figure 10 clearly shows the difference between the heights of the insole arches: the arch height of the left foot insole is 21 mm, while the arch height of the right insole is 28 mm, with a difference of 7 mm.



Figure 11. The shape of the support part of the insole

Figure 11 clearly shows the difference in shapes across the support area of the insoles.

The software package includes the following steps:

- Identification and segmentation of the zones of excessive pressure on the plantar part of the foot (demarcation using curved lines);
- Description of individual curves constituting the complex geometric shapes of the zones of excessive pressure on the pedograms using integral curves derived from the solution of the Dirichlet singular boundary-value problem, based on the corresponding mathematical algorithm;
- Geometric transformation (translation and rotation) of the curve segments to obtain accurate contours of the zones of excessive pressure;
- Development of computer programs describing the complex geometric shapes of the zones of excessive pressure based on the proposed mathematical algorithm and their implementation in the process of insole design;
- Export of the developed computer programs into formats compatible with CNC-controlled machine tools.

It should be noted that, unlike previously published studies, this work employs a mathematical research method that enables highly accurate description of the shapes of overloaded areas on the plantar surface of the diabetic foot.

Based on the conducted research, individual orthopedic insoles were manufactured for the 15 patients in the study group. The patients wore special orthopedic shoes daily, tailored to the specific anthropometric parameters of each individual's foot. The patients used the insoles in their daily footwear throughout the trial period. During the first 1–2 weeks, an intensive adaptation phase took place, accompanied by the initial compression of the EVA polymer. During this period, the material adapted to the patient's foot anatomy and load characteristics. By the 3rd–4th week of daily wear, the deformation of the EVA polymer significantly decreased, and its deformation properties transitioned into a stable phase. After 4 weeks, the subjective comfort of the individual insoles was evaluated. The majority of patients demonstrated an improved quality of life, which can be considered a positive indicator for the initial stage of observation. Long-term clinical outcomes are part of an ongoing, extended study and will be presented in future publications.

CONCLUSION

In this study, individual orthopedic insoles were designed for 15 patients with diabetic foot syndrome. For each patient, areas of excessive

plantar pressure were identified using pedograms. The complex geometric shapes of these overloaded zones were described with high accuracy using integral curves derived from the solution of a Dirichlet singular boundary-value problem. Based on the proposed mathematical algorithm, computer programs were developed and were exported into CNC-compatible formats for insole fabrication.

During the manufacturing of the insoles, EVA polymers with a hardness of 15–20 Shore A were used for overloaded areas, ultra-soft silicone-based materials with a hardness of 5–10 Shore A were applied in zones of ulcers and hyperkeratosis, and EVA polymers with a hardness of 40–45 Shore A were used for the insole frame. The selection of material hardness was based on plantar pressure values, as well as clinical data and patient-reported comfort.

Trial wear of the insoles demonstrated a reduction in peak pressure in overloaded zones, improved pressure distribution across the foot, and improvement in the clinical condition of ulcers and hyperkeratosis.

The proposed method shows that the combination of pedographic data, mathematical modeling, and the use of combined polymer materials makes it possible to design and manufacture individual orthopedic insoles that can contribute to the effective management of patients with diabetic foot syndrome.

Ethical Standards and Protection of Personal Data

All data presented in this article were collected and published in full compliance with ethical standards. No identifiable personal information is included, and every effort has been made to protect the privacy of the patients involved.

Conflicts of Interest

The authors declare that they have no conflicts of interest regarding this research.

Acknowledgements

The authors would like to thank the Shota Rustaveli National Science Foundation of Georgia for financially supporting this research. Grant FR № 217386.

REFERENCES

1. Saeedi, P., Petersohn, I., Salpea, P., Malanda, B., Karuranga, S., Unwin, N., Colagiuri, S., Guariguata, L., Motala, A.A., Ogurtsova, K., Shaw, J.E., Bright, D., Williams, R., IDF Diabetes Atlas Committee, Global and Regional Diabetes Prevalence Estimates for 2019 and Projections for 2030 and 2045: Results from the International Diabetes Federation Diabetes Atlas, 9th edition, *Diabetes Res Clin Pract*, **2019**, 157, 107843, https://doi.org/10.1016/j.diabres.2019.107843.
2. Manickum, P., Mashamba-Thompson, T., Naidoo, R., Ramklass, S., Madiba, T., Knowledge and Practice of Diabetic Foot Care – A Scoping Review, *Diabetes Metab Syndr*, **2021**, 15, 3, 783-793, https://doi.org/10.1016/j.dsx.2021.03.030.
3. Tan, M.K.H., Goodall, R., Hughes, W., Langridge, B., Shalhoub, J., Davies, A.H., A Methodological Assessment of Diabetic Foot Syndrome Clinical Practice Guidelines, *Eur J Vasc Endovasc Surg*, **2020**, 60, 2, 274-281, https://doi.org/10.1016/j.ejvs.2020.04.028.
4. Van, G.H., Amouyal, C., Bourron, O., Aubert, C., Carlier, A., Mosbah, H., Fourniols, E., Cluzel, P., Couture, T., Hartemann, A., Diabetic Foot Ulcer Management in a Multidisciplinary Foot Centre: One-Year Healing, Amputation and Mortality Rate, *J Wound Care*, **2021**, 1, 30, Sup6, S34-41, https://doi.org/10.12968/jowc.2021.30.Sup6.S34.
5. Cevera, J.J., Bolton, L.L., Kerstein, M.D., Options for Diabetic Patients with Chronic Heel Ulcers, *J Diabetes Complications*, **1997**, 1, 11, 6, 358-66, https://doi.org/10.1016/s1056-8727(96)00125-0.
6. Jones, F.W., Peltier, L.F., Structure and Function as Seen in the Foot, *Clin Orthop Relat Res*, **2001**, 1, 391, 3-6, https://doi.org/10.1097/00003086-200110000-00002.
7. Rome, K., Mechanical Properties of the Heel Pad: Current Theory and Review of the Literature, *Foot*, **1998**, 1, 8, 4, 179-85, https://doi.org/10.1016/S0958-2592(98)90026-8.
8. Bus, S.A., Akkerman, E.M., Maas, M., Changes in Sub-Calcaneal Fat Pad Composition and Their Association with Dynamic Plantar Foot

Pressure in People with Diabetic Neuropathy, *Clin Biomech*, **2021**, 1, 88, 105441, https://doi.org/10.1016/j.clinbiomech.2021.105441.
9. Buschmann, W.R., Jahss, M.H., Kummer, F., Desai, P., Gee, R.O., Ricci, J.L., Histology and Histomorphometric Analysis of the Normal and Atrophic Heel Fat Pad, *Foot Ankle Int*, **1995**, 16, 5, 254-8, https://doi.org/10.1177/107110079501600502.
10. Jahss, M.H., Michelson, J.D., Desai, P., Kaye, R., Kummer, F., Buschman, W., Watkins, F., Reich, S., Investigations into the Fat Pads of the Sole of the Foot: Anatomy and Histology, *Foot Ankle*, **1992**, 13, 5, 233-42, https://doi.org/10.1177/107110079201300502.
11. Ledoux, W.R., Blevins, J.J., The Compressive Material Properties of the Plantar Soft Tissue, *J Biomech*, **2007**, 1, 40, 13, 2975-81, https://doi.org/10.1016/j.jbiomech.2007.02.009.
12. Wang, Y.N., Lee, K., Shofer, J.B., Ledoux, W.R., Histomorphological and Biochemical Properties of Plantar Soft Tissue in Diabetes, *Foot*, **2017**, 1, 33, 1-6, https://doi.org/10.1016/j.foot.2017.06.001.
13. Wang, Y.N., Lee, K., Ledoux, W.R., Histomorphological Evaluation of Diabetic and Non-Diabetic Plantar Soft Tissue, *Foot Ankle Int*, **2011**, 32, 8, 802-10, https://doi.org/10.3113/FAI.2011.0802.
14. Wearing, S.C., Smeathers, J.E., Yates, B., Urry, S.R., Dubois, P., Bulk Compressive Properties of the Heel Fat Pad During Walking: A Pilot Investigation in Plantar Heel Pain, *Clin Biomech*, **2009**, 1, 24, 4, 397-402, https://doi.org/10.1016/j.clinbiomech.2009.01.002.
15. Chanda, A., Unnikrishnan, V., Novel Insole Design for Diabetic Foot Ulcer Management, *Proceedings of the Institution of Mechanical Engineers, Part H: Journal of Engineering in Medicine*, **2018**, 232, 12, 1182-95, https://doi.org/10.1177/0954411918808330.
16. Shalamberidze, M., Sokhadze, Z., Tatvidze, M., The Design of Individual Orthopedic Insoles for the Patients with Diabetic Foot Using Integral Curves to Describe the Plantar Over-Pressure Areas, *Comput Math Methods Med*, **2021**, 2021, 1, 9061241, https://doi.org/10.1155/2021/9061241.
17. Charanya, G., Patil, K.M., Narayanamurthy, V.B., Parivalavan, R., Visvanathan, K., Effect of Foot Sole Hardness, Thickness and Footwear on Foot Pressure Distribution Parameters in Diabetic Neuropathy, *Proceedings of the Institution of Mechanical Engineers, Part H: Journal of Engineering in Medicine*, **2004**, 1, 218, 6, 431-43, https://doi.org/10.1243/0954411042632117.
18. Rao, S., Saltzman, C.L., Yack, H.J., Relationships Between Segmental Foot Mobility and Plantar Loading in Individuals with and without Diabetes and Neuropathy, *Gait Posture*, **2010**, 1, 31, 2, 251-5, https://doi.org/10.1016/j.gaitpost.2009.10.016.
19. Healy, A., Naemi, R., Chockalingam, N., The Effectiveness of Footwear as an Intervention to Prevent or to Reduce Biomechanical Risk Factors Associated with Diabetic Foot Ulceration: A Systematic Review, *J Diabetes Complications*, **2013**, 1, 27, 4, 391-400, https://doi.org/10.1016/j.jdiacomp.2013.03.001.
20. Zhi, X., Wang, W., Xu, B., Zhou, J., Effectiveness of Pressure-Relieving Shoes/Insoles on Lowering the Plantar Pressure of Diabetic Foot: A Meta-Analysis, *Leather and Footwear Journal*, **2020**, 20, 4, 361-74, https://doi.org/10.24264/lfj.20.4.3.
21. Shalamberidze, M., Sokhadze, Z., Tatvidze, M., Construction of the Transverse-Vertical Shapes of the Orthopedic Boot-Tree by Means of the Solution to Singular Dirichlet Boundary Value Problem, *Bulletin of the Georgian National Academy of Sciences*, **2018**, 12, 1, 27-32, http://science.org.ge/bnas/t12-n1/05_Shalamberidze.pdf.
22. Shalamberidze, M., Sokhadze, Z., Tatvidze, M., Orthopedic Boot-Tree 3D Design by Means of the Integral Curves of Solutions of Differential Equations, *Complexity*, **2020**, 1-6, https://doi.org/10.1155/2020/4252790.

© 2026 by the author(s). Published by INCDTP-ICPI, Bucharest, RO. This is an open access article distributed under the terms and conditions of the Creative Commons Attribution license (http://creativecommons.org/licenses/by/4.0/).

A SYSTEMATIC APPROACH TO TEXTILE DESIGN: AN EXPERIMENTAL STUDY

Pinar ARSLAN*, Ozge OZTURK

Ankara Hacı Bayram Veli University, Faculty of Art and Design, Department of Textile Design, 06830, Ankara, Türkiye,

pinar.arslan@hbv.edu.tr, ozturk-ozge@hbv.edu.tr

Received: 04.03.2026 Accepted: 21.09.2026 https://doi.org/10.24264/lfj.26.3.2

A SYSTEMATIC APPROACH TO TEXTILE DESIGN: AN EXPERIMENTAL STUDY

ABSTRACT. Systematic creativity models provide structured frameworks for defining design problems, generating ideas, and evaluating solutions. Among these models, Osborn's Seven-Stage Theory offers a step-based process that supports creative thinking and problem-solving. This study aims to examine the applicability of Osborn's model in textile pattern design through an experimental approach. The research was conducted with second-year students from the Textile Design Department at Ankara Hacı Bayram Veli University. Within the scope of the study, seven students developed textile pattern designs by systematically applying the stages of Osborn's model. The resulting designs and processes were analyzed in terms of originality, conceptual consistency, and creative diversity. The findings indicate that the structured implementation of the model enhances systematic thinking, supports creative exploration, and contributes to the development of more original and coherent textile patterns. The study proposes a methodological framework for integrating systematic creativity models into textile design practice and education, thereby contributing to innovation-oriented design processes in the textile field.

KEY WORDS: digitalization; fabric design; innovation; creative process; pattern

O ABORDARE SISTEMATICĂ A DESIGNULUI TEXTIL: STUDIU EXPERIMENTAL

REZUMAT. Modelele sistematice de creativitate oferă cadre structurate pentru definirea problemelor de design, generarea ideilor și evaluarea soluțiilor. Dintre aceste modele, teoria în șapte etape a lui Osborn propune un proces etapizat care susține gândirea creativă și rezolvarea problemelor. Acest studiu își propune să examineze aplicabilitatea modelului lui Osborn în designul de modele textile printr-o abordare experimentală. Cercetarea a fost realizată cu studenți din anul al doilea de la Departamentul de Design Textil al Universității Ankara Hacı Bayram Veli. În cadrul studiului, șapte studenți au dezvoltat modele textile aplicând în mod sistematic etapele modelului lui Osborn. Modelele și procesele rezultate au fost analizate din perspectiva originalității, coerenței conceptuale și diversității creative. Rezultatele indică faptul că implementarea structurată a modelului îmbunătățește gândirea sistematică, susține explorarea creativă și contribuie la dezvoltarea unor modele textile mai originale și coerente. Studiul propune un cadru metodologic pentru integrarea modelelor sistematice de creativitate în practica și educația designului textil, contribuind astfel la procesele de design orientate spre inovare în domeniul textil.

CUVINTE CHEIE: digitalizare; design textil; inovație; proces creativ; model

UNE APPROCHE SYSTÉMATIQUE DU DESIGN TEXTILE : ÉTUDE EXPÉRIMENTAL

RÉSUMÉ. Les modèles systématiques de créativité offrent des cadres structurés pour définir les problèmes de conception, générer des idées et évaluer des solutions. Parmi ces modèles, la théorie en sept étapes d'Osborn propose un processus structuré qui soutient la pensée créative et la résolution de problèmes. Cette étude vise à examiner l'applicabilité du modèle d'Osborn dans la conception de motifs textiles à travers une approche expérimentale. La recherche a été menée auprès d'étudiants de deuxième année du département de design textile de l'université Ankara Hacı Bayram Veli. Dans le cadre de l'étude, sept étudiants ont développé des motifs textiles en appliquant systématiquement les étapes du modèle d'Osborn. Les créations et les processus ont été analysés en termes d'originalité, de cohérence conceptuelle et de diversité créative. Les résultats indiquent que la mise en œuvre structurée du modèle renforce la pensée systématique, favorise l'exploration créative et contribue au développement de motifs textiles plus originaux et cohérents. L'étude propose un cadre méthodologique pour l'intégration des modèles systématiques de créativité dans la pratique et l'enseignement du design textile, contribuant ainsi aux processus de conception orientés vers l'innovation dans le domaine textile.

MOTS CLÉS : numérisation ; design textile ; innovation ; processus créatif ; motif

* *Correspondence to: Pinar ARSLAN, Ankara Hacı Bayram Veli University, Faculty of Art and Design, Department of Textile Design, 06830, Ankara, Türkiye, pinar.arslan@hbv.edu.tr*

INTRODUCTION

Creativity and the skill of creative thinking – topics that have intrigued thinkers and philosophers since antiquity and continue to captivate modern scientists – remain among the most fundamental traits that distinguish humankind from other living beings. Initially explored within the field of philosophy, creativity has since become a subject of theoretical inquiry in various disciplines, including psychology, social sciences, fine arts, and education. A commonly agreed upon definition of creativity in interdisciplinary studies is that it involves "new ideas, different perspectives, or original products," and creativity is assessed based on the design or output that results from this process [1, 2]. Since the Renaissance, Western civilization has focused heavily on the technical structures and mechanisms associated with creativity [3]. As a result, from that period to the present day, both our ancestors and we ourselves have channeled creative impulses into the making of technical artifacts, thereby contributing to the application and advancement of creativity science. Creativity – expressed as the development of a solution to a problem, the invention of a new method, or the formulation of an original idea – emerges from the encounter between a highly conscious individual and their own world [4]. The term itself derives from the Latin word *creare*, meaning "to bring forth," "to create," or "to give birth" [5, 6]. According to Batı [7] creativity can emerge by developing our minds in the right environment using the right methods at the right time. Craft [8], on the other hand, describes creativity as a lifelong skill, defining it as the capacity for self-expression, intelligence, and imagination. Creativity has also been considered as an invention, a scientific theory, an improved product, or a novel design idea that involves questioning the status quo, exploring alternative solutions, and generating original ideas [9-11]. Design can be defined as a thought process that responds to a desired goal, a component of an intelligible whole, and a synthesis of material and form created to serve a specific purpose [12]. According to [13] who describes design as consisting of 98% common sense and 2% of what could be called a mystical component—creativity—the textile industry is a multifaceted field that requires an understanding of design, management, and technology for success. In this context, the design creation process holds a central place in both the evaluation and formation of design. This process supports the emergence of knowledge and experience through diverse reasoning mechanisms while ensuring the integration of design with visual and aesthetic values [14, 15]. Throughout history, scholars have developed theories and methodologies aimed at explaining the concept of design, along with approaches that analyze design activity as a cognitive process [16-19]. Especially in the field of textile design (weaving, knitting, printing), a creative process exists through which designers transform abstract ideas in their minds into concrete forms, thereby facilitating the emergence of original and innovative products. This study aims to develop a creative and innovative approach in pattern design by explaining Osborn's Seven-Stage Theory and integrating it into the textile design process. In line with this goal, the research problem focuses on the applicability of Osborn's Seven-Stage Theory (Orientation, Preparation, Analysis, Hypothesis, Incubation, Synthesis, Verification) in guiding undergraduate textile design students in developing digital textile pattern design variations.

EXPERIMENTAL

Materials and Methods

In this study, the methodology involved explaining the stages of Osborn's Seven-Stage Theory based on accessible literature, and conducting an experimental study with second-year undergraduate students enrolled in the Textile Composition course offered by the Textile Design Department. Information on Osborn's Seven-Stage Theory was presented to the students, who were then instructed to develop their designs in accordance with these stages. The theory was employed to help students understand how the creative process unfolds during textile pattern design and to ensure that the process—from idea formation

to product realization—could be systematically monitored, revised, and applied. Each of the model's seven stages was implemented separately, ultimately resulting in the production of textile pattern designs.

The study population comprised second-year undergraduate students enrolled in the Textile Composition course offered by the Textile Design Department at Ankara Hacı Bayram Veli University, while the sample consisted of seven participants randomly selected from two sections of the same course. To explore how the creative process is shaped through the stages of the creative process model and to evaluate the applicability of Osborn's Seven-Stage Theory in textile pattern design, a semi-structured interview form containing 25 questions was developed. The identities of the students interviewed were kept confidential, and they were referred to as "participants" in the study. In references supporting the analysis of data tables, participant citations were coded as "participant number." The interview form regarding the design process was administered to all seven participants, and, with their consent, the interviews were audio-recorded. The collected data were analyzed, tabulated, and then interpreted and explained in the section titled Applications of Pattern Design in Textiles. According to [20] semi-structured interviews lie between structured and unstructured interview types. In this method, the researcher follows a general framework but may adapt questions according to the characteristics of the interviewees, thus exploring various dimensions of the subject matter. In other words, semi-structured interviews offer a more flexible approach compared to structured interviews. The researcher prepares a form containing planned questions in advance, but during the interview, they may pose additional or alternative questions to influence the course of the conversation and encourage participants to elaborate on their responses in greater detail [21, 22].

OSBORN MODEL

Alex Osborn's creative process model, which grants equal status to analysis and imagination, consists of seven stages [17]. Also known as the Seven-Stage Theory, the phases of this creative process model can be described as follows:

1. Orientation (Identifying the Problem): While significant ideas can sometimes emerge spontaneously and unexpectedly, this does not occur consistently without conscious effort. However, creative effort increases productivity and enables the generation of more ideas. Throughout the entire process, it is essential to maintain focus on the primary objective. Starting from the notion that "a well-defined problem is half solved," a clearly framed problem serves as a key component in approaching the solution. Therefore, identifying the research problem and the fundamental goals and objectives to be achieved is critically important in this stage.

2. Preparation (Gathering Relevant Data): In the second stage of the creative process—preparation—both existing knowledge stored in memory and newly collected data related to the creative problem are needed. When the data obtained through effort and experience are internalized, they can lead to insights into potential solutions. Even if the mind is initially overwhelmed with an abundance of ideas, a sudden spark may reveal a creative solution that is potentially the best among them.

3. Analysis (Breaking Down the Relevant Material): Analysis functions as a component throughout the orientation, preparation, synthesis, and verification stages. It particularly helps in better defining objectives during the orientation phase and supports more effective guidance during preparation. This stage entails evaluating a problem from multiple perspectives using critical thinking and fostering creative thinking. By distinguishing between judgment-oriented elements and idea-generating elements, it enables a clearer assessment of the issue, thus allowing potential creative ideas to emerge.

4. Hypothesis (Accumulating Alternatives Through Ideas): Following the identification of objectives and the collection of data, the solution to a creative problem becomes closely linked to the diversity of hypotheses generated. Tentative development of alternative hypotheses can trigger new perspectives, increasing the likelihood of uncovering ideas related to problem-solving. Each new hypothesis can guide deeper

investigations and play a key role in reaching a solution. Creative thinking enhances this stage by enabling the connection between ideas, even those initially deemed impractical, to form new and innovative solutions. This holistic approach evaluates problem-solving not only through logic but also through creative, innovative, and open-minded thinking.

5. Incubation (Relaxing to Invite Illumination): The incubation stage, often referred to as the "surprise phase" of the creative process, denotes a period of spontaneous insight that arises without deliberate effort. This is the stage where brilliant ideas often surface unexpectedly. During this phase, the researcher does not actively focus on the problem; instead, the subconscious mind continues working in the background, often while engaging in routine activities or unrelated tasks. It marks the beginning of the emergence of solution ideas, although these are not yet fully formed or concrete.

6. Synthesis (Bringing the Parts Together): Most ideas result from combinations or refinements of other ideas. The synthesis stage, the most productive phase of the creative process, functions in contrast to the analysis stage. The more thoroughly a problem is analyzed from the beginning, the higher the likelihood of identifying and integrating the solution components. Synthesis relies on an inductive approach, combining several ideas within a logical framework under a general conceptual umbrella.

7. Verification (Judging the Emerging Ideas): The final stage is critical for any creative project. The verification process involves evaluating the outcomes, not only through personal judgment but also by seeking the opinions of others. This phase ensures the validation of not just the final results but also a review of previous stages, including goal alignment and hypothesis examination. Ultimately, testing the project outcomes represents the most definitive form of verification.

FINDINGS

Textile Pattern Design Applications

Among the participants, three (P1–P2–P3) developed pattern designs using the mind mapping method based on the theme "The Language of Sculpture/Modern Typography," while four participants (P4–P5–P6–P7) followed the theme "Met Gala," all applying the stages of Osborn's Seven-Stage Theory. The participants' pattern design processes were examined through a 25-question semi-structured interview form. The responses given by the participants were analyzed, presented in separate tables for each stage, and interpreted accordingly. Furthermore, these tables were supported with participant statements and explanations.

Orientation: Identifying the Problem

In the orientation stage, students were required to focus on a specific problem. As the design process evolves around the design problem, the problem must be defined clearly and explicitly at this stage. Through collaborative idea and suggestion sharing, the students identified a common design problem as follows: "To adopt a creative and innovative approach in textile pattern design, creating original printed fabric patterns based on a theme that are visually, aesthetically, and functionally meaningful, and transforming these patterns into a final product." The general and specific objectives related to this identified problem are outlined below.

General Objective: The general objective of the study is to integrate the stages of Osborn's Seven-Stage Theory into the creative process of textile pattern design and to prepare the pattern designs in line with these stages.

Specific Objectives:

1. How is a theme determined in textile pattern design?

2. How is the mind mapping method applied in theme-based printed textile fabric design?

3. How are visual, motif, color, material, and technique researches conducted to contribute to the pattern design process in line with the chosen theme?

4. How is the digital printing pattern design process carried out based on the theme?

5. How should the prepared pattern designs be evaluated in terms of aesthetics, functionality, and manufacturability, and how is the final design formed?

Table 1: Orientation phase

Question	K1, K2, K3 (Group 1)	K4, K5, K6, K7 (Group 2)
Sources used in theme research	Inspired by visuals from the documentary *Abstract: The Art of Design*, specifically the episode on *Paula Scher: Graphic Design*, detailed photographs, drawings, and graphic materials of Ancient Greek and Roman sculptures and columns were used. Additional resources included graphic books, studies on Greek and Phrygian alphabets, and artificial intelligence tools.	Visuals of Met Gala outfits from 2024 and earlier were examined via websites, social media, and online magazines. The visuals related to annually selected Met Gala themes were utilized for analysis.
Factors considered in theme selection and the importance of the theme	In textile pattern design, the aesthetic and structural features of Ancient Greek and Roman sculptures – such as depth, form effect, and the applicability of typography – were considered. Within the theme, the influence of sculpture on aesthetic perception, architectural inspirations, and the use of typography were emphasized, resulting in a design that reflected a modern-retro balance.	As a prestigious event where fashion and art merge under a unique concept each year, the Met Gala inspired designs based on iconic and striking styles worn by celebrities. The application of selected themes in outfits and patterns led to expressions that incorporated symbolic motifs reflecting the theme's essence.
Identified sub-themes and their rationale	In order to design subjective, detailed, and field-oriented patterns, typography was divided into sub-themes.	The main theme was not divided into sub-themes.

When examining the sources used in theme research during the orientation stage as presented in Table 1, it was found that participants in Group 1 (P1–P2–P3) were inspired by an art documentary focused on graphic design. They utilized artistic and historical resources such as Ancient Greek and Roman sculptures, drawings, graphic books, and artificial intelligence tools. In contrast, participants in Group 2 (P4–P5–P6–P7) drew inspiration from fashion influences—particularly the contemporary Met Gala event—and made use of digital platforms such as social media and online magazines to access event visuals. Accordingly, it can be stated that the participants in Group 1 adopted a more artistic and academic approach from a historical and traditional perspective, while those in Group 2 were more influenced by contemporary and popular culture, drawing inspiration from modern fashion trends.

Participant P1 stated, "We started out from a graphic design documentary. Since we felt a connection, we chose typography." Similarly, P2 commented, "After watching the documentary, some concepts became clearer in our minds. But that was a graphic designer, and we are textile designers. So we couldn't reflect it the same way. We focused more on the textile surface and used AI to preview such content." On the other hand, P4 remarked, "At that time (2024), the Met Gala visuals shared on social media caught our attention, and we were curious to see how the extravagant garments from the Met Gala would look as textile fabric patterns." When examining the factors considered during the theme selection process and the significance of the chosen themes, it was observed that participants from both groups first assessed the applicability of their selected themes to textile pattern design. In this context, Group 1 developed a theme that synthesized aesthetic and structural qualities by combining sculptural forms with typography, resulting in a blend of modern and retro influences. Group 2, on the other hand, created a theme based on the fusion of fashion and art, focusing on iconic red carpet looks of celebrities. Thus, it can be concluded that each group's theme selection was shaped by their own creative thinking and sources of inspiration. Participant P2 remarked, "We were fascinated by the idea of reflecting the spirit of female goddesses through sculptures and combining that with typography in an architectural context. Typography allowed us to reflect the modern aspect, while the sculptural elements brought in a retro feel that we didn't want to lose." Participant P4 stated, "The Met Gala is typically regarded as significant by fashion designers. While designers focus on the garment itself, as textile designers, we wanted to transfer the forms of Met Gala outfits and

elements like plants and flowers into our pattern designs."

When the identified sub-themes and their rationales were reviewed, it was found that Group 1 divided their main theme into sub-themes, whereas Group 2 developed their pattern designs based solely on the main theme, without further subdivision. The participants from Group 1 explained their reasons for subdividing the theme as follows:

P1 stated, "Since typography can be used in many fields, we needed to define which area of textile design we would focus on." P2 added, "We wanted to draw conclusions from our main headings to guide our design process." P3 noted, "We aimed to create more detailed and varied designs by structuring our work through sub-themes." In contrast, the Group 2 participants shared a common view that, since they explored Met Gala through different time periods, there was no need to develop detailed sub-themes.

Preparation: Gathering Relevant Data

Preparation is the stage where data related to the design problem is systematically collected. At this stage, students conduct comprehensive research using written and visual sources aimed at generating innovative, original, and creative printed fabric pattern design ideas. Deciding on a specific design theme to guide the formation of a creative and original design idea is a priority in this phase. Based on written and visual source reviews, Group 1 selected "The Language of Sculpture/Modern Typography" as their theme, while Group 2 developed their theme based on the idea of the "Met Gala".

Table 2: Preparation phase

Question	K1, K2, K3 (Group 1)	K4, K5, K6, K7 (Group 2)
Factors considered in motif, color, and color palette research	Within the theme, brown, cream, and their tones were chosen to emphasize sculpture, and warm colors were selected to create unity in typography.	In order to reflect the glamorous aspect of the Met Gala, colors used in costumes from past eras were combined with contemporary trend colors.
Contribution of the color palette to the theme	The use of brown, cream, and their tones to highlight sculpture added a nostalgic and mystical feeling, while the inclusion of warm colors reflected a modern spirit.	The selected patterns and colors provided iconic forms and integrity in the designs.
Order of visual-motif-color palette selections	Color Palette – Visual – Motif	Motif – Visual – Color Palette Visual – Color Palette – Motif

In the preparation stage, as seen in Table 2, when analyzing the factors considered in motif, color, and color palette research and the contributions of the selected colors to the theme, it was observed that Group 1 (P1–P2–P3) chose brown, cream, and their tones to emphasize the sculptural form and used warm tones to ensure visual unity with typography. Group 2 (P4–P5–P6–P7), on the other hand, selected colors that reflect the historical aspect of the Met Gala, combining past-era colors with current trend colors to achieve integrity; this color choice in Group 1's designs created a mystical and nostalgic atmosphere, while in Group 2's designs it contributed to visual coherence and striking impact. Accordingly, Group 1 favored a more traditional approach by selecting classic and natural tones, aiming to reinforce their theme through nostalgic color choices. Group 2, in contrast, aimed for a more vibrant and expressive aesthetic by incorporating modern color trends and emphasizing eye-catching and contemporary elements.

P1: "We used sculptural tone colors. I agree with P3." P3: "We mostly used brown and cream tones. I believe these colors, being associated with sculptures, gave that old mystical atmosphere." P2: "At first, we tried to integrate the colors individually in our designs. We focused on warm tones and added blue and its undertones. To maintain coherence in the theme, we determined a common color palette that would not disrupt the sculptural effect. The colors reflected both a nostalgic calmness and a modern spirit." P4–

P5–P6–P7: “We blended the patterns and colors on the garments, achieving striking forms and coherence in the designs,” they stated as a shared opinion.

When the order of Visual–Motif–Color Palette selections was examined, Group 1 participants listed them as “Color Palette–Visual–Motif,” while Group 2 participants listed them as “Motif–Visual–Color Palette” and “Visual–Color Palette–Motif.” Accordingly, it can be said that Group 1 first determined the color palette to establish a theme-appropriate framework and then drew inspiration from visuals and motifs; whereas Group 2 determined the colors starting from either the motif or the visual.

The participants expressed their sequences as follows: P1–P2–P3: “Color Palette–Visual–Motif”; P4 and P5: “Motif–Visual–Color Palette”; P6 and P7: “Visual–Color Palette–Motif.”

Analysis: Breaking Down the Relevant Material

Mind Mapping is a powerful graphical technique associated with imagination, consensus, flexibility, and other cognitive skills that encourages creative thinking, explores all creative possibilities related to a specific theme/topic, and helps generate ideas that unlock the brain’s potential. The main topic is gathered in a central image. Main themes related to the topic radiate outward from the central image in branches and are interconnected. These branches consist of keywords or key visuals, graphics, or drawings appropriate to the main and sub-themes. The structure of the branches is characterized as an interconnected node system [23].

In the formation and development of the design idea, the mind mapping method was used in this research as a supportive tool for:

a) Analyzing the main design idea in more detail by dividing it into sub-themes,

b) Associating the main theme/topic with its related sub-theme branches,

c) Evaluating the main theme/topic from a broader perspective.

In the mind map created by Group 1, the main theme “The Language of Sculpture/Modern Typography” is divided into various sub-themes including pattern, sculpture, graffiti, pop art, typefaces, and color palettes. The sub-themes are supported by keywords and key visuals (see Figure 1).

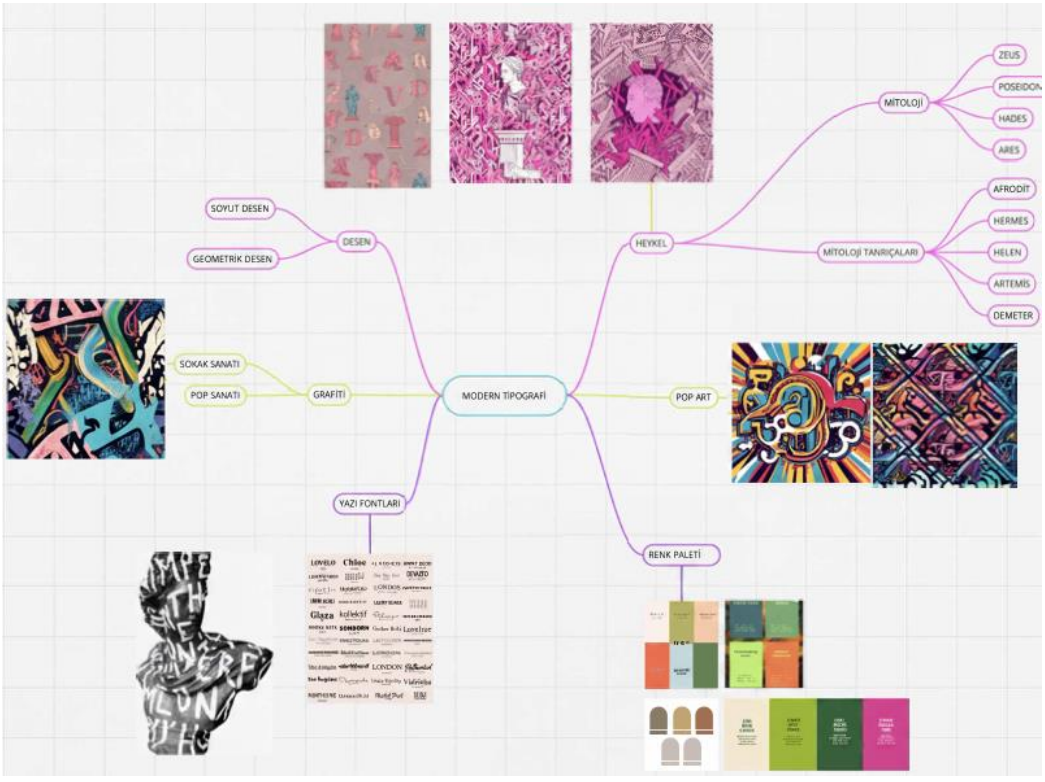


Figure 1. The language of sculpture/modern typography mind map

In the Group 2 mind map, after determining the main theme "Met Gala," [24] key visuals and color palettes related to appropriate sub-themes were included (see Figure 2).

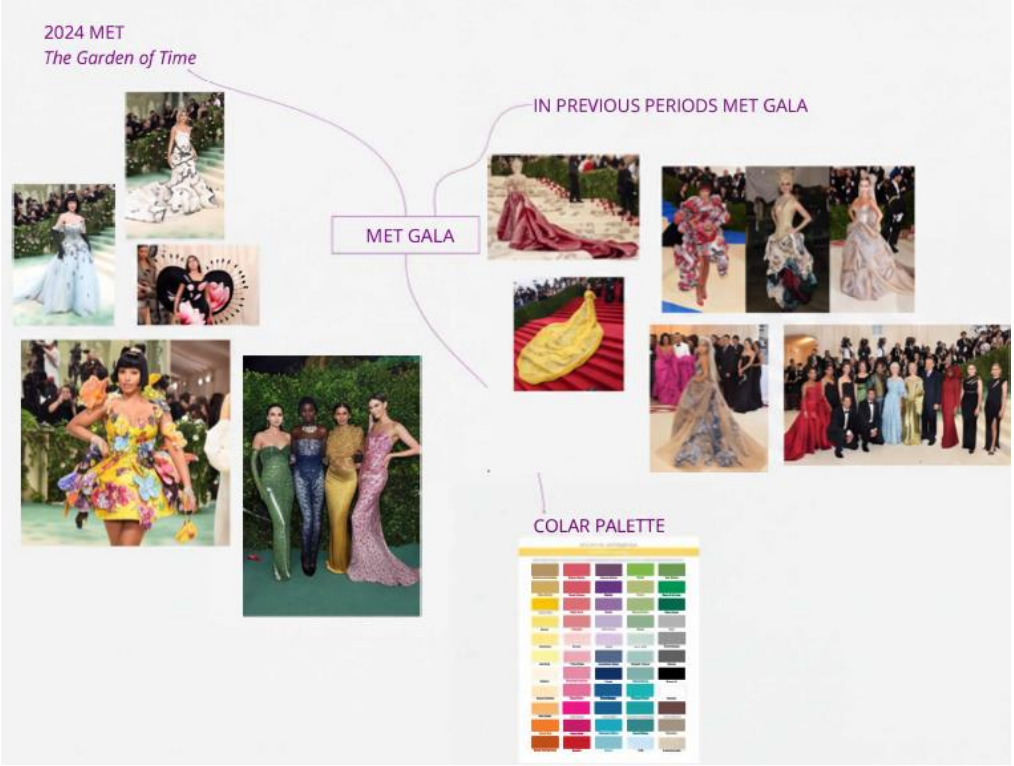


Figure 2. The Met Gala mind map

When examining the mind map created with main and sub-theme topics in Table 3 related to the analysis stage, it was observed that Group 1 (P1–P2–P3) shaped their main themes around the titles of modern typography, mythology, and goddesses, and in order to express the applications of these themes in textile pattern design, they divided them into sub-theme components such as sculpture, typefaces, color palette, and pop-art. Group 2 (P4–P5–P6–P7), on the other hand, did not divide their main theme Met Gala into sub-themes but drew inspiration from visual references of garments spanning the years 2016–2024. Regarding this topic, participants stated the following during the interviews:

Table 3: Analysis phase

Question	K1, K2, K3 (Group 1)	K4, K5, K6, K7 (Group 2)
Mind map created with main theme and sub-theme topics	The subheadings Modern Typography – Sculpture – Mythology / Mythological Goddesses were identified. In order to determine the areas of use of modern typography in textile pattern design, the main theme and sub-themes were defined as pattern, sculpture, typefaces, color palette, graffiti, and pop art. The defined sub-themes were categorized internally (See Figure 1).	Met Gala and time periods were determined. In order to identify the areas of use for textile pattern design, Met Gala outfits from 2016 to 2024 were examined [24] (See Figure 2).
Relationship between themes and pattern designs	Typography was generally used as the background, while sculpture was used in motifs. To preserve historical coherence, the alphabet of the period when the sculpture was created was preferred, ensuring integrity between typography and sculpture.	Based on the 2024 Met Gala theme, coherence was ensured by selecting suitable time periods and iconic styles from previous Met Gala designs.

Question	K1, K2, K3 (Group 1)	K4, K5, K6, K7 (Group 2)
Determining the type of repeat (rapport)	A repeat style was chosen that matched the pattern and ensured visual unity without losing rhythm or flow.	A unit repeat was used to achieve visual unity according to rapport rules, with particular attention paid to the harmony between the design and the surface shape of the fabric.

P1: "We identified modern typography as our main theme. Then we thought about what we could do with typography and in which fields. To reflect our theme more effectively in textile pattern design, we divided it into six subheadings: pattern (abstract and geometric), sculpture (mythology and mythological goddesses), color palette, and typefaces" (see Figure 3).



Figure 3. The language of sculpture / modern typography theme (P1)

P2: "To reflect modern influences in our designs, we wanted to use the colors of the pop-art movement adopted by a graphic artist and researched how we could apply these colors in our textile pattern designs." P4: "Our main theme was the theme defined for the 2024 Met Gala. As a sub-theme, we considered the earlier periods of Met Gala. For example, in some of my designs, I combined the 2024 theme with elements from the 2016–2020 period." P5: "At the end of creating our mind map, we were able to progress from parts to whole." P7: "We divided our main theme into time periods and then continued our work."

When the relationship between themes and pattern designs was analyzed, it was found that Group 1 (P1–P2–P3) created visual integrity between typography and sculpture by using the alphabet and writing styles of the historical period to which the sculpture belonged. Group 2 (P4–P5–P6–P7), meanwhile, ensured visual coherence by incorporating garment visuals, colors, and motifs from the 2024 Met Gala and earlier periods. Accordingly, it can be said that Group 1 achieved thematic and design coherence through typography and artistic elements, while Group 2 achieved this coherence by comparing past and contemporary understandings of fashion.

Participants' views in the interview form on this topic were as follows:

P1: “I used the contours and hair of the sculptural forms in my designs to create typographic elements. This way, I combined sculpture and typography.” P2: “The backgrounds prepared with typography were merged with sculpture motifs to create connections. For example, when using a Greek sculpture, we used the Greek alphabet.” P3: “On the lines of the sculpture columns, I wrote the materials used in textiles with different alphabets to create background cohesion. For instance, when highlighting the Aphrodite sculpture, I narrated her story in the background using typography.” P4–P5–P6–P7: “Since our main and sub-themes were all related to Met Gala, we did not combine independent topics. We incorporated forms from past outfits suitable for 2024 and ensured coherence in our pattern designs,” they stated as a shared opinion.

When analyzing the determination of the repeat type, it was found that Group 1 (P1–P2–P3) applied a structured and visually attentive approach that followed repeat rules and paid attention to the rhythm of the pattern. Group 2 (P4–P5–P6–P7) also followed repeat rules and paid attention to visual coherence. Accordingly, it can be said that both groups selected their repeat types in alignment with the fabric appearance appropriate to their theme-based designs.

On this topic, the participants stated: P1: “We determined it based on achieving a fabric-like appearance in our pattern designs.” P3: “We paid attention to ensuring pattern integrity, rhythm continuity, and avoiding loss of design elements.” P5: “We considered the unit size to be used in the pattern and how it would look on fabric.” P4–P6–P7: “First, we created a unit repeat and then analyzed which repeat type would yield better results before making our decision.”

Hypothesis: Accumulating Alternatives Through Ideas

According to the mind mapping method, Group 1 divided their main theme, “The Language of Sculpture – Modern Typography,” into five distinct sub-themes: Pattern – Sculpture – Graffiti – Pop Art – Typefaces, and linked these sub-themes to each other through branches using key visuals and keywords. Group 2, on the other hand, created their mind map in line with the main theme “Met Gala” by using key visuals (outfit visuals from various years of the Gala). However, it should be noted that this group did not elaborate on their main theme through sub-themes and relied solely on visual materials.

Within the scope of the design problem – to create original printed fabric designs based on the theme with a creative and innovative approach in textile pattern design and to transform these designs into final products in terms of visual, aesthetic, and functional aspects – the following alternative hypotheses have been formulated:

1. The student will be able to design more diverse and creative pattern variations (color, texture, motif, composition, etc.) by determining the main and sub-themes through the mind mapping method.

2. Through the process of identifying main and sub-themes, the student will be able to enhance their creative thinking skills by being inspired by keywords and visuals or by abstracting them, and will be able to generate more innovative and original ideas in the digital textile pattern design process.

3. The student will be able to produce a greater number and variety of patterns (color, motif, composition) based on the target pattern determined through the mind mapping method.

4. The student will be able to design original and innovative textile patterns through a design process that includes main and sub-themes evaluated by expert assessment.

5. The student will be able to transfer creative pattern design ideas in accordance with the elements of textile pattern design, composition rules, and digital design principles.

Based on the alternative hypotheses above, the study’s general hypothesis is formulated as follows: “The student will be able to enhance their creative thinking skills by identifying main and sub-themes through the mind mapping method and will be able to design original and innovative patterns based on expert evaluation and analysis.”

Table 4: Thought formation phase

Question	K1, K2, K3 (Group 1)	K4, K5, K6, K7 (Group 2)
Pattern proposal development	Pattern units for each repeat type were drawn and evaluated at the sketch stage using the Illustrator program.	Clothing visuals from the years 2016–2024 were examined, and pattern units for each repeat type were drawn and evaluated at the sketch stage using the Illustrator program.
Elements considered in pattern proposals	Among design principles, particular attention was given to balance, unity, contrast, and proportion, as well as balanced use of background and motif colors.	Among design principles, attention was paid especially to balance and unity; harmony between design elements; color selection; and contrast between light and dark tones, as well as appropriate use of the same colors and tones.

In Table 4, which pertains to the idea generation stage, the development of pattern proposals was examined. It was found that participants from both groups drew their patterns in the Illustrator program and evaluated them at the sketch stage for each type of repeat (rapport). Accordingly, it can be stated that the participants created units from the motifs/visuals they intended to use in their pattern designs in accordance with their theme, drew them in Illustrator, and tested these drawings across various repeat types within the program.

From the interview form, participants from Group 1 (P1–P2–P3) stated a shared opinion: “We drew our units in Illustrator and placed them for each type of rapport and then decided accordingly. For example, if we needed to use a sculpture silhouette unit, we tested it in diagonal and repeated rapport types. Afterwards, we chose to use the unit in diagonal and repeated rapports because we couldn’t use it in block rapport. For block rapport, we mostly referred to architectural patterns.”

Participants from Group 2 (P4–P5–P6–P7) also expressed a shared opinion: “We analyzed different gala periods to identify usable units, then drew the units in Illustrator and placed them in each type of rapport and decided accordingly.”

When examining the elements considered in the pattern proposals, it was observed that participants from both groups focused on design principles such as balance, unity, and contrast. While Group 1 paid particular attention to the balance between background, motif, and color, Group 2 focused on the contrast between light and dark tones. Accordingly, it can be said that Group 1 (P1–P2–P3) approached the process from a broader perspective, concentrating on design principles and the integration of motifs with the background, whereas Group 2 (P4–P5–P6–P7) adopted a more specific method, focusing particularly on color contrast and tonal transitions. The designs created by the students on this topic are included in the synthesis stage.

During the interviews P2 stated: “We paid attention to rhythm, emphasis, and balance principles from the design rules. We wanted to reflect the sculptures without distorting their overall structure, and for that, we used their original colors. In typography, we used slightly more vivid colors in order to preserve the typeface and complement the sculptures.” P4 stated: “We focused on rules such as proportion and balance from the design principles, as well as on color usage. For example, we prepared some of our pattern designs in tone-on-tone and with contrasting colors. This gave the patterns more dimension and made them visually striking.” P5 stated: “We particularly paid attention to maintaining unity in our pattern designs.”

Incubation: Relaxing to Invite Illumination

This stage can be described as the moment when no new ideas can be produced and designers begin to engage with different topics – essentially, distancing themselves from the problem. It is a phase where designers may feel the need to withdraw or take a break from the process.

Table 5: Incubation phase

Question	K1, K2, K3 (Group 1)	K4, K5, K6, K7 (Group 2)
Approach followed when ideas could not be generated	The participants distanced themselves from the pattern production process, engaged with different topics, and re-analyzed the documentary previously watched during the theme research.	The participants distanced themselves from the pattern production process and engaged with different topics.

When examining the approach followed when ideas could not be generated in Table 5 – Incubation Stage, it was found that Group 1 (P1–P2–P3) distanced themselves from the pattern creation process, engaged with different topics, and re-analyzed the documentary they had watched during the theme research. Group 2 (P4–P5–P6–P7) participants, on the other hand, were observed to have also engaged with different topics. Accordingly, it can be stated that within the context of creativity in the pattern development process, the incubation stage varies among participants and is a subjective experience. Regarding the approaches followed when ideas could not be generated, the participants stated:

P1: "I engaged with different topics." P2 and P3: "I rewatched and analyzed the documentary." P4: "I examined different time periods to generate ideas." P5: "I engaged with different topics and continued after taking a break." P6: "I agree with P7. I also engaged with other things." P7: "I designed patterns while listening to music."

Synthesis: Bringing the Pieces Together

At this stage, in line with the main and sub-themes specified in the mind mapping method, elements such as motif, color, and composition were combined to complete the pattern designs. The participants explained their designs accordingly. The explained pattern designs are presented in the following tables.

Table 6: Synthesis phase

Question	K1, K2, K3 (Group 1)	K4, K5, K6, K7 (Group 2)
Changes made in the patterns and their effects	Changes such as color palette adjustments and the use of typography on the outer contours of the sculpture were made to ensure unity and balance within the patterns.	Changes such as alterations in the color palette, background, and dimensional differences in motifs were made, and the resulting patterns were completed aesthetically with an added sense of depth.
Strengths and weaknesses of the designs in terms of aesthetics	As a weakness, some designs did not adequately reflect design principles; as a strength, the unity achieved between patterns and their complementary relationships were emphasized.	As a weakness, visual complexity and confusion caused by background effects and varying motif dimensions were noted; as a strength, successful use of different color combinations was highlighted.
Potential applications of the patterns in terms of functionality (e.g., home textiles, scarves, fabrics)	The patterns were mostly prepared for scarves, shawls, and home textiles, with intended use areas clearly defined.	The designs were mostly prepared for scarf and home textile use. Additionally, some patterns were evaluated as suitable for apparel design due to their aesthetic appeal.

When examining the changes made in the patterns and their effects in Table 6 – Synthesis Stage, it was observed that Group 1 (P1–P2–P3) generally made changes to the color palette, outer contours of sculptural forms, and typography usage in an effort to ensure unity and balance in their designs; whereas Group 2 (P4–P5–P6–P7) attempted to add depth to their designs through the effect of dimension, by making changes to the color palette, background, and motif sizes. Accordingly, while both groups made adjustments in their color palettes, it can be said that Group 1 focused on changes in typography and sculptural contours to achieve design unity, and Group 2 made changes to backgrounds and motif sizes. Participants expressed these changes as follows:

P2: “I was inspired by the color palette and sculptures and wrote the letters like columns. I ensured design unity by paying attention to the balance between filled and empty spaces” (see Figure 4).



Figure 4. The language of sculpture / modern typography theme (P2)

P3: “I separated the upper part of the sculpture from the color palette and created unity by connecting it with typography and the background” (see Figure 5).

P4: “I made changes to the colors. In some patterns, I added texture effects to the background to establish the background-motif interaction. This way, I ensured unity” (see Figure 6).



Figure 5. The language of sculpture / modern typography theme (P3)



Figure 6. The language of sculpture / modern typography theme (P4)

P5: “I made changes in the colors. The changes we made completed our designs aesthetically” (see Figure 7).

P6: “I changed the sizes. With color changes, I created a sense of dimension and depth in the motifs. The changes I made to the background color altered the appearance of the motifs” (see Figure 8).



Figure 7. The language of sculpture / modern typography theme (P5)

P7: “I made changes in the colors to adapt to the present day, stay true to the theme, and reflect my originality. I ensured unity through background effects” (see Figure 9).



Figure 8. The language of sculpture / modern typography theme (P6)



Figure 9. The language of sculpture / modern typography theme (P7)

When examining the strengths and weaknesses of the pattern designs in terms of aesthetics, it was found that the common weakness among participants in both groups was a lack of adherence to design principles in some of their patterns. As for the strengths, Group 1 (P1–P2–P3) designed their patterns in a way that complemented one another, while Group 2 (P4–P5–P6–P7) achieved visual depth in their patterns through effective use of color. Accordingly, while both groups shared a common weakness in terms of design principle implementation, the strength of Group 1 was the internal coherence among their patterns, whereas Group 2 demonstrated strength in combining different colors harmoniously to create visually cohesive designs. Participants expressed the strengths and weaknesses of their patterns as follows: P1: "As a weakness, I had a pattern that felt monotonous. As a strength, my patterns created unity with one another." P2: "As a weakness, I had a pattern where I couldn't establish a proper balance between filled and empty space. As a strength, I would say my patterns complemented each other." P3: "As a weakness, the use of letters created very fine lines. As a strength, my designs achieved overall unity." P4: "As a weakness, the patterns I selected were more suited for block rapport. As a strength, I used botanical units and different colors together." P5: "As a weakness, I couldn't maintain scale consistency in some of my patterns. As a strength, I can highlight the color harmony I achieved." P6: "As a weakness, some of the colors I used were not in harmony. As a strength, I would say I used different dimensions and harmonious color combinations across my designs." P7: "As a weakness, my intention to create background effects caused some patterns to appear visually complex. As a strength, I would say that I managed to establish harmony despite the complexity through the color combinations I used." When examining the potential applications of the pattern designs in terms of functionality, it was observed that participants from both groups generally designed their patterns for scarves, shawls, and home textiles; as an alternative, some participants from Group 2 (P4–P5–P6–P7) also designed certain patterns to be used as wallpapers. Accordingly, it can be stated that both groups generally identified common areas of functionality for their pattern designs. P1 and P2: "I designed my patterns to be suitable for use in scarves and shawls." P3: "I designed my patterns to be suitable for scarves, shawls, and home textiles (e.g., cushion covers)." P4 and P5: "I designed my patterns to be suitable for scarves and home textiles (e.g., cushions, bedspreads)." P6: "I designed my patterns to be suitable for scarves and home textiles. I believe some of my patterns could also be used as wallpaper." P7: "I designed my patterns to be suitable for scarves and home textiles. Some of my patterns could also be used as fabric."

Verification: Judging the Ideas that Emerged

At this stage, initial feedback on the patterns was provided by the course instructor. Final adjustments were made prior to the committee evaluation. Subsequently, a committee composed of faculty members from the Textile Design Department was formed, and the ideas emerging from the students' pattern designs were evaluated by the committee.

Table 7: Verification phase

Question	K1, K2, K3 (Group 1)	K4, K5, K6, K7 (Group 2)
Production technique and related adjustments	The motifs planned for use in the patterns were evaluated in terms of which printing technique would yield better results, and the appropriate technique was selected. The color mode was adjusted to suit the chosen printing technique.	The motifs planned for use in the patterns were evaluated in terms of which printing technique would yield better results, and the appropriate technique was selected. The color mode was adjusted to suit the chosen printing technique.
Key points in the design process	Choosing a color palette appropriate to the theme and blending nostalgic elements with modernity.	Using historical references from various periods in fashion and incorporating them into textile design.

Question	K1, K2, K3 (Group 1)	K4, K5, K6, K7 (Group 2)
Evaluation of the pattern designs	Throughout the pattern design process, revisions were made under the supervision of the design advisor; fabric type was selected, and the final pattern designs were evaluated by printing samples.	Throughout the pattern design process, revisions were made under the supervision of the design advisor; fabric type was selected, and the final pattern designs were evaluated by printing samples.

In Table 7, which pertains to the verification stage, an examination of the production technique and the corresponding changes revealed that both groups worked in accordance with the digital printing technique and made color mode adjustments to ensure better visual outcomes after printing. Accordingly, it can be said that the pattern designs of both groups were printed using the digital printing technique, following appropriate color mode modifications.

Participants from Group 1 (P1–P2–P3) and Group 2 (P4–P5–P6–P7) expressed the production technique and the related changes as follows: “We prepared our designs according to the digital printing technique and made color mode adjustments in the patterns to be produced.”

When examining the key points of the design process, it was observed that for Group 1, the focus was on combining nostalgic elements with modernity through a color palette compatible with the theme; while Group 2 emphasized the use of forms from various fields in pattern design. Accordingly, it can be said that Group 1 focused on the balance of color and nostalgia-modernity, whereas Group 2 concentrated on incorporating forms from different application areas. P2 stated: “We focused on combining nostalgic elements with modernity through the color palette.” P7 stated: “We focused on adapting motifs and forms used in past clothing designs to today's context by using them in different areas such as scarves and home textiles.” Regarding the evaluation of pattern designs, it was determined that both groups revised their patterns under the supervision of their course advisors and finalized their pattern designs accordingly. Therefore, it can be concluded that both groups followed a similar path during the evaluation process. Participants from Group 1 (P1–P2–P3) and Group 2 (P4–P5–P6–P7) stated: “When creating our patterns in accordance with our theme, we exchanged ideas with our advisor and received approval at each stage. We made revisions by paying attention to the appropriateness and rules of rapport types.” In addition, the final pattern designs printed on fabric using the selected printing technique by Group 1 (P1–P2–P3) and Group 2 (P4–P5–P6–P7) were presented and evaluated during the committee exam by the faculty members of the Department of Textile Design at the Faculty of Art and Design, Ankara Hacı Bayram Veli University. The final pattern designs were evaluated according to a specified assessment scale in the committee exam (see Table 8).

Table 8: Evaluation scale

		5 DIAGONAL (STYLE) REPEAT PATTERN DESIGNS (25 POINTS)			5 BLOCK REPEAT PATTERN DESIGNS (25 POINTS)		
GROUP INFORMATION		Relevance to Theme (5 pts)	Compliance with Composition Principles (10 pts)	Originality, Innovation, and Compliance with Design Principles (10 pts)	Relevance to Theme (5 pts)	Compliance with Composition Principles (10 pts)	Originality, Innovation, and Compliance with Design Principles (10 pts)
1 GROUP 1	P1	5	5	10	5	10	10
		5	10	10	5	10	10
		5	8	8	5	8	8
		Avg. 5	8	9	5	9	9

GROUP INFORMATION		5 DIAGONAL (STYLE) REPEAT PATTERN DESIGNS (25 POINTS)			5 BLOCK REPEAT PATTERN DESIGNS (25 POINTS)		
		Relevance to Theme (5 pts)	Compliance with Composition Principles (10 pts)	Originality, Innovation, and Compliance with Design Principles (10 pts)	Relevance to Theme (5 pts)	Compliance with Composition Principles (10 pts)	Originality, Innovation, and Compliance with Design Principles (10 pts)
GROUP 2	P2	5	10	10	5	10	10
		5	10	10	5	10	10
		5	7	7	5	6	5
		Avg. 5	9	9	5	9	8
	P3	5	5	8	5	5	8
		5	10	9	5	10	8
		5	8	8	5	7	7
		Avg. 5	8	8	5	7	8
	P4	5	10	10	5	10	10
		5	10	10	5	10	10
		5	8	8	5	8	8
		Avg. 5	9	9	5	9	9
	P5	5	8	10	5	6	10
		5	10	10	5	10	10
		5	7	10	5	6	10
		Avg. 5	8	10	5	7	10
	P6	5	10	10	5	6	10
		5	10	10	5	10	10
		5	9	10	5	9	10
		Avg. 5	10	10	5	8	10
	P7	5	8	10	5	8	10
		5	10	10	5	10	10
		5	10	10	5	10	10
		Avg. 5	9	10	5	9	10

Upon examining the evaluation scale table prepared in accordance with the five alternative hypotheses determined during the fourth stage (Hypothesis – Generating Alternatives Through Ideas) of Osborn's 7-Stage Model (see Table 8), the following conclusions can be drawn:

For the hypothesis "The student will be able to design more diverse and creative pattern variations by determining the main and sub-themes through the mind mapping method", it was observed that the students were able to produce various designs using different colors, motifs, and compositions, For the hypothesis "The student will be able to develop creative thinking skills and generate more innovative and original ideas in the digital textile pattern design process by being influenced by keywords and visuals or through abstraction in the process of determining the main and sub-themes", the originality and innovativeness of the students' designs indicated that their creative thinking and original design skills had improved accordingly. For the hypothesis "The student will be able to create a greater number and variety (in terms of color, motif, composition) of designs based on the pattern goal determined through the mind mapping method", it was found that each participant increased diversity by designing five diagonal and five block repeat pattern designs. For the hypothesis "The student will be able to design original and innovative textile patterns based

on a design process involving main and sub-themes evaluated by experts", expert evaluations confirmed that this hypothesis was realized. For the hypothesis "The student will be able to convey creative pattern design ideas in accordance with textile pattern design elements, composition rules, and digital design principles", the fact that the scores under the heading "compliance with composition principles" in the table were 8 and above indicates that participants paid attention to digital design principles.

As a result, the data presented in the table supports the general hypothesis: "The student will be able to enhance creative thinking skills by determining main and sub-themes using the mind mapping method and will be able to design original and innovative patterns based on expert evaluation analyses." The participants enhanced their creative thinking skills by determining main and sub-themes through the mind mapping method in line with the stages of Osborn's 7-Stage Model, and they designed original and innovative patterns based on expert evaluations.

RESULTS AND DISCUSSIONS

The findings of this study demonstrate that the integration of Osborn's 7-Stage Model into the textile design process provides a structured and systematic approach to supporting creativity during the stages of idea development, conceptualization, and concretization. The students' development of original design approaches based on different sources of inspiration, along with the gradual use of methods such as mind mapping, research, concept development, and digital pattern creation, reveals that the model has an adaptable and flexible structure that enables the emergence of creative idea alternatives. Furthermore, the individual thoughts and differences emerging during the Incubation stage are directly associated with the student's/designer's individual experiences, aesthetic preferences, perception, and interpretation styles, which influence the resulting design outcomes.

The involvement of expert opinions during the verification stage enabled the developed designs to be evaluated not only in terms of aesthetics but also regarding applicability, producibility, and functionality through professional feedback. This process enabled the systematic evaluation of whether the original, creative, and innovative design process had been implemented in a coherent and acceptable manner. These findings support the view that the creative process has a non-linear structure influenced by individual differences, while also demonstrating that the creative process in textile design can be addressed through a systematic approach. In this context, the studies by Arslan [16], titled "*Creative Process in Textile Pattern Design: Wallas' Four-Stage Model*," and Arslan and Çepni [27], titled "*Creative Textile Design: A Wallas Model-Based Approach*," have shown the applicability of creative process models by systematically addressing creative ideas within the textile design process.

The application of Osborn's 7-Stage Model in this study was limited to a relatively small sample of second-year undergraduate students enrolled in the Textile Composition course offered by the Department of Textile Design, which constitutes an important limitation of the research. Since the creative design outcomes were obtained from a specific course context, educational setting, and participant group, the findings cannot be directly generalized to textile design students at different academic levels. This limitation is attributable to potential differences in students' prior knowledge, design competencies, creative thinking skills, and readiness levels, which may influence both the design process and the quality of the resulting creative outcomes. Furthermore, the educational environment differs substantially from professional design practice. Unlike industrial design processes, educational projects are generally conducted without commercial constraints such as client requirements, production costs, delivery schedules, and market competitiveness. Therefore, the applicability and effectiveness of the model observed in this study may not fully reflect its performance in professional textile and fashion design settings. Similarly, in the creative design ideas generated by professional design teams in the textile and fashion industry through this approach, factors such as customer needs, demands, expectations,

product delivery schedules, and commercial requirements should be taken into consideration. It should not be overlooked that creative ideas may be shaped according to the extent to which the model responds to sectoral expectations and requirements. Particularly when considering the originality and innovativeness of design ideas developed in educational contexts alongside their ability to meet sectoral expectations, it should be acknowledged that creativity and originality may be subject to certain limitations.

Future research should evaluate Osborn's 7-Stage Model with larger groups of student participants in academic contexts, as well as with designers at different levels of professional experience and professional design teams within the textile and fashion industry. Furthermore, applying the model to different design disciplines may contribute to the analysis of creative outputs based on measurable criteria such as originality, applicability, aesthetic value, and functionality. Thus, the generalizability of the model, its capacity to support creativity in structured design processes, and its limitations in practice can be demonstrated through more comprehensive data. In addition, comparative studies involving different educational institutions, larger sample sizes, and cross-cultural contexts would provide stronger evidence regarding the robustness and generalizability of the proposed approach.

In conclusion, this study demonstrates that Osborn's 7-Stage Model contributes to students' ability to manage their creative processes in a planned manner, develop alternative solutions to design problems, and produce original and innovative pattern designs. It also contributes to the literature by demonstrating the applicability of creative process models in textile design. In this context, the model can be considered an applicable and effective approach in the textile pattern design process. Furthermore, the study is significant in terms of promoting the wider use of creative thinking models in textile design education, where originality and innovation are becoming increasingly important, and encouraging further investigation of their applicability across different design disciplines.

CONCLUSIONS

In the first and crucial stage of the creative process – Orientation – participants conducted comprehensive research to define their design problems and, based on their findings, determined the themes upon which they would develop their pattern designs. During the Preparation stage, participants collected data such as colors, motifs, and visuals that would support their idea generation processes related to their chosen themes.

In the Analysis stage, participants used the mind mapping method to break down their main themes into sub-themes. At this stage, the two groups followed different paths: Group 1 divided their design process into more detailed sub-themes using the mind mapping method, whereas Group 2 did not break down their main theme into detailed sub-themes but instead adopted a direct approach aligned with their central theme. In the Hypothesis stage, participants identified alternative hypotheses in line with the main problem and transformed these into a single general hypothesis statement, from which they developed various pattern design proposals. The Incubation stage – characterized by the need for rest or a break in the pattern design process – varied depending on individual differences. While some participants chose to take a break from pattern production, others continued to work throughout the process. During the Synthesis stage, participants reviewed the pattern designs they had developed up to that point within the scope of their themes, refining elements such as color, motif, and repeat to form cohesive final designs. In the Verification stage, participants made final revisions in accordance with the selected production technique and produced their final designs using the digital printing method. The completed designs were then evaluated by a committee consisting of faculty members from the Textile Design Department. In conclusion, this study demonstrates how Osborn's 7-Stage Model can be integrated into the textile pattern design process. While Group 1 (The Language of Sculpture/Modern Typography) developed their designs with a historical and artistic approach by focusing on typographic and sculptural forms, Group 2 (Met Gala) adopted a perspective rooted in popular

culture and fashion. Both groups systematically carried out their design processes by supporting the stages of the 7-Stage Model with methods such as mind mapping, repeat pattern analysis, and digital pattern development techniques.

Through the refinements made in the Synthesis and Verification stages, the designs were improved in terms of aesthetics, functionality, and producibility, resulting in final patterns suitable for digital printing. In this context, Osborn's 7-Stage Model was successfully integrated into the textile pattern design process and contributed to generating original and innovative results in pattern design by enhancing idea generation at every stage of the creative process.

Acknowledgements

We sincerely thank the undergraduate students Buket Hatice Kabaçalı (P1), Rümeysa Demir (P2), Sueda Kılıç (P3), Sıla Fatma Türkmen (P4), Rümeysa Okyay (P5), Elif Yaren Bilgin (P6), Aybüke Coşkun (P7) for their valuable support and contributions to this study.

REFERENCES

1. Yeşilyurt, E., Creativity and Creative Thinking: A Comprehensive Review Study with All Dimension and Stakeholders (in Turkish), *OPUS Int J Soc Res*, **2020**, 15, 25, 3874-3915, https://doi.org/10.26466/opus.662721.
2. Kurtuldu, E., Önlü, N., Creativity, Creative Thinking, Future and Foresight in Design (in Turkish), In: *Proceedings of the II International Symposium on Art and Research*, Çukurova University, **2018**, 105-112.
3. Johansson, F., *The Medici Effect: Breakthrough Insights at the Intersection of Ideas, Concepts, and Cultures* (in Turkish), translated by D. Tayanç, 2nd ed., MediaCat, İstanbul, **2013**, 16-17.
4. May, R., *The Courage to Create* (in Turkish), translated by A. Oysal, Metis Publications, İstanbul, **2013**, 83-96.
5. Aslan, A.E., Creativity in the Conceptual Dimension (in Turkish), *Turk Psychol Couns Guid J*, **2001**, 2, 16, 15-21, https://doi.org/10.17066/pdrd.72200.
6. Kahraman, Z., Determining the Creative Personality Characteristics of Textile and Fashion Design Department Students: The Case of Cankiri Karatekin University (in Turkish), *Journal of Ankara University Faculty of Fine Arts,* **2023**, 5, 2, 394-419, https://doi.org/10.58608/augsfd.1201522.
7. Batı, U., *Making Perfect Decisions and the Art of Persuasion: Using the Brain Effectively* (in Turkish), 4th ed., Dogan Book, İstanbul, **2020**, 143.
8. Craft, A., Creative Thinking in The Early Years of Education, *Early Years: An International Journal of Research and Development*, **2003**, 23, 2, 143-154, https://doi.org/10.1080/09575140303105.
9. Torrance, E.P., Goff, K., A Quiet Revolution, *J Creat Behav*, **1989**, 23, 2, 136-145, https://doi.org/10.1002/j.2162-6057.1989.tb00683.x.
10. Öncü, T., A Comparison of the Creativity Levels of 12–14-Year-Old Children by Age and Gender Using the Torrance Tests of Creative Thinking–Figural Test (in Turkish), *Journal of Ankara University Faculty of Languages, History and Geography,* **2003**, 43, 1, 221-237.
11. Arkan Sezgin, K., Baysal, Z.N., Examining the Effects of Thinking Skills Program Developed for the Primary School 3rd-Grade Students on Their Creativity Levels (in Turkish), *Hayef J Educ*, **2019**, 16, 1, 19-47, https://doi.org/10.26650/hayef.2019.19008.
12. Önlü, N., Creativity and Functionality in Design: Its Place in Textile Design (in Turkish), *Atatürk University Journal of Social Sciences Institute*, **2010**, 3, 1, 85-95.
13. Studd, R., The Textile Design Process, *The Design Journal*, **2002**, 5, 1, 35-39, https://doi.org/10.2752/146069202790718567.
14. Chan, C.S., *Style and Creativity in Design*, Springer International Publishing AG, Cham, Switzerland, **2015**, 1-6.
15. Arslan, P., Creative Process in Textile Pattern Design: Wallas' Four-Stage Model, *The Journal of Academic Social Science Studies*, **2021**, 14, 85, 199-218, http://doi.org/10.29228/JASSS.49901.
16. Wallas, G., *The Art of Thought*, Harcourt Brace Jovanovich, New York, **1926**.
17. Osborn, A.F., *Applied Imagination; Principles and Procedures of Creative Thinking*, Charles Scribner's Sons, New York, **1953**.
18. Mednick, S.A., The Associative Bases of the Creative Process, *Psychol Rev*, **1962**, 69, 220-232, https://doi.org/10.1037/h0048850.
19. Rothenberg, A., The Janusian Process in Scientific Creativity, *Creat Res J*, **1996**, 9, 207-209, https://doi.org/10.1001/archpsyc.1971.01750090001001.
20. Akman Dömbekci, H., Erişen, M.A., Interview Technique in Qualitative Research (in Turkish), *Anadolu University Journal of Social Sciences*, **2022**, 22, 2, 141-160, https://doi.org/10.18037/ausbd.1227330.
21. Türnüklü, A., Interview: An Effective Qualitative Research Technique that Can Be Used in Educational Sciences Research (in Turkish),

Educational Administration: Theory and Practice, **2000**, 24, 543-559.
22. Sert, H., Ölçer Demirkıran, S., Arslan Göz, P., Beler, H., A Qualitative Research Method: Interview (in Turkish), *Journal of Social, Humanities and Administrative Sciences*, **2023**, 9, 71, 4071-4075, http://doi.org/10.29228/JOSHAS.74031.
23. Buzan T., Buzan, B., *The Mind Map Book*, Dutton Book, New York, **1993**, 59.
24. Allaire, C. Met Gala 2024: The Best Red Carpet Looks (in Turkish), Vogue, **2024** [accessed 2025], available from: https://vogue.com.tr/unlu-stili/met-gala-2024-en-iyi-kirmizi-hali-gorunumleri-21914.
25. Arslan, P., Çepni, K. Creative Textile Design: A Wallas Model-Based Approach, *New Des Ideas*, **2025**, 9, 3, 847-864, https://doi.org/10.62476/ndi.93847.

© 2026 by the author(s). Published by INCDTP-ICPI, Bucharest, RO. This is an open access article distributed under the terms and conditions of the Creative Commons Attribution license (http://creativecommons.org/licenses/by/4.0/).

INFLUENCE OF FATLIQUOR CHEMISTRY ON FOGGING AND ODOUR CHARACTERISTICS OF AUTOMOTIVE LEATHER: A COMPARATIVE STUDY OF COMMERCIAL FATLIQUORS

Ali YORGANCIOGLU*

Ege University, Faculty of Engineering, Department of Leather Engineering, 35100, Izmir, Turkiye, e-mail: ali.yorgancioglu@ege.edu.tr

Received: 08.06.2026 Accepted: 21.09.2026 https://doi.org/10.24264/lfj.26.3.3

INFLUENCE OF FATLIQUOR CHEMISTRY ON FOGGING AND ODOUR CHARACTERISTICS OF AUTOMOTIVE LEATHER: A COMPARATIVE STUDY OF COMMERCIAL FATLIQUOR

ABSTRACT. Fogging and odour emissions are among the most important quality requirements for automotive leather due to their direct impact on passenger comfort, interior air quality and driving safety. Fatliquors are indispensable components in leather manufacture, providing softness, flexibility, fullness and durability; however, they are also recognized as one of the major sources of volatile substances responsible for fogging and odour formation. Therefore, the selection of appropriate fatliquor systems is critical for the production of automotive leathers with low emission characteristics. In this study, commercially available fatliquors supplied by three different suppliers with different chemical compositions, including phosphoester-based, fish-oil-based, ester-based, lecithin-containing and synthetic formulations were comparatively evaluated. Automotive leathers prepared with these fatliquors were characterized in terms of fogging behaviour according to DIN EN ISO 17071 and odour performance according to the VDA 270 method. In addition, the effects of fatliquor chemistry on the physical performance of leather were assessed through tensile strength, tear strength and colour fastness with accelerated ageing analysis. The results revealed substantial differences among the evaluated fatliquors in terms of fogging and odour performance. Gravimetric fogging values ranged from 6.8 to 20.8 mg, with synthetic oil, phosphoester and lecithin-based fatliquors generally showing relatively lower fogging tendencies, whereas certain fish oil and ester-based formulations exhibited comparatively higher fogging values. Odour ratings varied between 3.0 and 4.5, and no direct relationship was observed between fogging and odour performance. Notably, considerable differences were also observed among commercial products belonging to the same chemical class, indicating that formulation-specific characteristics play an important role in emission behaviour. These findings demonstrate that fatliquor chemistry and formulation characteristics should be carefully considered when selecting low-emission fatliquors for automotive leather.

KEYWORDS: automotive leather, fatliquor, fogging, odour emission, strength

INFLUENȚA COMPOZIȚIEI CHIMICE A AGENȚILOR DE UNGERE ASUPRA CARACTERISTICILOR DE CONDENSARE ȘI CELE OLFACTIVE ALE PIELII PENTRU TAPIȚERIE AUTO: UN STUDIU COMPARATIV AL AGENȚILOR DE UNGERE COMERCIALI

REZUMAT. Caracteristicile privind condensarea și cele olfactive se numără printre cele mai importante cerințe de calitate pentru pielea utilizată în industria auto, datorită impactului direct al acestora asupra confortului pasagerilor, calității aerului din habitaclu și siguranței la volan. Agenții de ungere sunt elemente indispensabile în fabricarea pielii, conferindu-i acesteia moliciune, flexibilitate, plinătate și durabilitate; cu toate acestea, sunt recunoscuți și ca fiind una dintre principalele surse de substanțe volatile responsabile pentru formarea de condens și a mirosurilor. Prin urmare, alegerea unor sisteme adecvate de ungere este esențială în vederea obținerii pieilor pentru tapițerie auto cu emisii reduse. În cadrul acestui studiu, au fost evaluate comparativ diverse produse comerciale de ungere provenind de la trei furnizori diferiți și având compoziții chimice variate – inclusiv formulări pe bază de fosfoesteri, ulei de pește, esteri, lecitină și produse sintetice. Pielea pentru tapițerie auto prelucrată cu acești agenți a fost caracterizată din punctul de vedere al formării de condens (conform standardului DIN EN ISO 17071) și olfactiv (conform metodei VDA 270). De asemenea, a fost evaluată influența compoziției chimice a agenților de ungere asupra proprietăților fizice ale pielii, analizându-se rezistența la rupere, rezistența la sfâșiere și rezistența culorii în condiții de îmbătrânire accelerată. Rezultatele au evidențiat diferențe semnificative între agenții de ungere evaluați în ceea ce privește performanța legată de formarea de condens și miros. Valorile gravimetrice pentru formarea de condens au variat între 6,8 și 20,8 mg; în general, agenții sintetici, cei pe bază de fosfoesteri și cei cu conținut de lecitină au prezentat tendințe de a forma condens relativ mai scăzute, în timp ce anumite formule pe bază de ulei de pește și esteri au înregistrat valori comparativ mai ridicate. Notele acordate pentru miros au variat între 3,0 și 4,5, neobservându-se o corelație directă între performanța privind caracteristicile de condensare și cele olfactive. Este de remarcat faptul că s-au observat diferențe considerabile chiar și între produsele comerciale aparținând aceleiași clase chimice, ceea ce indică faptul că proprietățile specifice ale formulei joacă un rol important în ceea ce privește emisiile. Aceste rezultate demonstrează că, la alegerea agenților de ungere cu emisii reduse pentru pielea destinată tapițeriei auto, trebuie luate în considerare cu atenție compoziția chimică și caracteristicile formulei.

CUVINTE-CHEIE: piele pentru tapițerie auto, agent de ungere, formare de condens, miros, rezistență

INFLUENCE DE LA COMPOSITION CHIMIQUE DES PRODUITS DE NOURRISSAGE SUR LES CARACTÉRISTIQUES DE CONDENSATION ET OLFACTIVES DES CUIRS AUTOMOBILES : UNE ÉTUDE COMPARATIVE DE PRODUITS COMMERCIAUX

RÉSUMÉ. Les caractéristiques de condensation et olfactives figurent parmi les exigences de qualité les plus importantes pour les cuirs automobiles, en raison de leur impact direct sur le confort des passagers, la qualité de l'air intérieur et la sécurité de conduite. Les produits de nourrissage sont des composants indispensables à la fabrication du cuir, car ils lui confèrent douceur, souplesse, plénitude et durabilité ; toutefois, ils sont également reconnus comme l'une des principales sources de substances volatiles responsables de la formation de condensation et d'odeurs. Par conséquent, le choix de systèmes de nourrissage appropriés est crucial pour produire des cuirs automobiles à faibles émissions. Dans cette étude, des produits de nourrissage disponibles dans le commerce, fournis par trois entreprises différentes et

* *Correspondence to: Ali YORGANCIOGLU, Ege University, Faculty of Engineering, Department of Leather Engineering, 35100, Izmir, Turkiye, Tel.: +90 232 311 2644, e-mail: ali.yorgancioglu@ege.edu.tr*

présentant des compositions chimiques variées — notamment des formulations à base de phosphoesters, d'huile de poisson, d'esters, de lécithine et de produits synthétiques — ont été évalués comparativement. Les cuirs automobiles traités avec ces produits ont été caractérisés en termes de comportement au condensation (selon la norme DIN EN ISO 17071) et de performance olfactive (selon la méthode VDA 270). De plus, l'influence de la chimie de ces produits sur les propriétés physiques du cuir a été évaluée par des analyses de résistance à la traction, de résistance à la déchirure et de solidité des couleurs après vieillissement accéléré. Les résultats ont révélé des différences significatives entre les produits évalués en ce qui concerne la condensation et les odeurs. Les valeurs gravimétriques pour la formation de condensation s'échelonnaient de 6,8 à 20,8 mg ; les produits synthétiques, à base de phosphoesters et à base de lécithine présentaient généralement une tendance au condensation relativement plus faible, tandis que certaines formulations à base d'huile de poisson ou d'esters affichaient des valeurs plus élevées. Les notes d'odeur variaient entre 3,0 et 4,5, et aucune corrélation directe n'a été observée entre la formation de condensation et la performance olfactive. Il convient de noter que des différences considérables ont également été observées entre des produits commerciaux appartenant à une même classe chimique, ce qui indique que les caractéristiques spécifiques de la formulation jouent un rôle important dans le comportement en matière d'émissions. Ces conclusions démontrent que la chimie et les caractéristiques de formulation des produits de nourrissage doivent être prises en compte avec soin lors de la sélection de produits à faibles émissions pour les cuirs automobiles.
MOTS-CLÉS : cuir automobile, produit de nourrissage, condensation, émission d'odeurs, résistance mécanique

INTRODUCTION

Leather is one of the premium materials in automotive interiors owing to its excellent combination of comfort, durability, flexibility, aesthetic appearance and breathability [1–3]. As consumer expectations and automotive quality standards continue to increase, the performance requirements imposed on automotive leather have become increasingly stringent. In addition to conventional mechanical properties and appearance characteristics, special attention is now given to volatile emissions originating from interior materials because of their influence on passenger comfort, interior air quality and driving safety [4, 5].

Among the emission-related phenomena encountered in automotive interiors, fogging is regarded as one of the most critical quality parameters. Fogging refers to the evaporation of volatile substances from interior materials under elevated temperatures followed by their condensation on cooler surfaces, particularly vehicle windshields [4]. The resulting condensate forms a haze-like layer that may impair visibility and contribute to safety concerns. Since the 1990s, the automotive industry has devoted considerable attention to fogging behaviour, leading to the development of standardized evaluation procedures such as DIN 75201 and subsequently, ISO 17071 for leather materials [4, 5]. Today, fogging performance remains an essential requirement for automotive leather approval.

Leather fogging may originate from various components used on leather goods and during leather manufacture, including finishing chemicals, adhesives, plasticizers and fatliquors [4]. Among these, fatliquors are widely recognized as one of the most significant contributors to fogging behaviour because they contain volatile organic compounds capable of migrating from the leather matrix under thermal conditions [6, 7].

Fatliquors are indispensable chemicals in leather processing, where they lubricate collagen fibres, reduce interfibrillary friction and impart softness, fullness, flexibility, and mechanical strength to the finished leather [8–10]. Recent developments have also focused on the design of functional fatliquors capable of providing additional performance benefits, such as antimicrobial activity, enhanced softness and improved sustainability [10, 11]. Traditionally, fatliquors have been produced from fish oils, vegetable oils, synthetic lubricants, phosphoesters, sulfated oils and various combinations thereof [6, 11].

In addition to fogging, odour emission represents another important quality parameter for automotive leather. Leather is known to release various volatile compounds originating from raw materials, processing chemicals, fatliquors, finishing products, and degradation reactions occurring during manufacture and service life. Although odour does not directly impair visibility, it can significantly affect passenger comfort and perceived product quality. For this reason, odour characteristics of automotive trim materials are commonly evaluated using sensory assessment methods such as VDA 270, which remain widely accepted within the automotive industry. Previous studies have highlighted that leather production has

historically been associated with odour-related concerns and that volatile emissions from leather products can contribute to nuisance and discomfort when not adequately controlled [12].

The relationship between fatliquor chemistry and volatile emissions has attracted increasing scientific interest in recent years. Wang *et al*. (2011) demonstrated that fatty spew and fogging are closely related phenomena and reported that fatty acid methyl esters, particularly methyl palmitate, methyl oleate and methyl stearate, are among the principal compounds associated with these defects [13]. Their findings suggested that highly mobile oil components can migrate from the collagen matrix and contribute to both surface exudation and volatile emissions. Similarly, Li *et al*. (2025) reported that fatliquors possessing low molecular weight, low melting points and high aliphatic ester content exhibit greater migration potential within leather, thereby increasing the risk of fogging-related defects [14].

Recent studies have further revealed that the fogging behaviour of leather is strongly governed by the interaction strength between fatliquor molecules and collagen fibres. Lyu *et al*. (2020) showed that improving the fixation of fatliquors within the collagen network effectively suppresses the migration of low-molecular-weight compounds and significantly reduces fogging values [15]. In another study, the incorporation of polymeric structures and reactive functional groups into fatliquor formulations enhanced leather performance while simultaneously satisfying automotive fogging requirements [16]. Zhang *et al*. (2022) systematically investigated the influence of fatliquor molecular structure on fogging behaviour and demonstrated that the introduction of hydroxyl, amino, and carboxyl functionalities strengthened intermolecular interactions with collagen fibres, thereby reducing migration and lowering fogging values [17]. More recently, phosphorylated and esterquat-based fatliquors have been reported to exhibit stronger interactions with leather fibres, improved fixation and reduced migration compared with conventional fatliquor systems [11, 14].

Despite these important advances, most previous investigations have focused on the synthesis and characterization of newly developed low-fogging fatliquors. Comparatively little information is available regarding the behaviour of commercially available fatliquors currently used by the leather industry. In practice, leather manufacturers employ a wide range of commercial fatliquors differing substantially in their chemical composition, including phosphoester-based, fish-oil-based, ester-based, lecithin-containing and synthetic formulations. However, comprehensive studies correlating the chemical nature of these commercial products with fogging behaviour, odour performance and leather properties remain limited.

Therefore, the objective of the present study was to evaluate the influence of fatliquor chemistry on the fogging and odour characteristics of automotive leather using commercially available fatliquors representing different chemical classes. The findings provide new insights into the relationship between fatliquor composition, migration behaviour, volatile emissions and leather properties, contributing to the development and selection of low-emission fatliquors for automotive leather applications.

MATERIALS AND METHODS

Materials

Wet-blue cattle hides were supplied by DD Demir Deri San. ve Tic. A.Ş. (Bursa, Turkiye). Commercially available fatliquors representing different chemical classes, including phosphoester-based, fish-oil-based, ester-based, lecithin-containing and synthetic formulations were supplied by three different companies from Turkiye. The main properties of the different chemical-based commercial fatliquors used in this study were provided by the three respective chemical manufacturers and are presented in Table 1.

Table 1: Properties of different chemical-based commercial fatliquors

Chemical Class	Commercial Fatliquor	Solids Content (%)	pH (1:10)	Main Characteristics
Phosphoester-based	SUPPLIER 1 (P-SUP1)	47.5	6.5–7.5	High penetration, oxidation resistance, excellent electrolyte and chrome stability, high lightfastness, promotes uniform dyeing and fullness.
	SUPPLIER 2 (P-SUP2)	59.0	6.0–8.0	High penetration and distribution, non-oxidizing character, excellent lightfastness, improves uptake of other fatliquors and dye uniformity.
	SUPPLIER 3 (P-SUP3)	47.0	6.0–7.0	Soft and waxy handle, good hard-water and chrome stability, suitable for white and pastel leathers, improves colour uniformity.
Lecithin-based	SUPPLIER 1 (L-SUP1)	52.5	6.0–7.0	Very soft handle, low specific gravity, silky and warm touch, excellent penetration and dyeing performance.
	SUPPLIER 2 (L-SUP2)	75	6.5–7.5	Very soft and supple handle, silky surface texture, high lightfastness and heat resistance, low odour
	SUPPLIER 3 (L-SUP3)	42.5	6.0–7.5	Soft, warm and slightly moist handle, high penetration, low density.
Fish oil-based	SUPPLIER 1 (F-SUP1)	62.5	6.0–7.0	Soft, full and waxy handle, high penetration, excellent softness and fullness.
	SUPPLIER 2 (F-SUP2)	75	6.0–7.0	Very soft and elastic handle, high electrolyte stability, excellent penetration.
	SUPPLIER 3 (F-SUP3)	65.0	6.0–8.0	High internal softness, silky handle, good brightness and penetration.
Ester-based	SUPPLIER 1 (E-SUP1)	57.5	7.5–8.5	General-purpose fatliquor providing softness and fullness, high lightfastness, improves mechanical strength and grain tightness.
	SUPPLIER 2 (E-SUP2)	70	7.0–8.0	Excellent fullness, tight grain, springy handle, high lightfastness and yellowing resistance, high exhaustion
	SUPPLIER 3 (E-SUP3)	50.0	6.0–7.0	Full handle, medium softness, silky touch, good grain tightness.
Synthetic oil-based	SUPPLIER 1 (S-SUP1)	47.0	6.0–7.0	Soft and full handle, good penetration and distribution, suitable for white and light-coloured leathers.
	SUPPLIER 2 (S-SUP2)	65	6.5–7.5	Full, soft and light handle; very low specific gravity; produces a tight and fine grain; excellent heat and light fastness.
	SUPPLIER 3 (S-SUP3)	48.5	6.0–7.0	High emulsification power, excellent electrolyte stability, promotes penetration of other oils and homogeneous lubrication.

Leather Production

The production recipe for wet-blue (chrome tanned) leathers is outlined in Table 2, covering the processes of neutralization and fatliquoring. To eliminate the influence of retanning and dyeing chemicals on the evaluated properties, all experimental leathers were processed according to a simplified wet-blue formulation containing only 6% fatliquor (based on shaved weight). No retanning agents or dyestuffs were applied. The control sample underwent the same processing conditions but received no fatliquor treatment.

Table 2: Leather production recipe

Process	%	Chemicals	Temperature (°C)	Time (min.)	Remarks
Re-Wetting	200	Water	30		
	1	Acetic acid		40	Drain
Neutralization	100	Water	30		
	1.5	Sodium formate		30	
	0.8	Sodium bicarbonate		2x30	pH 5.2, Drain
Washing x3	200	Water	30		Drain
Fatliquoring	80	Water	50		
	6	Fatliquor agent		60	
	1	Formic acid		60	pH 4
Drain-Washing-Horsing up overnight					

Fogging Test

The fogging characteristics of the leather samples were determined according to DIN EN ISO 17071 using the gravimetric method. Prior to testing, leather specimens were conditioned for 7 days. Two circular test pieces (80 mm diameter) were cut from each sample and placed in glass beakers. An aluminium foil collector was positioned above the specimens and the assembly was maintained at 100 ± 1 °C for 16 h. Volatile compounds released from the leather condensed on the cooled aluminium foil surface. After the test, the aluminium foil was conditioned in a desiccator and reweighed. The fogging value was calculated from the mass increase of the aluminium foil and expressed as milligrams (mg) of condensed volatile material. Lower fogging values indicate lower emission of volatile substances from the leather samples.

Odour Analysis

The odour characteristics of the leather samples treated with different fatliquors were evaluated according to VDA 270 – Determination of the odour characteristics of trim materials in motor vehicles [18]. The VDA 270 method is based on sensory evaluation of material or component specimens after storage in closed test vessels under defined conditions. A standard 1-L glass vessel is used, and the test conditions are selected according to the material and the applicable specification. In the present study, variants D4 and D5 were applied. Both variants involve conditioning of the specimens at 50 °C for 2 h. The distinction between the two variants is the presence of water in the test vessel: D4 is performed with water in the test vessel, whereas D5 is performed without water. Thus, D4 and D5 were used to evaluate the odour characteristics of the leather under humid and dry thermal conditioning, respectively.

Prior to testing, the samples were preconditioned for seven days under standard atmospheric conditions. Test specimens with an approximate size of A4, or an equivalent sample amount of approximately 100 g, were placed in the test vessels and conditioned according to the respective VDA 270 variant.

Odour intensity was evaluated by a six-member sensory panel consisting of three female and three male assessors aged between 27 and 38 years. The odour intensity was rated using the six-point VDA 270 scale, where 1 represents “very weak, not perceptible odour”, 2 “weak, perceptible but not annoying”, 3 “distinct but not annoying”, 4 “strong, annoying”, 5 “very strong, more annoying”, and 6 “extremely strong, extremely annoying and disgusting.” In addition to the numerical intensity rating, qualitative odour descriptors were recorded when applicable.

Physical Properties of Fatliquored Leathers

The tensile properties of the leather samples, including tensile strength and percentage elongation at break were evaluated in accordance with TS EN ISO 3376. Tear resistance was determined according to TS EN ISO 3377-1 using the single-edge tear method. All mechanical measurements were carried out using a Shimadzu AG-IS universal testing machine. The resistance of leather samples to colour change under accelerated ageing conditions was evaluated according to TS EN ISO 17228 standard method. Test specimens were exposed in a ventilated laboratory oven under controlled temperature conditions. Two ageing conditions were applied: 60 ± 2 °C for 72 ± 1 h and 100 ± 2 °C for 144 ± 1 h (TS EN ISO 17228-Method 6C and 6D). After ageing, the specimens were conditioned under standard laboratory conditions and visually assessed against the unaged reference specimens. Colour change was evaluated using the grey scale for colour change and reported as grey scale ratings.

RESULTS AND DISCUSSION

The gravimetric fogging values of the leathers treated with different commercial fatliquors are presented in Table 3.

Table 3: Gravimetric fogging values of leathers treated with different commercial fatliquors

Chemical Class	Sample Code	Fogging Value (mg)
Phosphoester-based	P-SUP1	11.70 ± 1.24
	P-SUP2	11.20 ± 0.37
	P-SUP3	8.40 ± 0.72
Lecithin-based	L-SUP1	8.00 ± 0.29
	L-SUP2	9.80 ± 0.47
	L-SUP3	9.50 ± 0.19
Fish oil-based	F-SUP1	10.80 ± 1.16
	F-SUP2	15.20 ± 1.35
	F-SUP3	9.00 ± 0.89
Ester-based	E-SUP1	12.50 ± 0.31
	E-SUP2	11.20 ± 0.15
	E-SUP3	12.80 ± 0.37
Synthetic oil-based	S-SUP1	6.80 ± 0.34
	S-SUP2	8.70 ± 0.20
	S-SUP3	20.80 ± 0.19

Considerable differences were observed among the evaluated samples, with fogging values ranging from 6.8 to 20.8 mg. This wide variation clearly indicates that the chemical nature of the fatliquor plays a decisive role in the emission behaviour of automotive leather. Since all leathers were processed using the same wet-blue substrate and identical processing recipe, except for the fatliquor type, the differences in fogging performance can mainly be attributed to the composition, volatility, molecular mobility and collagen-binding ability of the fatliquors listed in Table 1.

Among the phosphoester-based fatliquors, P-SUP3 showed the lowest fogging value (8.4 mg), followed by P-SUP2 (11.2 mg) and P-SUP1 (11.7 mg). Phosphoester-based fatliquors are generally expected to exhibit improved fixation within the collagen matrix due to their polar phosphate-containing groups, which may enhance interaction with chrome-tanned collagen fibres. This is consistent with recent findings indicating that phosphorylated fatliquors can show stronger interactions with leather fibres and lower migration tendency compared with conventional oil-based systems [14]. However, the differences among P-SUP1, P-SUP2 and P-SUP3 demonstrate that the presence of phosphoester functionality alone is not sufficient to determine fogging behaviour. Other formulation parameters, such as active matter content, the proportion of natural or synthetic oil components, emulsifier type and the presence of low-molecular-weight fractions, may also influence the amount of volatile material released during heating.

The lecithin-based group exhibited relatively low and close fogging values, ranging from 8.0 to 9.8 mg. L-SUP1 gave the lowest value within this group (8.0 mg), while L-SUP2 and L-SUP3 showed fogging values of 9.8 and 9.5 mg, respectively. According to Table 1, these products are characterized by soft handle, high penetration, low density and good dyeing behaviour. Lecithin-containing fatliquors may provide effective lubrication and fibre distribution due to their polar phospholipid structure. The comparatively narrow fogging range of this group suggests that lecithin-based systems may offer a balanced combination of softness and moderate emission behaviour. Nevertheless, despite their favourable handle properties, their fogging values remained higher than the best-performing synthetic oil-based product, indicating that low fogging cannot be predicted solely from softness or penetration ability.

Fish-oil-based fatliquors showed more variable fogging behaviour. F-SUP3 exhibited the lowest fogging value in this group (9.0 mg), whereas F-SUP1 and F-SUP2 showed higher values of 10.8 and 15.2 mg, respectively. Fish-oil-based fatliquors are traditionally known for imparting excellent softness, fullness, waxy handle and internal lubrication, as also summarized in Table 1. However, their chemical structure, typically rich in long-chain unsaturated fatty components, may also increase the risk of oxidation, degradation and migration under thermal conditions. The

relatively high fogging value of F-SUP2 suggests the presence of more mobile or volatile oil fractions, despite its high penetration and electrolyte stability. This agrees with the general understanding that fatliquors containing weakly bound oil components can migrate from the leather matrix and contribute to fogging formation [6, 7]. Wang *et al*. (2013) also reported that fatty acid methyl esters associated with fatliquor composition may contribute to both fatty spew and fogging phenomena [13].

In the ester-based group, fogging values were relatively close to each other, with E-SUP1, E-SUP2 and E-SUP3 giving values of 12.5, 11.2 and 12.8 mg, respectively. These results indicate that ester-based fatliquors showed moderate-to-high fogging tendency compared with lecithin-based and some phosphoester-based systems. As shown in Table 1, this group is associated with fullness, tight grain, springy handle, lightfastness and yellowing resistance. However, ester-rich structures may contain relatively mobile aliphatic ester fractions, which can migrate more readily under elevated temperature. This interpretation is supported by Li *et al*. (2025), who reported that fatliquors with low molecular weight, low melting point and high aliphatic ester content exhibit greater migration potential within leather [14]. Therefore, although ester-based fatliquors may provide desirable physical and handle properties, their formulation should be carefully optimized for automotive leather applications where low emission performance is required.

The synthetic oil-based group showed the widest variation in fogging behaviour. S-SUP1 exhibited the lowest fogging value among all tested samples (6.8 mg), whereas S-SUP3 showed the highest value (20.8 mg). S-SUP2 also displayed a relatively low fogging value of 8.7 mg. This result is particularly important because it demonstrates that synthetic oil-based classification alone does not guarantee low fogging performance. The markedly high value of S-SUP3 may be related to its strong emulsification capacity and ability to promote penetration of other oils, as indicated in Table 1. Although such characteristics are technologically advantageous for homogeneous lubrication, they may also facilitate the mobility of low-molecular-weight or weakly fixed oil components within the leather matrix. In contrast, S-SUP1 and S-SUP2 appear to contain less volatile or better-fixed components, resulting in substantially lower fogging values.

The results in Table 3 show that the fogging behaviour of fatliquored automotive leather is governed by a combination of fatliquor chemistry, molecular mobility, volatility and interaction with collagen fibres. The lowest fogging values were obtained with S-SUP1, L-SUP1, P-SUP3 and S-SUP2, while the highest values were observed for S-SUP3 and F-SUP2. These findings support the concept that low fogging is not determined only by the general chemical class of the fatliquor, but by the specific formulation chemistry within each class.

Odour is a critical quality parameter for automotive interior materials because it directly influences passenger comfort and perceived product quality. Unlike fogging, which primarily affects visibility and safety, odour emissions influence consumer acceptance and can lead to rejection of otherwise technically satisfactory materials. The odour characteristics of the leather samples produced with different commercial fatliquors are presented in Table 4.

Table 4: Odour characteristics of leathers treated with different commercial fatliquors

Chemical Class	Sample Code	D4 Rating	D4 Odour Description	D5 Rating	D5 Odour Description
	P-SUP1	4.0	Pungent	3.0	None
Phosphoester-based	P-SUP2	3.0	Fatty, fruity	3.5	Nut-like
	P-SUP3	3.5	Burnt, sour	3.5	Coffee-like
	L-SUP1	4.0	Pungent, sour	3.5	None
Lecithin-based	L-SUP2	4.0	None	3.5	None
	L-SUP3	3.5	Musty, old	3.0	None
	F-SUP1	3.0	None	3.0	None
Fish oil-based	F-SUP2	3.5	Fecal	3.0	None
	F-SUP3	3.5	Fruity, chemical, fecal	4.0	Chemical, fecal

Chemical Class	Sample Code	D4 Rating	D4 Odour Description	D5 Rating	D5 Odour Description
	E-SUP1	3.5	Fatty, fruity	3.0	None
Ester-based	E-SUP2	3.5	Fatty	3.0	None
	E-SUP3	4.0	Fecal	3.5	Fecal
	S-SUP1	4.5	Fecal, sour	4.0	Fecal
Synthetic oil-based	S-SUP2	3.0	None	3.0	None
	S-SUP3	3.0	Fatty	3.0	None

The D4 odour ratings of the investigated leathers ranged from 3.0 to 4.5, while D5 ratings varied between 3.0 and 4.0 (Table 4). These results demonstrate that fatliquor chemistry has a significant influence on the sensory characteristics of automotive leather. However, unlike the fogging results presented in Table 3, the odour ratings did not show a direct relationship with gravimetric fogging values, indicating that the mechanisms governing volatile mass emission and odour perception are not necessarily identical. Among the phosphoester-based fatliquors, P-SUP2 exhibited the lowest D4 rating (3.0), while P-SUP1 and P-SUP3 showed slightly higher values of 4.0 and 3.5, respectively. The odour descriptors associated with this group included pungent, fatty, fruity, burnt and sour notes. Interestingly, although all three products belong to the same chemical class and displayed relatively similar fogging behaviour (Table 3), their odour profiles differed considerably. This finding suggests that odour perception is influenced not only by the total quantity of emitted substances but also by the chemical identity of specific volatile compounds. Small amounts of highly odorous substances may significantly affect sensory evaluation even when overall volatile emissions remain relatively low.

The lecithin-based fatliquors produced moderate odour ratings. L-SUP1 and L-SUP2 both exhibited D4 values of 4.0, whereas L-SUP3 showed a lower value of 3.5. Lecithin-containing systems contain phospholipid structures that generally provide good lubrication and compatibility with collagen fibres. Nevertheless, the presence of natural lipid fractions may contribute to the formation of characteristic odour compounds during thermal conditioning. The pungent and sour notes observed for L-SUP1 and the musty odour detected for L-SUP3 may originate from oxidation products of natural oil components or residual low-molecular-weight compounds present in the formulation.

The fish-oil-based group exhibited particularly interesting behaviour. F-SUP1 showed the lowest odour intensity among all tested samples, with D4 and D5 ratings of 3.0 and no detectable odour descriptors. In contrast, F-SUP2 and especially F-SUP3 generated more pronounced odour characteristics, including fecal, fruity and chemical notes. Fish-oil-based fatliquors are traditionally valued for their excellent softness and lubrication properties (Table 1), but they may also contain unsaturated fatty components susceptible to oxidative degradation. The formation of aldehydes, ketones and short-chain oxidation products during thermal exposure can contribute significantly to odour generation. The markedly different behaviour observed among the three fish-oil-based products further demonstrates that formulation details and purification level may be more important than the general chemical class itself.

The ester-based fatliquors generally exhibited acceptable odour performance, with D4 ratings between 3.5 and 4.0. E-SUP1 and E-SUP2 were characterized primarily by fatty and fruity notes, whereas E-SUP3 produced a more pronounced fecal odour. As indicated in Table 1, ester-based products are designed to provide fullness, grain tightness and favourable handle properties. However, ester-containing formulations may generate volatile decomposition products under elevated temperatures, particularly when low-molecular-weight ester fractions are present. The higher odour intensity observed for E-SUP3 suggests that the composition of the ester fraction plays a significant role in determining sensory performance.

The synthetic oil-based group displayed the greatest variation in odour behaviour. S-SUP2 and S-SUP3 exhibited the lowest odour

ratings (3.0), whereas S-SUP1 produced the highest odour intensity among all evaluated samples, with D4 and D5 ratings of 4.5 and 4.0, respectively. Notably, S-SUP1 also exhibited the lowest fogging value in Table 3 (6.8 mg). This observation clearly demonstrates that low fogging does not necessarily correspond to low odour. Although S-SUP1 emitted relatively small quantities of volatile material, the emitted compounds apparently possessed a high odour impact and were perceived as fecal and sour by the sensory panel. Conversely, S-SUP3 exhibited the highest fogging value (20.8 mg) while receiving one of the lowest odour ratings. Such behaviour highlights the fundamental difference between gravimetric fogging measurements and sensory odour evaluation. Fogging quantifies the mass of condensed volatile substances, whereas odour assessment depends on the sensory threshold and perception of specific compounds.

A comparison of Tables 3 and 4 reveals that no direct correlation exists between fogging values and odour ratings. For example, S-SUP1 exhibited the lowest fogging value but the highest odour intensity, whereas S-SUP3 exhibited the highest fogging value but one of the lowest odour ratings. Similarly, F-SUP1 demonstrated moderate fogging behaviour while producing the most favourable odour performance. These findings suggest that fogging and odour should be evaluated as complementary but independent parameters when assessing automotive leather emissions.

The tensile strength, elongation at break and tear strength values of the experimental leathers are presented in Table 5.

Table 5: Strength properties of leathers treated with different commercial fatliquors

Chemical Class	Sample Code	Tensile Strength (N/mm²)	Elongation (%)	Single Tear Load (N)
	P-SUP1	26.00 ± 0.85	70.30 ± 1.45	47.30 ± 1.20
Phosphoester-based	P-SUP2	21.40 ± 0.72	73.20 ± 1.80	76.20 ± 2.15
	P-SUP3	23.50 ± 1.68	68.60 ± 2.25	65.40 ± 1.90
	L-SUP1	27.50 ± 0.90	70.20 ± 1.35	55.10 ± 1.65
Lecithin-based	L-SUP2	26.40 ± 0.78	71.50 ± 1.60	48.50 ± 1.40
	L-SUP3	27.00 ± 0.82	68.70 ± 1.50	50.10 ± 1.30
	F-SUP1	25.80 ± 0.75	65.40 ± 1.20	75.40 ± 2.10
Fish oil-based	F-SUP2	26.40 ± 0.88	68.70 ± 1.65	73.20 ± 1.95
	F-SUP3	28.70 ± 0.95	72.40 ± 1.70	68.40 ± 1.80
	E-SUP1	26.70 ± 2.80	79.00 ± 2.10	80.00 ± 2.30
Ester-based	E-SUP2	25.40 ± 1.70	75.80 ± 1.85	82.40 ± 2.45
	E-SUP3	18.60 ± 0.65	71.60 ± 1.55	59.10 ± 1.75
	S-SUP1	29.50 ± 2.05	72.40 ± 1.60	52.40 ± 1.50
Synthetic oil-based	S-SUP2	31.50 ± 3.12	75.60 ± 2.90	59.50 ± 1.65
	S-SUP3	32.20 ± 1.18	78.10 ± 2.05	57.00 ± 1.60
Control	Control	25.60 ± 0.82	63.10 ± 1.30	47.30 ± 1.25

All fatliquored samples exhibited higher elongation values than the control leather, confirming the beneficial lubricating effect of fatliquors on collagen fibre mobility and flexibility. The control sample showed an elongation value of 63.1%, whereas the fatliquored leathers exhibited elongation values ranging from 65.4% to 79.0%, demonstrating that the incorporation of lubricating agents effectively reduced interfibrillar friction within the collagen network.

Significant differences were observed in tensile strength depending on fatliquor chemistry. The highest tensile strength values were obtained for the synthetic oil-based group, particularly S-SUP3 (32.2 N/mm²), S-SUP2 (31.5 N/mm²) and S-SUP1 (29.5 N/mm²), all of which exceeded the control value of 25.6 N/mm². According to the characteristics summarized in Table 1, synthetic oil-based fatliquors are designed to provide homogeneous lubrication, high emulsification stability and effective penetration into the leather structure. These properties may contribute to a more uniform stress distribution during tensile loading, resulting in improved tensile performance. The superior behaviour of the synthetic oil-based products suggests that efficient fibre lubrication and

homogeneous oil distribution play a critical role in maximizing tensile strength. The lecithin-based fatliquors also exhibited relatively high tensile strength values, ranging from 26.4 to 27.5 N/mm². The highest value within this group was observed for L-SUP1 (27.5 N/mm²). Lecithin-containing systems are characterized by excellent penetration and softening ability (Table 1), which may facilitate uniform fibre lubrication without excessive fibre separation. The relatively narrow variation observed within this group indicates a consistent effect of lecithin-containing formulations on tensile performance.

A different trend was observed for tear strength. The highest tear resistance values were obtained with the ester-based fatliquors, particularly E-SUP2 (82.4 N) and E-SUP1 (80.0 N), followed by P-SUP2 (76.2 N), F-SUP1 (75.4 N) and F-SUP2 (73.2 N). These values were substantially higher than the control sample (47.3 N). The superior tear strength of the ester-based group may be associated with the fullness, grain tightness and structural reinforcement characteristics reported in Table 1. Within the phosphoester-based group, P-SUP2 displayed a remarkable tear strength value (76.2 N) despite exhibiting only moderate tensile strength (21.4 N/mm²). Ester-based fatliquors are specifically formulated to improve grain compactness and fibre cohesion, which can enhance resistance against localized stress concentration during tearing. This observation is consistent with the technical characteristics of E-SUP1 and E-SUP2, which emphasize fullness, tight grain structure and mechanical reinforcement.

Interestingly, the sample exhibiting the highest tensile strength (S-SUP3) did not show the highest tear strength, whereas E-SUP2 exhibited the highest tear resistance despite only moderate tensile strength. This finding highlights the different structural requirements governing tensile and tear properties. Tensile strength is influenced primarily by overall fibre cohesion and stress distribution, whereas tear strength is more closely associated with fibre mobility, fibre interlocking and the ability of the collagen network to dissipate localized stresses. Similar observations have been reported in previous studies, where different fatliquor chemistries affected tensile and tear properties through distinct lubrication mechanisms [9, 16].

Another noteworthy observation is the absence of a direct relationship between mechanical performance and emission behaviour. For example, S-SUP3 exhibited the highest tensile strength but also the highest fogging value (20.8 mg) in Table 3, whereas S-SUP1 combined the lowest fogging value (6.8 mg) with excellent tensile performance. Similarly, E-SUP2 provided the highest tear strength despite only moderate fogging behaviour. These results indicate that high mechanical performance does not necessarily correspond to low-emission characteristics and vice versa. Therefore, the selection of automotive fatliquors should be based on a balanced evaluation of both physical performance and emission-related properties.

The resistance of the leather samples to colour change after accelerated ageing is presented in Table 6. The grey scale ratings obtained after ageing at 60 °C for 72 h and 100 °C for 144 h revealed noticeable differences among the evaluated fatliquor systems.

Table 6: Colour change assessment of leather samples after accelerated ageing

Chemical Class	Sample Code	60°C ± 2°C / 72 h ± 1 h	100°C ± 2°C / 144 h ± 1 h
	P-SUP1	3/4	2/3
Phosphoester-based	P-SUP2	3	2
	P-SUP3	3	2
	L-SUP1	3	1/2
Lecithin-based	L-SUP2	3	1/2
	L-SUP3	3	1
	F-SUP1	3	2
Fish oil-based	F-SUP2	2/3	2
	F-SUP3	3	2
	E-SUP1	3	2
Ester-based	E-SUP2	2	2
	E-SUP3	1/2	1/2

Chemical Class	Sample Code	60°C ± 2°C / 72 h ± 1 h	100°C ± 2°C / 144 h ± 1 h
	S-SUP1	3/4	3
Synthetic oil-based	S-SUP2	4	3/4
	S-SUP3	3/4	3/4
Control	Control	3/4	2/3

Among the investigated fatliquors, the synthetic oil-based group demonstrated the best overall ageing performance. S-SUP2 exhibited the highest colour stability, with grey scale ratings of 4 and 3/4 under mild and severe ageing conditions, respectively. Similarly, S-SUP1 and S-SUP3 maintained relatively high ratings throughout the ageing process. These results are consistent with the excellent heat and light fastness characteristics reported for synthetic oil-based products in Table 1. The phosphoester-based fatliquors also showed good resistance to colour change. P-SUP1 exhibited ageing performance comparable to the control leather, while P-SUP2 and P-SUP3 showed only slightly lower ratings. The favourable behaviour of this group may be attributed to their oxidation resistance and high lightfastness properties.

In contrast, lecithin-based and ester-based fatliquors generally exhibited lower ageing resistance. The most pronounced colour deterioration was observed for E-SUP3, which showed grey scale ratings of only 1/2 under both ageing conditions. Similarly, L-SUP3 displayed substantial colour change after severe ageing, indicating a higher susceptibility to thermal oxidation.

The results indicate that synthetic oil-based and phosphoester-based fatliquors provide superior colour stability, whereas certain lecithin-based and ester-based formulations are more prone to thermal discoloration. These findings demonstrate that, in addition to fogging, odour and mechanical performance, ageing resistance should also be considered when selecting fatliquors for automotive leather applications.

CONCLUSIONS

This study comparatively evaluated the influence of eleven commercial fatliquors from three different suppliers representing phosphoester-based, lecithin-based, fish oil-based, ester-based and synthetic oil-based systems on the fogging, odour, mechanical and ageing performance of automotive leather.

The results demonstrated that fatliquor chemistry plays a decisive role in the fogging behaviour of automotive leather. Gravimetric fogging values varied from 6.8 to 20.8 mg, revealing substantial differences among commercially available formulations. In general, synthetic oil-based, phosphoester-based and lecithin-based fatliquors exhibited lower fogging tendencies, whereas certain fish oil-based and ester-based formulations showed comparatively higher fogging values. However, significant variations were also observed among products belonging to the same chemical class, indicating that fogging behaviour is governed not only by the general fatliquor type but also by formulation-specific characteristics such as molecular composition, volatility, migration tendency and interaction with collagen fibres.

Odour ratings ranged between 3.0 and 4.5, confirming that fatliquor composition strongly influences the sensory characteristics of automotive leather. No direct relationship was observed between fogging and odour performance, demonstrating that the amount of emitted volatile material and its sensory perception are controlled by different mechanisms. Consequently, fogging and odour should be considered as complementary but independent evaluation parameters in automotive leather assessment.

The mechanical performance of leather was also affected by fatliquor chemistry. Synthetic oil-based formulations generally produced the highest tensile strength values, while ester-based fatliquors provided superior tear resistance and elongation. Furthermore, synthetic oil-based and phosphoester-based systems exhibited the highest resistance to colour change after accelerated ageing, indicating superior thermal stability compared with several lecithin-based and ester-based formulations.

The findings demonstrate that the selection of fatliquors for automotive leather should not be based solely on softness and handle characteristics. Instead, a balanced evaluation of fogging, odour, mechanical performance and ageing resistance is required. The results provide valuable guidance for leather manufacturers and chemical suppliers in the development of low-emission fatliquor systems capable of meeting increasingly stringent automotive performance requirements.

REFERENCES

1. Thomson, R., Leather, in: E. May, M. Jones (Eds.), *Conservation Science: Heritage Materials*, The Royal Society of Chemistry, Cambridge, **2006**.
2. Covington, A.D., *Tanning Chemistry: The Science of Leather*, Royal Society of Chemistry, Cambridge, **2009**.
3. Heidemann, E., *Fundamentals of Leather Manufacturing*, Eduard Roether KG, Darmstadt, **1993**.
4. Götz, O., Factors Determining the Occurrence of Fogging Behaviour of Automotive Leathers, *J Soc Leather Technol Chem*, **1999**, 83, 149-154.
5. Page, C., Noger, J., Dickhaut-Güdemann, S., Fogging for Automotive Leathers – The New EN 14288/ISO 17071 Test Method, *J Soc Leather Technol Chem*, **2005**, 89, 121-127.
6. Reetz, I., Izquierdo, F., Fischer, C., Segura, R., Mähner, P., Drexler, J., Fatliquoring from a Viewpoint of Sustainability, *J Am Leather Chem Assoc*, **2012**, 107, 85-92.
7. Fu, L., Liu, J., Automotive Leather Fogging and Volatile Emissions: Current Challenges and Developments, *J Soc Leather Technol Chem*, **2008**, 92, 145-152.
8. Ma, J., Wang, T., Yu, S., Zhang, Y., Lyu, B., Preparation and Application of Dialdehyde Nanocellulose Reinforced Jatropha Oil Based Polymer Emulsions as Leather Fatliquors, *Cellulose*, **2021**, 28, 331-346, https://doi.org/10.1007/s10570-020-03494-y.
9. Kalyanaraman, C., Rao, J.R., Nair, B.U., Leather Fatliquoring: An Overview of Chemistry and Applications, *J Am Leather Chem Assoc*, **2012**, 107, 249-260.
10. Yorgancioglu, A., Emulsification and Application of a Thymol Loaded Antibacterial Fatliquor for Leather Industry, *J Ind Text*, **2021**, 51(3), 470–485, https://doi.org/10.1177/1528083720941117.
11. Yorgancioglu, A., Onem, E., Sabyrkhanova, S., Production of an Esterquat-Based Novel Softening Agent and Its Impact on Leather and Textile Quality, *ACS Omega*, **2025**, 10(9), 9289–9300, https://doi.org/10.1021/acsomega.4c09502.
12. Akyüz, F., Odor: An Important Problem in Leather Industry, Proceedings of the International Leather Engineering Congress (IAFLI), **2010**, 110–116.
13. Wang, Y., Liao, X., He, Q., Shi, B., Determination of Fatty Spew on Leather by GC-MS, *J Am Leather Chem Assoc*, **2011**, 106, 179-183.
14. Li, R., Yang, C., Liu, Y., Yu, Y., A Novel Approach for Analyzing the Migration Behavior of Fatliquors within Leather, *Collagen Leather*, **2025**, 7, 8, https://doi.org/10.1186/s42825-025-00189-7.
15. Lyu, B., Luo, K., Wang, Y., Gao, D., Ma, J., Sodium Alginate Oxide Assembly Layered Double Hydroxide and Its Structure–Activity Relationship to Anti-Fogging Properties and Flame Retardancy of Leather, *Appl Clay Sci*, **2020**, 190, 105559, https://doi.org/10.1016/j.clay.2020.105559.
16. Ma, J., Wang, T., Yu, S., Zhang, Y., Lyu, B., Preparation and Application of Dialdehyde Nanocellulose Reinforced Jatropha Oil Based Polymer Emulsions as Leather Fatliquors, *Cellulose*, **2021**, 28, 331-346, https://doi.org/10.1007/s10570-020-03494-y.
17. Zhang, Y., Liu, C., Ma, J., Zhang, W., Fan, Q., Ma, Z., Relationship between the Structure of Modified Ricinoleic Acids via the Thiol–Ene Click Reaction and the Fogging Value of Fatliquored Leather, *ACS Sustain Chem Eng*, **2022**, 10, 13288-13300, https://doi.org/10.1021/acssuschemeng.2c02364.
18. VDA 270. Determination of the Odour Characteristics of Trim Materials in Motor Vehicles, German Association of the Automotive Industry (Verband der Automobilindustrie e.V), **2022**, 4p.

© 2026 by the author(s). Published by INCDTP-ICPI, Bucharest, RO. This is an open access article distributed under the terms and conditions of the Creative Commons Attribution license (http://creativecommons.org/licenses/by/4.0/).

DEODORIZATION OF LEATHER TANNERY WASTE WATER TOXIC GASES USING SPENT COFFEE GROUNDS: A COMPREHENSIVE REVIEW

Megabi Adane YIZENGAW*

Leather Engineering Department, Ethiopian Institute of Textile and Fashion Technology, P.O. Box: 1037, Bahir Dar University, Bahir Dar, Ethiopia, email: megadane123@gmail.com

Received: 09.06.2026 Accepted: 21.09.2026 https://doi.org/10.24264/lfj.26.3.4

DEODORIZATION OF LEATHER TANNERY WASTE WATER TOXIC GASES USING SPENT COFFEE GROUNDS: A COMPREHENSIVE REVIEW

ABSTRACT. The leather tanning industry is a major contributor to economic development worldwide; however, it is also associated with significant environmental challenges, particularly the generation of toxic and malodorous gases from wastewater treatment processes. Emissions such as hydrogen sulfide (H_2S), ammonia (NH_3), and volatile organic compounds (VOCs) not only create severe odor nuisances but also pose substantial risks to human health, workplace safety, and environmental quality. Conventional odor control technologies, including chemical scrubbing, activated carbon adsorption, and biological filtration, often suffer from high operational costs, energy demands, and secondary waste generation, highlighting the need for sustainable alternatives. This review critically examines the potential of spent coffee grounds (SCG), an abundant agro-industrial by-product, as an innovative and eco-friendly adsorbent for deodorizing tannery wastewater gases. Owing to their porous structure, high carbon content, and rich surface chemistry containing hydroxyl, carboxyl, and phenolic functional groups, SCG exhibit remarkable capabilities for capturing and transforming hazardous gaseous pollutants through physical adsorption, chemisorption, and redox mechanisms. The review discusses the sources and formation pathways of toxic tannery gases, evaluates existing odor control technologies and their limitations, and explores the physicochemical characteristics and gas-removal mechanisms of SCG. Furthermore, it highlights current research advances, regeneration potential, and opportunities for integrating SCG into sustainable wastewater treatment systems. Although challenges related to adsorption efficiency, material standardization, and large-scale implementation remain, the valorization of spent coffee grounds represents a promising circular-economy strategy that simultaneously addresses waste management and industrial air pollution.

KEYWORDS: leather tannery wastewater, spent coffee grounds, odor control, adsorption, circular economy

DEZODORIZAREA GAZELOR TOXICE REZULTATE DIN APELE UZATE ALE TĂBĂCĂRIILOR FOLOSIND ZAȚUL DE CAFEA: O ANALIZĂ CUPRINZĂTOARE

REZUMAT. Industria de pielărie contribuie semnificativ la dezvoltarea economică mondială; totuși, aceasta este asociată și cu provocări ecologice majore, în special generarea de gaze toxice și urât mirositoare în procesele de tratare a apelor uzate. Emisii precum hidrogenul sulfurat (H_2S), amoniacul (NH_3) și compușii organici volatili (COV) nu doar că provoacă un disconfort olfactiv sever, dar prezintă și riscuri considerabile pentru sănătatea umană, siguranța la locul de muncă și calitatea mediului. Tehnologiile convenționale de control al mirosurilor – inclusiv spălarea chimică a gazelor, adsorbția pe cărbune activ și filtrarea biologică – implică adesea costuri operaționale ridicate, un consum mare de energie și generarea de deșeuri secundare, ceea ce subliniază necesitatea unor alternative sustenabile. Această lucrare analizează critic potențialul zațului de cafea – un produs secundar agroindustrial abundent – ca adsorbent inovator și ecologic pentru dezodorizarea gazelor provenite din apele uzate ale tăbăcăriilor. Datorită structurii poroase, conținutului ridicat de carbon și chimiei de suprafață bogate în grupări funcționale hidroxil, carboxil și fenolice, zațul de cafea prezintă capacități remarcabile de captare și transformare a poluanților gazoși periculoși prin mecanisme de adsorbție fizică, chemosorbție și reacții redox. Lucrarea discută sursele și căile de formare a gazelor toxice din tăbăcării, evaluează tehnologiile existente de control al mirosurilor și limitările acestora și explorează caracteristicile fizico-chimice și mecanismele de eliminare a gazelor specifice zațului de cafea. De asemenea, sunt evidențiate progresele actuale ale cercetării, potențialul de regenerare și oportunitățile de integrare a zațului de cafea în sisteme sustenabile de tratare a apelor uzate. Deși persistă provocări legate de eficiența adsorbției, standardizarea materialului și implementarea la scară largă, valorificarea zațului de cafea reprezintă o strategie promițătoare în cadrul economiei circulare, care abordează simultan gestionarea deșeurilor și poluarea industrială a aerului.

CUVINTE CHEIE: ape uzate din tăbăcării, zaț de cafea, controlul mirosurilor, adsorbție, economie circulară

DÉSODORISATION DES GAZ TOXIQUES ISSUS DES EAUX USÉES DE TANNERIE À L'AIDE DE MARC DE CAFÉ : UNE SYNTHÈSE APPROFONDIE

RÉSUMÉ. L'industrie du tannage du cuir contribue largement au développement économique mondial ; toutefois, elle est également associée à des défis environnementaux majeurs, notamment l'émission de gaz toxiques et malodorants lors des processus de traitement des eaux usées. Des émissions telles que le sulfure d'hydrogène (H_2S), l'ammoniac (NH_3) et les composés organiques volatils (COV) engendrent non seulement d'importantes nuisances olfactives, mais présentent également des risques considérables pour la santé humaine, la sécurité au travail et la qualité de l'environnement. Les technologies conventionnelles de contrôle des odeurs — telles que le lavage chimique des gaz, l'adsorption sur charbon actif et la filtration biologique — souffrent souvent de coûts d'exploitation élevés, d'une forte consommation énergétique et de la production de déchets secondaires, soulignant ainsi la nécessité d'alternatives durables. Cette synthèse examine de manière critique le potentiel du marc de café, un sous-produit agro-industriel abondant, en tant qu'adsorbant innovant et écologique pour la désodorisation des gaz issus des eaux usées de tannerie. Grâce à son structure poreuse, son forte teneur en carbone et la richesse de son chimie de surface (présence de groupements fonctionnels hydroxyle, carboxyle et phénolique), le marc de café présente des capacités

* *Correspondence to: Megabi Adane YIZENGAW, Leather Engineering Department, Ethiopian Institute of Textile and Fashion Technology, P.O.Box: 1037, Bahir Dar University, Bahir Dar, Ethiopia, email: megadane123@gmail.com*

remarquables pour capturer et transformer les polluants gazeux dangereux via des mécanismes d'adsorption physique, de chimisorption et de réactions redox. L'article aborde les sources et les voies de formation des gaz toxiques de tannerie, évalue les technologies existantes de contrôle des odeurs ainsi que leurs limites, et explore les caractéristiques physico-chimiques du marc de café ainsi que les mécanismes d'élimination des gaz associés. Il met également en lumière les avancées actuelles de la recherche, le potentiel de régénération du matériau et les opportunités d'intégration du marc de café dans des systèmes durables de traitement des eaux usées. Bien que des défis subsistent concernant l'efficacité d'adsorption, la normalisation du matériau et la mise en œuvre à grande échelle, la valorisation du marc de café constitue une stratégie prometteuse d'économie circulaire, répondant simultanément aux enjeux de gestion des déchets et de pollution atmosphérique industrielle.
MOTS-CLÉS : eaux usées de tannerie, marc de café, contrôle des odeurs, adsorption, économie circulaire

INTRODUCTION

The centuries' old leather tanning industry is essential for producing leather goods used worldwide in fashion, automotive, furniture, and various other sectors [1]. However, leather processing is known to generate significant environmental pollution, particularly through its wastewater discharges and gaseous emissions [1, 2]. Tannery wastewater typically contains a complex mixture of toxic chemicals, including heavy metals like (chromium), organic pollutants, sulfides, and nitrogen compounds. These contaminants not only pollute aquatic ecosystems but also contribute to the release of malodorous and hazardous gases such as hydrogen sulfide (H_2S), ammonia (NH_3), and volatile organic compounds (VOCs) during wastewater treatment and sludge handling. These gases pose serious health risks to tannery workers and neighboring communities, including respiratory issues, eye irritation, and in severe cases, toxicity or suffocation [1, 3].

Current conventional deodorization techniques for controlling these toxic gases largely rely on chemical scrubbers, bio-filtration, or activated carbon adsorption. While these approaches can be effective, they often involve high operating costs, generation of secondary waste, and complex disposal issues. Additionally, chemical scrubbers sometimes introduce harmful by-products, and activated carbon is costly and requires energy intensive regeneration. Therefore, developing cost effective, eco-friendly, and sustainable methods to deodorize tannery wastewater gases remains a serious task for environmental management in the leather tanning industry [3, 4].

In this review, spent coffee grounds (SCG) are being studied as a favorable bio-adsorbent material for environmental cleansing purpose. SCG is the residue left after brewing coffee and is generated in massive quantities worldwide estimated at several million tons annually [3, 5]. Valorization of SCG as a resource aligns with global sustainability and circular economy goals, turning waste into value added products. Chemically, SCG are rich in lignocellulosic materials, phenolic compounds, lipids, proteins, and nitrogen containing groups, which impart a variety of surface functional groups such as hydroxyl (-OH), carboxyl (-COOH), and amine ($-NH_2$) groups. These characteristics make SCG an effective adsorbent for a wide range of pollutants, including heavy metals, dyes, and organic contaminants [6, 7]. More recently, research has extended toward the application of SCG for the adsorption and neutralization of malodorous and toxic gases. Studies have demonstrated that SCG can physically adsorb gases due to their porous structure and chemically interact with gas molecules via surface functional groups. Additionally, the antioxidant properties of phenolic compounds present in SCG may contribute to chemical reduction reactions that degrade toxic gases [7, 8].

Despite these advantageous features, the use of SCG specifically for deodorization of leather tannery wastewater gases remains an evolving and relatively unrevealed study. There is a critical need to comprehensive review and consolidate existing knowledge on the effectiveness, mechanisms, and practical applicability of SCG for this purpose. Understanding the molecular level interactions

between SCG surface groups and tannery gas constituents is essential for optimizing adsorbent performance and designing scalable deodorization systems. The researcher discussed the nature and sources of tannery wastewater gases, the physicochemical properties of SCG relevant to gas adsorption, underlying removal mechanisms, integration strategies into existing wastewater treatment frameworks, and the challenges and future prospects of this SCG deodorization. By valorizing spent coffee grounds for tannery wastewater gas deodorization, the leather industry can move towards more sustainable wastewater management practices, reduce its environmental footprint, and promote circular waste utilization.

COMPOSITIONS OF TANNERY WASTEWATER

Leather tannery wastewater contains a diverse mixture of organic and inorganic pollutants. These pollutants originate from the wide range of chemical and mechanical operations involved in the conversion of raw hides into finished leather [1]. Each stage of the tanning process such as soaking, liming, deliming, pickling, tanning, and finishing contributes specific pollutants to the wastewater stream [9]. On average, tanneries generate approximately 30 to 50 cubic meters of wastewater per ton of raw hides processed, although this number can vary significantly based on the type of tanning process used (chrome tanning or vegetable tanning), the level of process automation, and the degree of water recycling or reuse implemented within the facility [10, 11].

Organic Compounds

These organic substances are introduced during early stages of processing, especially during soaking and liming, where blood, flesh, and decomposed skin tissues are removed [12]. The degradation of these animal derived materials in wastewater not only increases (biological oxygen demand) BOD and (chemical oxygen demand) COD but also contributes to the production of malodorous compounds and potential pathogen production if not properly treated [13]. High BOD values indicate a substantial presence of biodegradable organic matter, which consumes oxygen during microbial decomposition. COD represents the total quantity of oxygen required to chemically oxidize both biodegradable and non-biodegradable organics. The major contributors to this organic load include proteins, fats, carbohydrates, and residual organic tanning agents such as vegetable tannins or synthetic substitutes. Incomplete removal or degradation of these compounds can severely impact downstream biological treatment systems and pose environmental hazards when discharged into natural water bodies [1, 9].

Inorganic Compounds

In addition to the organic load, tannery wastewater contains a wide array of inorganic pollutants derived from the numerous chemicals used in tanning processes. Notable, among these are high concentrations of salts, including sodium chloride (NaCl), which is commonly used in the curing and pickling stages to preserve raw hides and facilitate the penetration of tanning agents [1]. Excessive salt concentrations contribute to raise total dissolved solids (TDS), which can inhibit microbial activity in biological treatment systems and increase the salinity of receiving water bodies, leading to ecological imbalances [14]. Alkalinity is introduced primarily through the use of calcium hydroxide (lime) during the liming stage, where it serves to loosen hair and swell collagen fibers in the hide [15]. Conversely, acidity arises from the use of strong acids such as sulfuric acid (H_2SO_4) or formic acid (HCOOH) during pickling and pH adjustment processes [1]. These opposing chemical conditions high pH from liming and low pH from pickling can result in fluctuations in wastewater pH, complicating treatment and posing challenges to maintaining neutralization and buffer capacity [16]. Other inorganic components include chromium salts, particularly trivalent chromium (Cr^{3+}), used in chrome tanning. Although chromium is less volatile, it poses long-term

environmental and health risks if not properly removed, especially if it oxidizes to hexavalent chromium (Cr^{6+}), a known carcinogen [17].

SOURCES AND FORMATION OF TOXIC GASES IN TANNERY

In leather tannery wastewater, both organic and inorganic pollutants, many of which can undergo biochemical and chemical transformations to produce hazardous gaseous emissions under aerobic and anaerobic conditions [18]. The raw effluent from various stages of the tanning process contains significant concentrations of sulfide compounds, ammonia, volatile fatty acids (VFAs), proteins, lipids, and other biodegradable organics [1]. Under anaerobic conditions, microbial degradation of these organics leads to the production of biogases such as methane (CH_4), hydrogen sulfide (H_2S), and ammonia (NH_3) [19].

Hydrogen Sulfide (H_2S)

Hydrogen sulfide (H_2S) is among the most hazardous and environmentally significant gaseous emissions associated with tannery wastewater treatment. The generation of H_2S in tannery effluents is primarily the result of anaerobic microbial processes, specifically the dissimulator's sulfate reduction by sulfate-reducing bacteria (SRB) [20]. These microorganisms utilize sulfate (SO_4^{2-}) or organic sulfur compounds such as amino acids containing sulfur (cysteine and methionine) as terminal electron acceptors during the degradation of organic matter under anoxic conditions, producing H_2S as a metabolic byproduct [21]. The concentration of H_2S in tannery wastewater environments can vary significantly depending on factors such as the organic load, temperature, pH, redox potential, and the presence of sulfate or sulfide-containing compounds (sodium sulfide, commonly used in the liming process) [1]. Despite this variability, H_2S levels can frequently exceed occupational safety thresholds. The gas is acutely toxic; concentrations as low as 10–20 parts per million (ppm) can cause eye and respiratory tract irritation, while prolonged or repeated exposure may lead to chronic neurological and pulmonary complications [22].

Ammonia (NH_3)

Ammonia (NH_3) is a significant volatile emission associated with tannery wastewater, primarily arising from the degradation of nitrogen containing organic compounds such as proteins, peptides, amino acids, urea, and ammonium salts [23]. These nitrogenous substances originate from animal residues (blood, skin, flesh) and chemical additives used during processes such as deliming and bating. Under aerobic and especially anaerobic conditions, microbial and enzymatic breakdown of these compounds leads to the formation and release of free ammonia into the gaseous phase [24]. In the context of tannery operations, ammonia emissions are especially concerning due to the high nitrogen (N) load in the effluent and the potential for volatilization during wastewater handling, storage, and treatment [25].

Volatile Organic Compounds (VOCs)

Volatile organic compounds in tannery emissions include a variety of hydrocarbons, aldehydes, ketones, and sulfur containing organic compounds. These arise from the decomposition of organic matter and chemicals used in tanning, such as solvents and degreasing agents [26]. Volatile Organic Compounds (VOCs) in tannery emissions comprise a diverse group of hydrocarbons, aldehydes, ketones, and sulfur-containing organic molecules that originate from both the degradation of organic matter and the volatilization of chemicals utilized throughout the leather processing stages [19]. These compounds are generated through multiple pathways. The microbial anaerobic and aerobic decomposition of proteinaceous and lipid-rich residues in wastewater releases various low-molecular-weight VOCs, while chemical solvents, degreasing agents, and tanning additives volatilize during mechanical agitation, heating, and drying processes [27]. Specifically, the breakdown of fats and oils produces ketones and aldehydes, whereas

sulfur-containing tanning agents and organic sulfur compounds can degrade into thiols and other sulfur-based VOCs. The emission of VOCs contributes significantly to the characteristic malodors associated with tanneries and poses potential health risks due to the carcinogenicity and toxicity of several compounds, such as benzene derivatives and formaldehyde [28, 29].

Other Sulfur Compounds

In addition to hydrogen sulfide (H_2S), tannery wastewater and associated processes can emit a range of other sulfur containing volatile compounds, including carbonyl sulfide (COS), methyl mercaptan (CH_3SH), and dimethyl sulfide (DMS). These sulfurous gases arise primarily from the microbial degradation and chemical transformation of sulfur containing organic matter and additives used in leather processing [30]. Carbonyl sulfide is typically formed through the oxidation of carbon disulfide (CS_2), a compound sometimes present in tanning formulations, or through microbial metabolism of sulfur-containing substrates under both aerobic and anaerobic conditions [21]. Methyl mercaptan and dimethyl sulfide are generated via the microbial breakdown of sulfur-containing amino acids such as methionine and cysteine, as well as through methylation reactions mediated by specific bacterial consortia in anaerobic sludge environments [31].

Nitrogen Oxides (NOx) and Carbon Oxides (COx)

Nitrogen oxides (NO_x) and carbon oxides (CO_x), although not typically generated directly from tannery wastewater itself, can be significant byproducts of tannery waste management practices, particularly during thermal treatment processes such as sludge incineration, combustion, or pyrolysis [32]. NO_x species, primarily nitric oxide (NO) and nitrogen dioxide (NO_2), are formed via high-temperature oxidation of nitrogenous compounds present in the sludge or combustion air, through mechanisms including the thermal fixation of atmospheric nitrogen (thermal NO_x) and the oxidation of fuel-bound nitrogen (fuel NO_x) [33]. Similarly, carbon oxides carbon monoxide (CO) and carbon dioxide (CO_2) are produced from the incomplete and complete oxidation of organic carbonaceous matter contained within tannery sludge and other solid wastes [34].

Table 1: Summary of gas Emission Sources within Tannery Processes [1, 35]

Process Steps	Emission Sources	Major toxic Gases
Soaking	Decomposition of residual blood, manure, and skin tissue	VOCs, NH_3
Liming	Hair removal using sodium sulfide and lime	H_2S
Deliming	Neutralization of lime using ammonium salts	NH_3
Pickling	Application of sulfuric acid and salt to prepare for tanning	Acidic fumes, VOCs
Tanning	Use of chromium (III) salts or vegetable tannins	VOCs, NH_3
Post-tanning (Drying, Fatliquoring)	Thermal decomposition and chemical reactions with oils and fats	VOCs
Sludge Treatment	Anaerobic breakdown of organic sludge from wastewater systems	H_2S, NH_3, VOCs

ODOR CONTROL TECHNIQUES

As global attention shifts toward more sustainable and inclusive industrial practices, aligning tannery emission controls with both regulatory standards and practical field realities becomes paramount [36]. So, the control of gaseous emissions, particularly malodorous compounds originating from tannery wastewater, is a complex task that needs a strategic, sustainable and specific approach [1]. Effective odor management must therefore balance technical efficiency, economic feasibility, and environmental sustainability [37]. To this end, a range of control technologies has been developed and applied, including physical methods (ventilation, and gas condensation), chemical treatments (scrubbing, with oxidants or alkaline solutions), biological processes (biofilters and bio-trickling filters), and adsorption-based systems (activated carbon and bio-based adsorbents) [38].

Physical Methods

In this method a range of mechanically driven processes aimed at reducing the concentration or presence of airborne pollutants through dilution, separation, or phase change mechanisms [39]. Unlike chemical or biological methods, physical techniques do not involve chemical reactions or microbial degradation but instead rely on physical principles such as air movement, temperature control, and mass transfer to mitigate odor emissions [40]. Due to their operational simplicity, relatively low cost, and immediate effectiveness, physical methods are commonly used to rapidly reduce odorous gas concentrations or to condition emissions prior to further treatment [41]. However, they are typically limited in their ability to address complex mixtures of gases, high concentration emissions, or substances with low odor thresholds. Their effectiveness is highly dependent on factors such as pollutant solubility, volatility, temperature, humidity, and flow rate, which must be carefully considered during system design and implementation [36].

Ventilation

Ventilation is one of the most basic physical methods employed for odor control. It operates by displacing odorous or contaminated air with ambient or treated fresh air to reduce the concentration of gaseous pollutants to levels below odor detection thresholds [38]. This approach is commonly applied in large, open processing areas, sludge handling zones, or during temporary peak emission events. The method is valued for its low cost, simplicity, and immediate effectiveness, especially in non-enclosed environments. However, ventilation alone does not neutralize or capture odorants it merely disperses them. This can shift rather than solve the pollution problem, potentially impacting nearby communities if not carefully managed [42]. Moreover, its effectiveness decreases significantly with high-load emissions or in enclosed spaces where proper airflow dynamics are difficult to maintain. As a result, ventilation is typically used in combination with other control systems, such as filters or scrubbers, to improve overall efficiency [43].

Condensation

Condensation is another physical method used for odor control, particularly targeting volatile organic compounds (VOCs) [19]. This technique involves cooling the gas stream to a temperature where condensable vapors undergo a phase change from gas to liquid, allowing for their collection and removal [44]. Condensation is especially useful for treating high-boiling-point VOCs and is often employed in pre-treatment or recovery processes, such as solvent reclamation. In odor control systems, condensation is typically used to pre-concentrate VOCs before further treatment [45].

Chemical Methods

Chemical odor control methods are based on the application of reactive agents that chemically neutralize, oxidize, or transform odorous compounds into less harmful or non-odorous substances [19]. These techniques are particularly effective against a wide range of volatile and reactive compounds, including hydrogen sulfide (H_2S), ammonia (NH_3), and various volatile organic compounds (VOCs) [43]. Common chemical treatment approaches include oxidation, acid-base neutralization, and chlorination. For example, oxidizing agents such as sodium hypochlorite, hydrogen peroxide, or potassium permanganate are frequently employed to degrade sulfur containing compounds and nitrogenous odorants [19]. Similarly, acidic or alkaline solutions are used to neutralize basic or acidic gases, respectively such as using sulfuric acid to neutralize ammonia or sodium hydroxide to scrub acidic gases [39].

Scrubbing

Scrubbing, particularly wet scrubbing is a widely adopted physical-chemical method in industrial odor control. This process involves passing odorous gases through a scrubbing

liquid commonly water, acidic, or alkaline solutions that absorbs or reacts with soluble pollutants. Wet scrubbers are particularly effective for treating water-soluble gases such as ammonia (NH_3) and hydrogen sulfide (H_2S), which are prevalent in tannery emissions [46]. In tannery operations, alkaline scrubbers (sodium hydroxide based) are often used to neutralize acidic gases, while oxidative scrubbers may employ agents like hydrogen peroxide or sodium hypochlorite to break down reactive sulfur compounds [1]. Although scrubbing offers high removal efficiency and flexibility, it requires regular monitoring of pH and chemical concentrations, generates secondary liquid waste, and demands additional treatment infrastructure for handling spent scrubbing fluids. The system's design must also consider gas-liquid contact time, temperature, and flow rates to ensure optimal performance [47].

Oxidation

Oxidation processes utilize strong oxidizing agents such as ozone (O_3) and chlorine (Cl_2) to chemically degrade odor causing molecules by breaking down complex sulfur and nitrogen containing compounds into less odorous or non-odorous substances [19]. These oxidants function through electron transfer reactions that alter the molecular structure of malodorous compounds, often converting them into inorganic species such as sulfate or nitrate ions [48]. Oxidation is particularly effective in targeting volatile sulfur compounds (hydrogen sulfide) and nitrogenous gases (ammonia, amines), which are common in tannery emissions. However, the use of chlorine can lead to the formation of chlorinated organic by-products, some of which are toxic or carcinogenic, necessitating stringent effluent monitoring and disposal protocols. Additionally, ozone, while a powerful oxidant, is highly reactive and can pose occupational safety risks if not properly controlled [39].

Neutralization

Neutralization techniques contain the addition of acidic or alkaline reagents to adjust the pH of the gas or liquid phase, facilitating the chemical conversion of odorous gases into less volatile or non-odorous salts [46]. For instance, the introduction of acidic agents can convert gaseous ammonia (NH_3) into ammonium salts (NH_4^+), effectively reducing its volatility and odor potential. Conversely, alkaline reagents are used to neutralize acidic gases such as hydrogen sulfide and sulfur dioxide, converting them into soluble sulfides or sulfates. The productivity of neutralization processes is highly dependent on precise dosage control, adequate mixing, and continuous monitoring of system parameters such as pH and reagent concentration [43]. Inadequate or excessive dosing can lead to incomplete neutralization or the formation of secondary pollutants, which can complicate waste handling and disposal. Moreover, neutralization reactions often generate secondary waste streams that require additional treatment, thus increasing operational complexity [47].

Biological Methods

Biological odor control technologies harness the natural metabolic capabilities of microorganisms to biodegrade, transform, or integrate odorous gaseous pollutants into less harmful substances, often converting them into carbon dioxide, water, and biomass. These methods are widely regarded as environmentally sustainable and cost-effective, especially for treating continuous, low- to moderate-concentration emissions typical of industrial processes such as tannery wastewater treatment and solid waste management [49, 50].

Biofilters

Bio filtration implicates passing contaminated air through a moist, porous medium commonly composed of natural materials such as compost, peat, wood chips, or soil which serves as a habitat for specialized microbial communities capable of degrading odorous compounds [51]. The biological oxidation of pollutants occurs as gases diffuse into the biofilm layer that coats the packing material, where aerobic microorganisms

metabolize target substances such as hydrogen sulfide (H_2S), ammonia (NH_3), and volatile organic compounds (VOCs) [43]. Biofilters are particularly effective under aerobic conditions, leveraging the metabolic pathways of chemoheterotrophic and autotrophic bacteria to convert malodorous gases into non-toxic end products like sulfate, nitrate, carbon dioxide, and biomass. However, biofilters require careful moisture management to prevent drying out or anaerobic zones, and the porous medium may degrade or compact over time, necessitating periodic replacement or transformation [19].

Bio-scrubbers

Bioscrubbers combine the gas absorption efficiency of wet scrubbers with the biological degradation capabilities of bioreactors, offering a two-stage process for odor control. In this system, the contaminated air is first passed through a liquid phase where soluble pollutants are absorbed [52]. The resulting liquid solution, enriched with absorbed contaminants, is then circulated through a bioreactor containing microbial populations that biodegrade the dissolved odorants. This separate design allows for independent control of gas liquid mass transfer and microbial activity, improving treatment efficiency and operational stability compared to conventional biofilters [53]. Bioscrubbers are particularly advantageous for treating gases with low solubility or those requiring controlled pH and nutrient conditions. However, the increased complexity of infrastructure, higher capital costs, and the need for continuous monitoring of microbial health, oxygen supply, and liquid parameters represent operational tasks [54].

Adsorption-Based Methods

Adsorption is a surface phenomenon where gaseous odor molecules are physically or chemically bound onto the surface of solid adsorbents, thereby removing them from the air stream. This process is highly effective for taking a wide variety of odorous compounds, including volatile organic compounds (VOCs), sulfur-containing gases (hydrogen sulfide), and nitrogenous compounds (ammonia) [55]. Adsorption-based methods are among the most widely applied odor control technologies due to their versatility, high removal efficiency, and relatively straightforward operation [56]. The success of adsorption depends primarily on the surface area, pore structure, and chemical properties of the adsorbent material. Common adsorbents include activated carbon, zeolites, silica gel, and bio-based materials [57].

Activated Carbon

Activated carbon which is widely regarded as the standard adsorbent due to its exceptionally high specific surface area (normally 500–1500 m^2/g) and well developed porous structure, which provide numerous active sites for the adsorption of volatile organic compounds (VOCs), hydrogen sulfide (H_2S), ammonia (NH_3), and other odor causing gases [58]. The adsorption mechanism on activated carbon primarily involves physical adsorption via van der Waals forces, accompanied by chemical interactions when soaked with reactive agents such as potassium iodide or metals to target specific pollutants [59].

Zeolites

Zeolites are micro-porous alumino silicate minerals characterized by uniform pore sizes and high ion exchange capacity, which enable selective adsorption of small molecules such as ammonia and certain VOCs [60]. Their crystalline structure imparts hydrophilic or hydrophobic properties, making some zeolites more resistant to moisture interference compared to activated carbon [61]. This moisture tolerance is advantageous in treating humid emissions common in tannery environments. However, zeolites generally exhibit lower adsorption capacities for sulfide gases such as hydrogen sulfide, limiting their standalone use in certain odor control applications [62].

LIMITATIONS OF CONVENTIONAL ODOUR CONTROL METHODS

Table 2: Overall summary of limitations of conventional odour control methods [63-66]

Odor control Technique	Mechanism of odor removal	Advantages	Limitations/gaps
Physical (Ventilation, Condensation)	Dilutes or condenses gases to lower odor concentrations	Simple, low cost, fast implementation	Not effective for high concentration or reactive gases
Chemical Scrubbing	Absorption of gases using liquid chemicals (NaOH, H_2O_2)	High removal efficiency for specific gases (H_2S, NH_3)	Chemical consumption, sludge generation, operational costs
Biological Filtration (Biofilters, Bio trickling filters)	Microbial degradation of pollutants in a packed bed or biofilm	Eco-friendly, low operational cost, suitable for continuous flow	Sensitive to environmental conditions (pH, moisture, temperature)
Activated Carbon Adsorption	Adsorbs VOCs and sulfur compounds onto porous carbon surface	High efficiency, compact system	Carbon replacement/regeneration needed, costly for large volumes

Strategies to Overcome Limitations

In recent years, the pursuit of sustainability in industrial pollution control is increasingly driven by both environmental imperatives and economic feasibility. In the context of the leather tanning industry a sector known for its intensive use of chemicals and high emission potential there is an urgent demand for eco-friendly and cost-effective deodorization technologies that do not transfer pollution from one medium to another (from air to water or solid waste), a challenge often observed in conventional treatment systems [67].

Spent Coffee Grounds (SCG)

Spent coffee grounds (SCG), a major byproduct of the coffee brewing industry, have recently gained attention as a sustainable, low cost adsorbent material for environmental applications, including the deodorization of toxic gases from industrial wastewater effluents [6]. The unique physicochemical properties of SCG make them particularly suitable for capturing and neutralizing harmful gases [68, 69].

Chemical Composition of (SCG)

Spent coffee grounds (SCG) primarily consist of lingo cellulosic biomass, forming a complex matrix of organic compounds that contribute to their adsorption capabilities. The main constituents include cellulose, hemicellulose, lignin, proteins, lipids, residual caffeine, and phenolic compounds. This diverse chemical composition provides a variety of functional groups on the SCG surface that serve as active sites for gas adsorption [70]. Among these, hydroxyl groups (-OH), mostly found in cellulose and hemicellulose, play a crucial role by facilitating hydrogen bonding and polar interactions with polar gases such as ammonia (NH_3) and hydrogen sulfide (H_2S). These polar interactions enhance the affinity of SCG for such gases, making them effective adsorbents in capturing malodorous and toxic compounds [71].

Additionally, carboxyl groups (-COOH), largely contributed by lignin and oxidized cellulose, enable acid-base interactions and can form ionic bonds with basic gases like ammonia, thereby improving adsorption capacity through electrostatic attraction. Phenolic groups, derived from lignin and residual antioxidant compounds in SCG, act as electron donors or acceptors, which allows them to participate in redox reactions that may aid in the transformation or neutralization of toxic gases [70]. Furthermore, nitrogen-containing groups from residual proteins and caffeine provide amine or amide functionalities capable of hydrogen bonding with acidic gases, further broadening the spectrum of interactions SCG can engage in. Together,

these chemical features support the potential of SCG as a versatile and effective adsorbent for industrial gas treatment applications [71].

Porous Structure and Surface Area of SCG

The adsorption efficiency of spent coffee grounds (SCG) is significantly influenced by their unique physical structure, which is characterized by a naturally porous and fibrous texture. This structure is a result of cellular wall degradation and water-soluble component removal during the brewing process, leading to increased surface exposure and internal void formation [70]. The porous nature of SCG serves as a critical feature in their function as an adsorbent. Firstly, the high specific surface area of SCG, often reported in the range of 1.2 to 5.4 m^2/g for raw grounds and exceeding 300 m^2/g after activation, provides a large number of adsorption sites, enhancing the material's capacity to capture gas molecules. Secondly, the presence of both micro-pores (<2 nm) and meso-pores (2–50 nm) enables the adsorption of a wide variety of gaseous pollutants, including hydrogen sulfide (H_2S), ammonia (NH_3), and volatile organic compounds (VOCs) [72]. These multiscale pore distributions improve adsorption kinetics by facilitating gas transport and diffusion throughout the matrix. Finally, the highly accessible surface of SCG ensures rapid contact between pollutant molecules and the material's functional groups (hydroxyl, carboxyl), allowing for efficient physisorption and chemisorption processes [72]. This combination of pore structure and accessible surface area makes SCG a compelling and sustainable alternative to conventional adsorbents, particularly for the treatment of odorous gases in industrial applications such as tannery emissions [73].

Surface Chemistry and Charge of SCG

The surface chemistry and electrostatic properties of spent coffee grounds (SCG) play a pivotal role in determining their gas adsorption behavior, particularly in environments such as tannery wastewater treatment, where acidic or basic gases are prevalent. SCG are composed of a complex matrix of lingo-cellulosic components primarily cellulose, hemicellulose, and lignin which contain a variety of oxygen- and nitrogen-containing functional groups [70]. These include hydroxyl (-OH), carboxyl (-COOH), amine ($-NH_2$), and phenolic (-PhOH) moieties that contribute to surface reactivity and charge distribution. At the slightly acidic to neutral pH values typical of tannery effluents (pH 5.5–7.5), carboxylic acid groups on the SCG surface can dissociate, imparting a negative surface charge [71]. This facilitates electrostatic interactions with positively charged species, such as ammonium ions (NH_4^+), or polar basic gases like ammonia (NH_3), via ion exchange or hydrogen bonding mechanisms. Moreover, the presence of redox-active phenolic groups inherited from the lignin and residual antioxidants in coffee grounds provides additional functionality [74]. These phenolic moieties can act as electron donors or acceptors, enabling redox reactions that may contribute to the oxidative degradation or transformation of sulfur-containing gases such as hydrogen sulfide (H_2S) into less volatile or less toxic forms (elemental sulfur or sulfate) [73]. Overall, the interplay between surface charge and functional group chemistry endows SCG with a dual adsorption mechanism: physisorption through surface area and porosity, and chemisorption through electrostatic and redox interactions, making them highly effective for capturing and neutralizing a range of odorous and hazardous gases from industrial sources [72, 73].

Mechanisms of Gas Removal Using Spent Coffee Grounds (SCG)

Spent coffee grounds (SCG) have emerged as promising bio-based adsorbents for the removal of odorous and toxic gases, particularly those associated with leather tanning wastewater such as ammonia (NH_3), hydrogen sulfide (H_2S), and volatile organic compounds (VOCs) [70]. The effectiveness of SCG in gas removal stems from a synergistic combination of physical adsorption, chemical interactions, and redox activity, all of which are mediated by the material's rich surface chemistry, porosity, and functional group diversity [72]. A mechanistic understanding of these processes is essential to optimize SCG

preparation, activation, and deployment strategies in sustainable odor control technologies [73].

Physical Adsorption

Physical adsorption refers to the non-covalent, reversible adherence of gas molecules onto the surface of SCG through weak intermolecular forces such as van der Waals attractions. SCG's high specific surface area and porous morphology comprising micro- and mesoporous enable the trapping of gas molecules by pore-filling mechanisms [75]. These pores provide abundant active sites and facilitate gas diffusion into the adsorbent matrix. The adsorption efficiency increases with the availability of fine pores that closely match the kinetic diameters of gas molecules like NH_3 (~2.6 Å) and H_2S (~3.6 Å) [68, 76].

Moreover, surface adherence plays a crucial role in the initial capture of VOCs and other weakly polar compounds. The interaction is primarily governed by dispersion forces, making the process rapid and non-selective. Environmental parameters such as temperature, pressure, and humidity significantly influence the adsorption dynamics. Moderate moisture levels may aid gas capture by forming a hydrated layer on SCG surfaces, which can increase the solubility of hydrophilic gases (e.g., NH_3), thereby enhancing their uptake. However, excessive water content can obstruct pore accessibility, reducing overall adsorption efficiency [75, 77].

Chemical Adsorption (Chemisorption)

In addition to physical adsorption, spent coffee grounds (SCG) facilitate chemical adsorption (chemisorption) through their diverse surface functional groups. Chemisorption involves stronger, often irreversible chemical bonds between gas molecules and the reactive sites on SCG, leading to more selective and effective removal of odorous gases [78]. One key mechanism is acid-base interaction, where basic gases like ammonia (NH_3) react with acidic groups such as carboxyl (-COOH) present in lignin and oxidized cellulose fractions of SCG. This interaction typically involves proton transfer or ionic bond formation, resulting in the generation of ammonium salts (NH_4^+) that become immobilized on the adsorbent surface. Additionally, hydrogen bonding plays a significant role: gases like NH_3 and hydrogen sulfide (H_2S) can form hydrogen bonds with hydroxyl (-OH) and amine (-NH) groups in SCG, which increases their adsorption affinity and retention time. Under alkaline or neutral pH conditions, electrostatic attractions occur as negatively charged carboxylate groups ($-COO^-$) on SCG surfaces attract positively charged gas species or ions, further enhancing selective adsorption capacity [79].

Redox Reactions and Gas Transformation

A distinctive advantage of SCG lies in their content of phenolic and other antioxidant compounds, which confer redox activity capable of chemically transforming toxic gases into less harmful species. For example, the reduction of hydrogen sulfide (H_2S) is facilitated by phenolic groups donating electrons, thereby converting H_2S into elemental sulfur (S^o) or other less volatile sulfur compounds. This redox transformation not only immobilizes sulfur gases but also reduces their toxicity and odor impact [80]. Similarly, although less extensively studied, SCG's redox-active functional groups may participate in the oxidation or breakdown of ammonia and volatile organic compounds (VOCs), potentially leading to mineralization or conversion into less harmful forms. These redox-mediated pathways add a layer of detoxification beyond simple adsorption, improving the overall sustainability and regeneration potential of SCG as bio-based deodorization agents [81].

Multimodal Adsorption and Synergistic Effects

The effectiveness of spent coffee grounds (SCG) in treating complex gaseous emissions from tannery wastewater systems is largely attributed to their capacity to engage in multimodal adsorption mechanisms, where physical, chemical, and redox interactions occur simultaneously or sequentially [82]. This synergistic behavior enhances the overall

adsorption efficiency, particularly in mixed-gas environments. For instance, sequential adsorption and transformation may occur when a gas such as ammonia (NH_3) is first captured through acid-base interactions with carboxylic groups, followed by chemical alteration via redox-active phenolics [83]. Additionally, competitive adsorption is an important factor; various gas species may vie for overlapping active sites on the SCG surface, which can influence the adsorption selectivity and kinetics. The presence of moisture also plays a crucial role by enhancing gas solubility, enabling hydrolysis reactions, and supporting protonation processes that aid in gas immobilization or conversion. These interdependent effects contribute to the robustness of SCG as a versatile adsorbent in dynamic industrial emission settings [84].

Regeneration and Reusability

The regeneration and reusability of SCG are critical parameters in assessing their feasibility as sustainable gas adsorbents. After saturation with odorous gases, regeneration can typically be achieved through mild thermal desorption (heating at 100–150°C) or solvent washing, especially for physically adsorbed species. This restores the porous structure and surface activity of SCG without significant degradation of the material [85]. However, the chemical stability of adsorbed compounds particularly those bound via chemisorption or transformed through redox reactions may limit complete regeneration. In such cases, stronger desorption methods or partial loss in adsorption capacity over cycles may be observed. Despite these limitations, SCG demonstrate promising recyclability, especially when used in systems where physical adsorption predominates. Optimizing regeneration protocols balancing temperature, treatment duration, and chemical additives can enhance both the economic viability and environmental performance of SCG-based odor control technologies [76].

Application Studies of Spent Coffee Grounds (SCG) for Deodorization

Studies involving SCG and SCG-derived materials have demonstrated the potential of these materials to interact with gaseous pollutants through physical adsorption, chemisorption, and related surface interactions. Reported performance depends strongly on the characteristics of the adsorbent and operating conditions, including particle size, surface modification, moisture content, gas concentration, flow rate, temperature, and contact time. Consequently, removal efficiencies reported under controlled laboratory conditions cannot be directly extrapolated to complex tannery wastewater gas streams [86].

For example, studies on modified coffee-ground materials and related bio-based systems have reported measurable removal of sulfur- and nitrogen-containing odorants under controlled experimental conditions. Such findings provide useful evidence for the adsorption potential of coffee-derived materials but do not, by themselves, demonstrate equivalent performance for real tannery wastewater emissions [87]. Surface modification methods, including thermal activation, chemical activation, and incorporation of additional functional materials, may improve surface area, porosity, and the availability of active functional groups. Nevertheless, the effectiveness of these modifications must be evaluated using standardized experimental conditions and, ultimately, under realistic tannery emission conditions [88].

Overall, existing studies support the potential of SCG as a sustainable adsorbent for odor-control applications, but direct evidence for the removal of H_2S, NH_3, and VOCs specifically from tannery wastewater gas remains limited. Further research using real tannery gas streams, representative gas mixtures, continuous-flow systems, and pilot-scale experiments is therefore required before quantitative removal efficiencies can be reliably assigned to tannery-specific applications [89]. Additionally, regeneration studies suggest that SCG can retain a significant

proportion of their adsorption capacity after multiple thermal desorption cycles at 100–150°C, thereby improving their lifecycle performance and economic feasibility [85].

CHALLENGES AND FUTURE DIRECTIONS

Despite the promising adsorption capacity of spent coffee grounds (SCG) for removing toxic gases from leather tannery wastewater, several challenges hinder their large-scale application. Raw SCG has relatively low surface area and porosity compared to commercial adsorbents like activated carbon, limiting its efficiency. Moreover, the variability in SCG composition due to differences in coffee types, roasting levels, and brewing methods can affect adsorption consistency and reproducibility. Additionally, the high moisture and oil content of SCG may require pre-treatment steps such as drying, carbonization, or chemical activation, which increase operational complexity and cost. There are also concerns regarding the regeneration and safe disposal of spent SCG adsorbents after use, particularly when saturated with hazardous substances. Future studies should focus on optimizing SCG modification techniques, such as pyrolysis, acid/base activation, or incorporation with other biomaterials, to enhance surface area, functional groups, and gas adsorption efficiency. Research is also needed to standardize SCG collection and treatment protocols to ensure consistent quality and performance. Moreover, integrating SCG-based adsorbents into hybrid systems with membranes or biofilters could improve removal efficiency and operational flexibility. Life cycle assessments and techno-economic analyses are essential to evaluate the sustainability and feasibility of SCG use at industrial scale. Lastly, in-depth studies on adsorption mechanisms, regeneration cycles, and long-term stability will be critical to establish SCG as a reliable, low-cost, and eco-friendly solution for treating tannery gas emissions.

CONCLUSIONS

The control of toxic and malodorous gases associated with leather tannery wastewater remains an important environmental challenge, particularly because emissions may contain hydrogen sulfide (H_2S), ammonia (NH_3), and volatile organic compounds (VOCs). Spent coffee grounds (SCG) represent a potentially sustainable bio-based adsorbent because of their lignocellulosic structure, surface functional groups, and availability as an agro-industrial residue.

Available studies indicate that SCG and SCG-derived materials can interact with gaseous pollutants through physical adsorption and chemical surface interactions. However, the reported removal efficiencies are highly dependent on experimental conditions, including adsorbent preparation, gas composition, pollutant concentration, humidity, temperature, flow rate, and contact time. Importantly, much of the available evidence has been obtained under controlled laboratory conditions or from applications involving gas streams and odor sources other than tannery wastewater. Therefore, these results should not be interpreted as direct evidence of equivalent removal performance for real tannery wastewater gases.

The specific application of SCG for tannery wastewater gas deodorization remains insufficiently validated. In particular, direct experimental data obtained using real tannery gas, streams are limited. Accordingly, SCG should currently be regarded as a promising research candidate rather than a fully demonstrated tannery-specific gas treatment technology.

Future research should prioritize systematic experiments using representative and real tannery waste water gas streams containing H_2S, NH_3, VOCs, and relevant gas mixtures. Studies should evaluate adsorption capacity, removal efficiency, selectivity, regeneration, long-term stability, and performance under realistic humidity, temperature, flow, and concentration conditions. Pilot-scale and field-based investigations, together with life cycle and

techno-economic assessments, will be necessary to determine the practical feasibility of SCG-based deodorization systems.

Within these limitations, the valorization of SCG remains consistent with circular-economy principles and provides a promising research direction for developing potentially low-cost and sustainable approaches to odor and gaseous-pollutant management in the leather industry.

REFERENCES

1. Zhao, J., Wu, Q., Tang, Y., Zhou, J., Guo, H., Tannery Wastewater Treatment: Conventional and Promising Processes, an Updated 20-year Review, *J Leather Sci Eng*, **2022**, 4, 1, 10, https://doi.org/10.1186/s42825-022-00082-7.
2. Stachowiak, N., Kowalonek, J., Kozlowska, J., Effect of Plasticizer and Surfactant on the Properties of Poly (Vinyl Alcohol)/Chitosan Films, *Int J Biol Macromol*, **2020**, 164, 2100-2107, https://doi.org/10.1016/j.ijbiomac.2020.08.001.
3. Abdul Mutalib, A.A., Jaafar, N.F., Miskam, M., Shafie, S., Comprehensive Functionality Analysis of Spent Coffee Grounds Activated Using a Microwave-Assisted Method, *J Dispers Sci Technol*, **2024**, 46, 1, 72-87, https://doi.org/10.1080/01932691.2023.2278495.
4. Rybarczyk, P., Removal of Volatile Organic Compounds (VOCs) From Air: Focus on Biotrickling Filtration and Process Modeling, *Processes*, **2022**, 10, 12, 2531, https://doi.org/10.3390/pr10122531.
5. Kumar, M.A., Sinha, D., Basheer, S.M., Biological Treatment of Volatile Organic Compounds (VOCs) and Odorous Compounds, in Selvasembian, R., van Hullebusch, E.D., Mal, J. (eds.), *Biotechnology for Environmental Protection*, **2022**, Springer, 131-164, https://doi.org/10.1007/978-981-19-4937-1_5.
6. Ahmed, H., Abolore, R.S., Jaiswal, S., Jaiswal, A.K., Toward Circular Economy: Potentials of Spent Coffee Grounds in Bioproducts and Chemical Production, *Biomass*, **2024**, 4, 2, 286-312, https://doi.org/10.3390/biomass4020014.
7. Priena, G.H., Handajani, M., Nisa, L.M., Utilization of Spent Coffee Grounds as Adsorbent: A Review, in *Proceedings of the 4th ITB Graduate School Conference - Innovation and Discovery for Sustainability*, July 6, **2023**, 727-739.
8. Zhao, N., Liu, Z., Yu, T., Yan, F., Spent Coffee Grounds: Present and Future of Environmentally friendly Applications on Industries-A Review, *Trends Food Sci Technol*, **2024**, 143, 104312, https://doi.org/10.1016/j.tifs.2023.104312.
9. Jallouli, S., Wali, A., Buonerba, A., Zarra, T., Belgiorno, V., Naddeo, V., Ksibi, M.,, Efficient and Sustainable Treatment of Tannery Wastewater by a Sequential Electrocoagulation-UV Photolytic Process, *J Water Process Eng*, **2020**, 38, 101642, https://doi.org/10.1016/j.jwpe.2020.101642.
10. Buljan, J., Král, I., Clonfero, G., *Introduction to Treatment of Tannery Effluents*, UNIDO, Vienna, **2011**.
11. Mallick, M.A.I., Malakar, R., Ghorai, N., Saha, A., Mukherjee, P., Sanyal, T., Revolutionizing Leather Industry Wastewater Treatment: A Game-Changing Approach for Sustainable Environmental Management, in: Roychoudhury, S., Sanyal, T., Sen, K., Sanyal, S.M. (eds.), *A Basic Overview of Environment and Sustainable Development*, vol. 2, **2023**, 390-407, https://doi.org/10.52756/boesd.2023.e02.027.
12. Dancila, A.M., Bosomoiu, M., Exploring the Possibilities of Using Recovered Collagen for Contaminants Removal—A Sustainable Approach for Wastewater Treatment, *Polymers*, **2024**, 16, 20, 2923, https://doi.org/10.3390/polym16202923.
13. Sultana, R., Rashid, T.U., Rahman, M.M., Enzymatic Approaches for Tannery Waste Valorization, in: Kumar, V., Verma, P. (eds.), *Biotechnological Applications in Industrial Waste Valorization*, **2025**, Springer, 407-435, https://doi.org/10.1007/978-981-96-2302-0_12.
14. Al Sharabaty, R., Sarsour, S., Leather Manufacturing Wastewater Characterization and Cleaner Production Options, Palestine Polytechnic University, **2017**.
15. George, J.S., Ramos, A., Shipley, H.J., Tanning Facility Wastewater Treatment: Analysis of Physical–Chemical and Reverse Osmosis Methods, *J Environ Chem Eng*, **2015**, 3, 2, 969-976, https://doi.org/10.1016/j.jece.2015.03.011.
16. Kebede, A.M., Andualem, G., Yiheyis, B., Kassie, M., Brihane, D., Extraction of Keratin Hydrolysate from Tannery Sheep Hair Waste for Industrial Application of Leather Processing, Thesis, **2023**.
17. Piera Framis, C., Assessment of Tannery Solid Waste Management: A Case of Sheba Leather Industry in Wukro (Ethiopia), Bachelor Thesis, Escola Tècnica Superior d'Enginyeria Industrial de Barcelona, **2018**.
18. Saxena, G., Chandra, R., Bharagava, R.N., Environmental Pollution, Toxicity Profile and Treatment Approaches for Tannery Wastewater and Its Chemical Pollutants, in: de Voogt, P.

(ed.), *Reviews of Environmental Contamination and Toxicology Volume 240*, **2016**, 31-69, https://doi.org/10.1007/398_2015_5009.
19. Metcalf and Eddy Inc., Tchobanoglous, G., Stensel, H.D., Tsuchihashi, R., Burton, F.L., *Wastewater Engineering Treatment and Resource Recovery*, 5th edition, **2014**, McGraw-Hill Education.
20. Roane, T.M., Pepper, I.L., Microscopic Techniques, in: Pepper, I.L., Gerba, C.P., Gentry, T.J. (eds.), *Environmental Microbiology*, 3rd edition, **2015**, Elsevier, 177-193, https://doi.org/10.1016/B978-0-12-394626-3.00009-0.
21. Bitton, G., *Wastewater Microbiology*, **2011**, John Wiley & Sons, https://doi.org/10.1002/9780470901243.
22. Carter, D.R., Adams, N.J., Hydrogen Sulfide in the Drilling Industry, SPE Deep Drilling and Production Symposium, **1979**, https://doi.org/10.2118/7854-MS.
23. Tchobanoglous, G., Leverenz, H., Comprehensive Source Control for Potable Reuse, *Front Environ Sci*, **2019**, 7, 95, https://doi.org/10.3389/fenvs.2019.00095.
24. Bosnic, M., Buljan, J., Daniels, R., Pollutants in Tannery Effluents, United Nations Industrial Development Organization, **2000**, p. 26.
25. Rich, V., Maier, R.M., Aquatic Environments, in: Pepper, I.L., Gerba, C.P., Gentry, T.J. (eds.), *Environmental Microbiology*, 3rd edition, **2015**, Elsevier, 111-138, https://doi.org/10.1016/B978-0-12-394626-3.00006-5.
26. Wang, H.L., Nie, L., Li, J., Wang, Y.F., Wang, G., Wang, J.H., Hao, Z.P., Characterization and Assessment of Volatile Organic Compounds (VOCs) Emissions from Typical Industries, *Chin Sci Bull*, **2013**, 58, 7, 724-730, https://doi.org/10.1007/s11434-012-5345-2.
27. Covington, A., Fundamentals of Leather Science, XXXIV IULTCS Congress, **2017**.
28. United States Environmental Protection Agency, National Management Measures to Control Non-Point Source Pollution for Urban Areas, EPA-841-B-05-004, November **2005**.
29. Panda, R.C., Rai, C.L., Sivakumar, V., Mandal, A.B., Odour Removal in Leather Tannery, *Adv Chem Eng Sci*, **2012**, 2, 02, 199-203, https://doi.org/10.4236/aces.2012.22024.
30. Lomans, B.P., van der Drift, C., Pol, A., Op den Camp, H.J.M., Microbial Cycling of Volatile Organic Sulfur Compounds, in: Bruzzone, R., Thomas, J.L. (eds.), *Cellular and Molecular Life Sciences*, **2002**, 59, 4, 575-588, https://doi.org/10.1007/s00018-002-8450-6.
31. Kesselmeier, J., Merk, L., Exchange of Carbonyl Sulfide (COS) Between Agricultural Plants and the Atmosphere: Studies on the Deposition of COS to Peas, Corn and Rapeseed, *Biogeochemistry*, **1993**, 23, 1, 47-59, https://doi.org/10.1007/BF00002922.
32. Sharma, N., Agarwal, A.K., Eastwood, P., Gupta, T., Singh, A.P. (eds.), *Air Pollution and Control*, **2018**, Springer, https://doi.org/10.1007/978-981-10-7185-0.
33. Lackner, M., Palotás, Á., Winter, F., *Combustion: From Basics to Applications*, **2013**, John Wiley & Sons, https://doi.org/10.1002/9783527667185.
34. Skrypski-Mäntele, S., Bridle, T., Environmentally Sound Disposal of Tannery Sludge, *Water Res*, **1995**, 29, 4, 1033-1039, https://doi.org/10.1016/0043-1354(94)00261-5.
35. Hansen, É., de Aquim, P.M., Gutterres, M., Environmental Assessment of Water, Chemicals and Effluents in Leather Post-Tanning Process: A Review, *Environ Impact Assess Rev*, **2021**, 89, 106597, https://doi.org/10.1016/j.eiar.2021.106597.
36. Wang, L.K., Pereira, N.C., Hung, Y.T. (eds.), *Air Pollution Control Engineering*, Vol. 1, **2004**, Springer, https://doi.org/10.1007/978-1-59259-778-9.
37. Frechen, F., Odour Emissions and Odour Control at Wastewater Treatment Plants in West Germany, *Water Sci Technol*, **1988**, 20, 4-5, 261-266, https://doi.org/10.2166/wst.1988.0175.
38. American Conference of Governmental Industrial Hygienists, *Industrial Ventilation: A Manual of Recommended Practice*, **1995**.
39. Cooper, C.D., Alley, F.C., *Air Pollution Control: A Design Approach*, **2010**, Waveland Press.
40. Belgiorno, V., Naddeo, V., Zarra, T., *Odour Impact Assessment Handbook*, **2012**, John Wiley & Sons, https://doi.org/10.1002/9781118481264.
41. Mukhopadhyay, A., Pandit, V., Control of Industrial Air Pollution through Sustainable Development, Environment, *Development and Sustainability*, **2014**, 16, 1, 35-48, https://doi.org/10.1007/s10668-013-9473-x.
42. Brancher, M., Griffiths, K.D., Franco, D., de Melo Lisboa, H., A Review of Odour Impact Criteria in Selected Countries Around the World, *Chemosphere*, **2017**, 168, 1531-1570, https://doi.org/10.1016/j.chemosphere.2016.11.160.
43. Stuetz, R.M., Frechen, F.-B. (eds.), *Odours in Waste Water Treatment: Measurement, Modelling and Control*, **2001**, IWA Publishing.
44. Vallero, D.A., *Fundamentals of Air Pollution*, **2025**, Academic Press, https://doi.org/10.1016/C2023-0-52324-9.
45. Sorrels, J.L., Baynham, A., Randall, D.D., Schaffner, K.S., Carbon Adsorbers, in: *EPA Air*

Pollution Control Cost Manual, US Environmental Protection Agency: Research Triangle Park, NC, USA, **2018**, 1-47.
46. Seinfeld, J.H., Pandis, S.N., *Atmospheric Chemistry and Physics: From Air Pollution to Climate Change*, **2016**, John Wiley & Sons.
47. De Nevers, N., *Air Pollution Control Engineering*, **2010**, Waveland Press.
48. Richardson, S.D., Postigo, C., The Next Generation of Drinking Water Disinfection By-products: Occurrence, Formation, Toxicity, and New Links with Human Epidemiology, in: Thompson, K.C., Gillespie, S., Goslan, E. (eds.), *Disinfection By-products in Drinking Water*, **2015**, Royal Society of Chemistry, https://doi.org/10.1039/9781782622710-00001.
49. Mohseni, M., Biological Treatment of Waste Gases Containing Inorganic Compounds, in: Shareefdeen, Z., Singh, A. (eds.), *Biotechnology for Odor and Air Pollution Control*, **2005**, Springer, 253-279, https://doi.org/10.1007/3-540-27007-8_12.
50. Singh, A., Shareefdeen, Z., Ward, O.P., Bioscrubber Technology, in: Shareefdeen, Z., Singh, A. (eds.), *Biotechnology for Odor and Air Pollution Control*, **2005**, Springer, 169-193, https://doi.org/10.1007/3-540-27007-8_8.
51. Rittmann, B.E., McCarty, P.L., *Environmental Biotechnology: Principles and Applications*, Vol. 6, **2001**, McGraw-Hill New York.
52. Daginnus, K., Marty, T., Trotta, N.V., Brinkmann, T., Whitfield, A., Roudier, S., *Best Available Techniques (BAT) Reference Document for Common Waste Gas Management and Treatment Systems in the Chemical Sector*, JRC Science for Policy Report, **2023**, https://doi.org/10.2760/220326.
53. Jadoun, S., Erfani, H., Khodayari, S., Kalantari, F., Fatahi, S., Gorjizadeh, F., A Review of Biological Methods for Air Pollution Control and Environmental Sustainability, *Water Air Soil Poll*, **2025**, 236, 10, 669, https://doi.org/10.1007/s11270-025-08315-1.
54. Anjumol, K.P., Kundu, P., Mishra, I.M., Anju, A.V., Current Progress and Perspectives of Various Biological Technologies for Treatment of Gaseous Pollutants: A State-of-the-Art Review, *J Inst Eng (India) Ser E*, **2025**, 106, 2, 277-307, https://doi.org/10.1007/s40034-025-00310-9.
55. Zhang, B., Ma, Z., Zhang, Y., Wang, L., Yan, J., Ling, S., Fang, X., Odor Control Technologies for Municipal Solid Waste Mechanical Biological Treatment Plant: A Review, *Clean Technol Environ Policy*, **2025**, 27, 7, 2741-2758, https://doi.org/10.1007/s10098-024-02952-6.
56. Khan, H., Arshad, M., Jalal, A., Khalid, U., Maqbool, A., Ansari, M., Hussain, S., Mechanistic and Data-Guided Design of Biochar Adsorbents for Gas Phase Pollution Control: A State-of-the-Art Review, *Environ Sci Pollut Res Int*, **2026**, 33, 6, 7424-7451, https://doi.org/10.1007/s11356-026-37767-z.
57. Liu, N., Ning, Z., Jia, Y., Ren, Y., Liu, W., Zhang, Y., Zhao, P., Sun, Peng, Zhang, J., Liu, J., Indoor Odor Pollution: An Interdisciplinary Review from Sources to Control and an Intelligent Building Environment Management Framework, *Buildings*, **2026**, 16, 4, 687, https://doi.org/10.3390/buildings16040687.
58. Elehinafe, F.B., Aondoakaa, E.A., Akinyemi, A.F., Agboola, O., Okedere, O.B., Separation Processes for the Treatment of Industrial Flue Gases–Effective Methods for Global Industrial Air Pollution Control, *Heliyon*, **2024**, 10, 11, https://doi.org/10.1016/j.heliyon.2024.e32428.
59. Chen, H., Zhang, C., Chang, Y., Liu, H., Chen, H., Xu, B., Wang, Y., Li, W., Xing, X., Formation and Control of Off-Odors in Aquatic Processing Products: A Review, *Food Sci Anim Prod*, **2025**, 3, 9240124, https://doi.org/10.26599/FSAP.2025.9240124.
60. Colomer, M.T., Special Issue "Design, Synthesis and Applications of Macroporous, Mesoporous, and Microporous Materials", *Int J Mol Sci*, **2024**, 25, 13, 7127, https://doi.org/10.3390/ijms25137127.
61. Czekaj, I., Sobuś, N., Odors Adsorption in Zeolites Including Natural Clinoptilolite: Theoretical and Experimental Studies, *Materials*, **2024**, 17, 13, 3088, https://doi.org/10.3390/ma17133088.
62. Zhu, X., Xin, Y., Yu, L., Liu, S., Han, D., Jia, J., Wang, J., Zhang, Z., Zeolite-based Materials Eliminating Nitrogen Oxides (NO x) and Volatile Organic Compounds (VOCs): Advances and Future Perspectives, *Catal Sci Technol*, **2024**, 14, 17, 4756-4774, https://doi.org/10.1039/D4CY00841C.
63. Talaie, A., Rezania, S., Tamadon, A., Kamyab, H., Mehranzamir, K., Ghasemi, M., Recent Advances in Air Purification Technologies for Volatile Organic Compound Removal: Mechanisms, Performance, and Future Perspectives, *Int J Environ Sci Technol*, **2026**, 23, 5, 397, https://doi.org/10.1007/s13762-026-07235-9.
64. Estrada, J.M., Kraakman, N.J.R.B., Muñoz, R., Lebrero, R., A Comparative Analysis of Odour Treatment Technologies in Wastewater Treatment Plants, *Environ Sci Technol*, **2011**, 45, 3, 1100-1106, https://doi.org/10.1021/es103478j.
65. Majidnia, Z., Fulazzaky, M.A., Photocatalytic Reduction of Cs(I) Ions Removed by Combined Maghemite-Titania PVA-Alginate Beads from Aqueous Solution, *J*

Environ Manag, **2017**, 191, 219-227, https://doi.org/10.1016/j.jenvman.2017.01.019.
66. Zong, P., Wang, S., Zhao, Y., Wang, H., Pan, H., He, C., Synthesis and Application of Magnetic Graphene/Iron Oxides Composite for the Removal of U(VI) from Aqueous Solutions, *Chem Eng J*, **2013**, 220, 45-52, https://doi.org/10.1016/j.cej.2013.01.038.
67. Akhtar, M.S., Ali, S., Zaman, W., Innovative Adsorbents for Pollutant Removal: Exploring the Latest Research and Applications, *Molecules*, **2024**, 29, 18, 4317, https://doi.org/10.3390/molecules29184317.
68. Pyrzynska, K., Spent Coffee Grounds as an Adsorbent Material for Metal Ions, *Materials*, **2026**, 19, 9, 1720, https://doi.org/10.3390/ma19091720.
69. Ungureanu, N., Vlăduț, N.-V., Sustainable Valorization of Spent Coffee Grounds Within the Circular Economy: Innovative Applications in Food, Agriculture, Environmental, and Industrial Sectors, *Sustainability*, **2026**, 18, 8, 4127, https://doi.org/10.3390/su18084127.
70. Mussatto, S.I., Machado, E.M.S., Martins, S., Teixeira, J.A., Production, Composition, and Application of Coffee and Its Industrial Residues, *Food Bioprocess Technol*, **2011**, 4, 5, 661-672, https://doi.org/10.1007/s11947-011-0565-z.
71. Ortega-Villar, R., Lizárraga-Mendiola, L., Coronel-Olivares, C., López-León, L.D., Bigurra-Alzati, C.A., Vázquez-Rodríguez, G.A., Effect of Photocatalytic Fe_2O_3 Nanoparticles on Urban Runoff Pollutant Removal by Permeable Concrete, *J Environ Manag*, **2019**, 242, 487-495, https://doi.org/10.1016/j.jenvman.2019.04.104.
72. Kobayashi, N., Noel, E.A., Barnes, A., Watson, A., Rosenberg, J.N., Erickson, G., Oyler, G.A., Characterization of Three *Chlorella sorokiniana* Strains in Anaerobic Digested Effluent from Cattle Manure, *Bioresour Technol*, **2013**, 150, 377-386, https://doi.org/10.1016/j.biortech.2013.10.032.
73. Travis, W., Gadipelli, S., Guo, Z., Superior CO_2 Adsorption from Waste Coffee Ground Derived Carbons, *RSC Adv*, **2015**, 5, 37, 29558-29562, https://doi.org/10.1039/C4RA13026J.
74. Broglia, M., Pinacci, P., Radaelli, M., Bottino, A., Capannelli, G., Comite, A., Vanacore, G., Zani, M.,, Synthesis and Characterization of Pd Membranes on Alumina-Modified Porous Stainless Steel Supports, *Desalination*, **2009**, 245, 1-3, 508-515, https://doi.org/10.1016/j.desal.2009.01.004.
75. Kempisty, P., Krukowski, S., Adsorption of Ammonia at GaN(0001) Surface in the Mixed Ammonia/Hydrogen Ambient-A Summary of *ab initio* Data, *AIP Adv*, **2014**, 4, 11, https://doi.org/10.1063/1.4901922.
76. Gora, E.H., Saldana, S.G., Casper, L.M., Sijercic, V.C., Giza, O.A., Sanders, R.L., Effect of Exhausted Coffee Ground Particle Size on Metal Ion Adsorption Rates and Capacities, *ACS Omega*, **2022**, 7, 43, 38600-38612, https://doi.org/10.1021/acsomega.2c04058.
77. Kante, K., Nieto-Delgado, C., Rangel-Mendez, J.R., Bandosz, T.J., Spent Coffee-Based Activated Carbon: Specific Surface Features and Their Importance for H_2S Separation Process, *J Hazard Mater*, **2012**, 201, 141-147, https://doi.org/10.1016/j.jhazmat.2011.11.053.
78. Bhatnagar, A., Hogland, W., Marques, M., Sillanpää, M., An Overview of the Modification Methods of Activated Carbon for Its Water Treatment Applications, *Chem Eng J*, **2013**, 219, 499-511, https://doi.org/10.1016/j.cej.2012.12.038.
79. Foo, K.Y., Hameed, B.H., Coconut Husk Derived Activated Carbon via Microwave Induced Activation: Effects of Activation Agents, Preparation Parameters and Adsorption Performance, *Chem Eng J*, **2012**, 184, 57-65, https://doi.org/10.1016/j.cej.2011.12.084.
80. Li, Y.-Q., Zhao, B.-H., Chen, X.-T., Zhang, Y.-Q., Yang, H.-S., Co-existence Effect of Copper Oxide Nanoparticles and Ciprofloxacin on Simultaneous Nitrification, Endogenous Denitrification, and Phosphorus Removal by Aerobic Granular Sludge, *Chemosphere*, **2023**, 312, 137254, https://doi.org/10.1016/j.chemosphere.2022.137254.
81. Rincón-Tomás, B., Lanzén, A., Sánchez, P., Estupiñán, M., Sanz-Sáez, I., Bilbao, M.E., Rojo, D., Mendibil, I., Pérez-Cruz, C., Ferri, M., Capo, E., Abad-Recio, I.L., Amouroux, D., Bertilsson, S., Sánchez, O., Acinas, S.G., Alonso-Sáez, L., Revisiting the Mercury Cycle in Marine Sediments: A Potential Multifaceted Role for Desulfobacterota, *J Hazard Mater*, **2024**, 465, 133120, https://doi.org/10.1016/j.jhazmat.2023.133120.
82. Kim, M.-S., Kim, J.-G., Adsorption Characteristics of Spent Coffee Grounds as an Alternative Adsorbent for Cadmium in Solution, *Environments*, **2020**, 7, 4, 24, https://doi.org/10.3390/environments7040024.
83. Cuccarese, M., Brutti, S., De Bonis, A., Teghil, R., Di Capua, F., Mancini, I.M., Masi, S., Caniani, D., Sustainable Adsorbent Material Prepared by Soft Alkaline Activation of Spent Coffee Grounds: Characterisation and Adsorption Mechanism of Methylene Blue from Aqueous Solutions, *Sustainability*, **2023**, 15, 3, 2454, https://doi.org/10.3390/su15032454.
84. Kebede, T., Taddesse, A.M., Hussen, A., Coffee Spent Supported Fe-Al-Zr Composite: Synthesis, Characterization and Its Adsorptive Dye

Removal from Tannery Wastewater, *Bull Chem Soc Ethiop*, **2023**, 37, 4, 875, https://doi.org/10.4314/bcse.v37i4.6.
85. Aouay, F., Attia, A., Dammak, L., Ben Amar, R., Deratani, A., Activated Carbon Prepared from Waste Coffee Grounds: Characterization and Adsorption Properties of Dyes, *Materials*, **2024**, 17, 13, 3078, https://doi.org/10.3390/ma17133078.
86. Al Balushi, J., Al Saadi, S., Ahanchi, M., Al Attar, M., Jafary, T., Al Hinai, M., Yeneneh, A.M., Basha, J.S., A Comprehensive Review on Sustainable Conversion of Spent Coffee Grounds into Energy Resources and Environmental Applications, *Biomass*, **2025**, 5, 3, 55, https://doi.org/10.3390/biomass5030055.
87. Wang, Y., Cui, R., Jiang, H., Bai, M., Lin, K., Zhang, M., Ren, L., Removal of Hydrogen Sulfide and Ammonia Using a Biotrickling Filter Packed with Modified Composite Filler, *Processes*, **2022**, 10, 10, 2016, https://doi.org/10.3390/pr10102016.
88. Kim, M.-S., Kim, S.-H., Jeong, M., Park, M.-K., Jo, Y.J. Kang, G.-U., Jung, D.-R., Lee, C.-I., Shin, J.-H.,, Fermented Coffee Grounds Diminish Livestock Odors: A Microbiome Study, *Agronomy*, **2021**, 11, 10, 1914, https://doi.org/10.3390/agronomy11101914.
89. Kim, J., Ryu, M.-S., Park, Y.K., Seo, J.-W., Lee, R., Yang, H.-J., Jeong, D.-Y., Effect of Spent Coffee Grounds and *Stenotrophomonas rhizophila* SRCM 116907 on the Removal of Ammonia and Sulfur Compounds in Cattle Manure, *J Anim Environ Sci*, **2024**, 26, 2, 76-86, https://doi.org/10.11109/JAES.2024.26.2.076.

© 2026 by the author(s). Published by INCDTP-ICPI, Bucharest, RO. This is an open access article distributed under the terms and conditions of the Creative Commons Attribution license (http://creativecommons.org/licenses/by/4.0/).

MECHANICAL BEHAVIOR OF BELT LEATHERS PRODUCED WITH DIFFERENT TANNING SYSTEMS

Fatih Furkan YILDIZ[1], Fatih YALÇIN [2], Nilay ORK EFENDIOGLU[1*], Hüseyin Ata KARAVANA[1]

[1]Ege University, Faculty of Engineering, Department of Leather Engineering, 35100, İzmir, Türkiye, nilay.ork@ege.edu.tr

[2]Usak University, Technology Transfer Office, 64100, Usak, Turkey, fatih.yalcin@usak.edu.tr

Received: 29.06.2026 Accepted: 22.09.2026 https://doi.org/10.24264/lfj.26.3.5

MECHANICAL BEHAVIOR OF BELT LEATHERS PRODUCED WITH DIFFERENT TANNING SYSTEMS

ABSTRACT. In this study, the effects of different tanning systems on the mechanical behavior of bovine belt leathers were comparatively investigated. Heavy bovine pickled hides were subjected to three commercial tanning systems: System I (Vegetable-based combination: 10% Mimosa + 10% Quebracho), System II (Synthetic-based combination: 10% Phenolic syntan + 15% White syntan), and System III (Chrome-focused combination: 7% Basic chromium sulphate + 10% Phenolic syntan). Following post-tanning, leather samples were evaluated according to TS EN ISO standards. Statistical analysis was performed using one-way ANOVA followed by Tukey's post-hoc test ($p < 0.05$) to determine significant differences among tanning systems. Experimental findings demonstrated that the tanning system plays a definitive role on leather performance. Tanning System III leathers exhibited superior mechanical properties, recording the highest mean thickness (3.80±0.06 mm), tensile strength (25.34±3.64 N/mm²), double edge tear strength (361.57±34.08 N), grain cracking force (65.00±15.00 kgf), grain bursting force (100.00±7.21 kgf), and stitch tear resistance (509.61±80.54 N). Furthermore, they displayed 0.00% extension set, indicating excellent dimensional stability required for premium belt production. Conversely, Tanning System II leathers demonstrated the highest elasticity with an elongation at break of 69.74±16.34% and a comparable single edge tear load (90.42±15.09 N) but displayed an extension set of 1.30±0.42%. Tanning System I leathers overall exhibited lower mechanical strength (tensile strength: 20.75±6.67 N/mm²; highest extension set: 2.22±1.53%), though they offered superior grain crack (12.71±0.57 mm) and bursting distension (15.41±0.34 mm). Under the conditions investigated, System III provided the most favorable overall mechanical performance for heavy-duty belt leather, while the specific synthetic and vegetable formulations used in Systems II and I, respectively, provided greater extensibility and grain distension. These findings are specific to the commercial tanning formulations investigated and should not be generalized to all vegetable, synthetic, or chrome tanning systems.

KEY WORDS: belt leather, chrome tanning, vegetable tanning, synthetic tanning, mechanical properties

COMPORTAMENTUL MECANIC AL PIEILOR PENTRU CURELE OBȚINUTE PRIN DIFERITE SISTEME DE TĂBĂCIRE

REZUMAT. În acest studiu s-au investigat comparativ efectele diferitelor sisteme de tăbăcire asupra comportamentului mecanic al pieilor bovine destinate fabricării curelelor. S-au tăbăcit piei bovine piclate de greutate mare utilizând trei sisteme comerciale de tăbăcire: Sistemul I (combinație pe bază de tananți vegetali: 10% Mimosa + 10% Quebracho), Sistemul II (combinație pe bază de tananți sintetici: 10% sintan fenolic + 15% sintan alb) și Sistemul III (combinație pe bază de crom: 7% sulfat bazic de crom + 10% sintan fenolic). După etapa de retăbăcire, probele de piele au fost evaluate conform standardelor TS EN ISO. Analiza statistică a fost realizată utilizând testul ANOVA unifactorial, urmat de testul post-hoc Tukey ($p < 0,05$), pentru a determina diferențele semnificative între sistemele de tăbăcire. Rezultatele experimentale au demonstrat că sistemul de tăbăcire joacă un rol determinant în performanța pielii. Pieile obținute prin Sistemul III de tăbăcire au prezentat proprietăți mecanice superioare, înregistrând cele mai ridicate valori medii pentru: grosime (3,80±0,06 mm), rezistență la rupere (25,34±3,64 N/mm²), rezistență la sfâșiere pe două margini (361,57±34,08 N), forță de crăpare a feței (65,00±15,00 kgf), forță de plesnire a feței (100,00±7,21 kgf) și rezistență la sfâșiere la cusătură (509,61±80,54 N). De asemenea, acestea au prezentat o deformare remanentă la întindere de 0,00%, indicând o stabilitate dimensională excelentă, necesară pentru producția de curele premium. În schimb, pieile obținute prin Sistemul II de tăbăcire au demonstrat cea mai mare elasticitate, cu o alungire la rupere de 69,74±16,34% și o forță de sfâșiere pe o singură margine comparabilă (90,42±15,09 N), dar au prezentat o deformare remanentă la întindere de 1,30±0,42%. În ansamblu, pieile prelucrate prin Sistemul de tăbăcire I au prezentat o rezistență mecanică mai scăzută (rezistență la rupere: 20,75 ± 6,67 N/mm²; alungire remanentă maximă: 2,22 ± 1,53%), însă au oferit performanțe superioare în ceea ce privește rezistența la crăparea feței (12,71 ± 0,57 mm) și la plesnirea feței (15,41 ± 0,34 mm). În condițiile studiate, Sistemul III a asigurat cea mai favorabilă performanță mecanică generală pentru pielea destinată curelelor cu regim intens de utilizare, în timp ce formulările sintetice și vegetale specifice, utilizate în Sistemele II, respectiv I, au conferit o extensibilitate și o capacitate de distensie a feței mai mari. Aceste rezultate sunt specifice formulelor comerciale de tăbăcire analizate și nu trebuie generalizate la toate sistemele de tăbăcire vegetală, sintetică sau cu săruri de crom.

CUVINTE CHEIE: piele pentru curele, tăbăcire în crom, tăbăcire vegetală, tăbăcire sintetică, proprietăți mecanice

LE COMPORTEMENT MÉCANIQUE DES CUIRS DE CEINTURE PRODUITS AVEC DIFFÉRENTS SYSTÈMES DE TANNAGE

RÉSUMÉ. Cette étude compare les effets de différents systèmes de tannage sur le comportement mécanique des cuirs de ceinture bovins. Des peaux de bovins épaisses, préalablement picklées, ont été soumises à trois systèmes de tannage commerciaux : le Système I (combinaison végétale : 10 % de mimosa et 10 % de quebracho), le Système II (combinaison synthétique : 10 % de tanin phénolique synthétique et 15 % de tanin blanc synthétique) et le Système III (combinaison à base de chrome : 7 % de sulfate de chrome basique et 10 % de tanin phénolique synthétique). Après tannage, les échantillons de cuir ont été évalués selon la norme TS EN ISO. Une analyse statistique a été réalisée par l'ANOVA à un facteur, suivie du test post-hoc de Tukey ($p < 0,05$) afin de déterminer les différences significatives entre les systèmes de tannage. Les résultats expérimentaux ont démontré que le système de tannage influence fortement les

* *Correspondence to: Nilay ORK EFENDIOGLU, Ege University, Faculty of Engineering, Department of Leather Engineering, 35100, İzmir, Türkiye, nilay.ork@ege.edu.tr*

performances du cuir. Les cuirs tannés selon le Système III ont présenté des propriétés mécaniques supérieures, avec une épaisseur moyenne (3,80 ± 0,06 mm), une résistance à la traction (25,34 ± 3,64 N/mm²), une résistance au déchirement des deux bords (361,57 ± 34,08 N), une force de fissuration de la fleur (65,00 ± 15,00 kgf), une force d'éclatement de la fleur (100,00 ± 7,21 kgf) et une résistance à l'arrachement au point de couture (509,61 ± 80,54 N) plus élevées. De plus, ils ont affiché un allongement à la rupture de 0,00 %, ce qui indique une excellente stabilité dimensionnelle, essentielle à la fabrication de ceintures haut de gamme. À l'inverse, les cuirs tannés selon le Système II ont démontré la plus grande élasticité, avec un allongement à la rupture de 69,74 ± 16,34 % et une résistance au déchirement d'un seul bord comparable (90,42 ± 15,09 N), mais un allongement à la rupture de 1,30 ± 0,42 %. Les cuirs tannés selon le Système I ont globalement présenté une résistance mécanique inférieure (résistance à la traction : 20,75 ± 6,67 N/mm² ; allongement maximal : 2,22 ± 1,53 %), malgré une meilleure résistance à la gerçure (12,71 ± 0,57 mm) et à l'éclatement (15,41 ± 0,34 mm) de la fleur. Dans les conditions étudiées, le Système III a offert les meilleures performances mécaniques globales pour les cuirs de ceintures robustes, tandis que les formulations synthétiques et végétales spécifiques utilisées respectivement dans les Systèmes II et I ont permis une extensibilité et un allongement de la fleur supérieurs. Ces résultats sont spécifiques aux formulations de tannage commerciales étudiées et ne doivent pas être généralisés à tous les systèmes de tannage végétaux, synthétiques ou au chrome.
MOTS-CLÉS : cuir de ceinture, tannage au chrome, tannage végétal, tannage synthétique, propriétés mécaniques

INTRODUCTION

Leather is a natural polymeric material characterized by a complex, three-dimensionally interwoven network of collagen fibers. Its mechanical properties are affected by many factors and used in evaluating the quality and suitability of leather [1]. In the leather industry, products designated for manufacturing bags, belts, wallets, and industrial accessories are broadly classified as leather goods. Depending on specific consumer demands, these leathers require structural adaptations ranging from a flexible, soft touch to an extremely compact, firm, and rigid character [2]. Historically, the evolutionary steps of tanning began when early humans discovered that certain plant woods, barks, roots, and seeds rich in natural polyphenolic tannins could systematically transform raw hides into non-putrescible, durable materials [3]. In the modern manufacturing of heavy-duty leather goods, the choice of the tanning system remains the most crucial chemical factor establishing macromolecular architecture and ultimate performance limits of the leather matrix.

Among various commercial leather applications, belt leathers occupy a highly demanding technical category. Unlike garment leathers, which are primarily designed to provide softness, drape, and wearer comfort, belt leathers are subjected to continuous mechanical stresses throughout their service life. During daily use, belts must maintain dimensional stability while resisting repeated tensile, bending, and torsional forces generated by fastening and body movements. In addition to these mechanical requirements, belt leathers are commonly used in direct contact with garments and are frequently exposed to perspiration. Therefore, adequate resistance to colour migration, perspiration fastness, and rubbing fastness are important quality attributes that directly affect user satisfaction and product durability. Owing to these requirements, belt leathers exhibit a structural character more closely related to sole and heavy leather products than to garment leathers, requiring a compact fiber structure, high firmness, and superior resistance to deformation [4, 5].

Traditionally, mineral tanning based on basic chromium (III) salts has been the universal standard due to its outstanding cross-linking efficiency, producing leather with exceptional hydrothermal stability and superior strength parameters [6]. However, the strict global environmental regulations and potential ecological footprints of chromium-bearing waste streams have accelerated the engineering of alternative chrome-free matrices.

To address these challenges, continuous efforts have been directed toward optimizing synthetic and vegetable tanning systems capable of providing mechanical properties comparable to conventional chrome tanning. Srinivasan *et al*. (2021) developed a pickle-free tanning approach combining vegetable tannins and aluminum salts and reported a compact fiber structure with high physical strength values [7]. Furthermore, current market trends favor leather products exhibiting enhanced natural appearance and

sustainable production characteristics, leading to renewed interest in vegetable tanning systems. Nevertheless, vegetable-tanned leathers often display higher hydrophilicity and different deformation behavior than chrome-tanned counterparts, requiring careful process optimization and retanning strategies to achieve the desired balance between firmness and flexibility [2].

Recent micro-mechanical characterizations —utilizing advanced methods such as instrumental indentation, zeta potential and surface topography—have confirmed that modern alternative tanning matrices induce highly specific structural profiles within the collagen network that differ fundamentally from traditional chrome baselines [8]. The structural variations induced by these chemical cross-links have direct statistical consequences for commercial performance. As demonstrated by Ork *et al*. (2014) through rigorous statistical modeling on identical bovine raw material, the type of tanning matrix dictates significant differences across physical strength, fastness, and elongation properties, directly determining the leather's suitability for specific high-performance leather goods applications [9].

Although extensive literature focuses on the chemistry or ecological aspects of alternative tanning systems, comparative studies evaluating the comprehensive mechanical performance of bovine belt leathers—including tensile strength, trouser tear strength, double-edge tear strength, grain distension, stitch tear resistance, and dimensional stability—remain remarkably scarce.

Therefore, this study systematically evaluates and contrasts the mechanical behavior of bovine belt leathers produced using three specific commercial tanning formulations: a vegetable combination of mimosa and quebracho, a synthetic combination of phenolic and white syntans, and a chrome-focused combination of basic chromium sulphate and phenolic syntan. By maintaining uniform mechanical operations and identical bovine raw materials across all trials, this paper establishes a precise quantitative baseline. All mechanical results were statistically analyzed using one-way ANOVA followed by Tukey's post-hoc test to ensure robust inter-group comparison and reliable differentiation of tanning effects ($p < 0.05$). The numerical trends and performance differentials observed herein not only elucidate the structural effects of different cross-linking mechanisms but also serve as a guide for selecting optimal tanning matrices based on the mechanical requirements of industrial belt manufacturing.

EXPERIMENTAL

Materials and Methods

In this study, heavy pickled bovine hides sourced from a commercial supplier operating in Bolu, Türkiye, were used as the primary research material. These hides were systematically divided into three experimental groups and processed using the three commercial tanning formulations described below under controlled conditions.

The chemical formulations utilized throughout the processing of the experimental leathers consisted of conventional tannery chemicals. Rather than evaluating theoretical pure single-agent baselines, this study specifically focused on practical recipes commercialized and utilized in current industrial belt leather production. Consequently, the experimental formulations were designed to reflect real-world tanneries' combination systems—such as integrating syntans into chrome matrices to achieve the required structural firmness and density—thereby offering direct insights for industrial applications. These processing chemicals were procured from local commercial suppliers based in Bolu, Türkiye. The specific cross-linking matrix agents utilized for each independent tanning system were determined as follows:

- System I (Vegetable-Based Combination): Commercial natural polyphenolic extracts of mimosa (10%) and quebracho (10%) were utilized as the primary tanning agents to crosslink and stabilize the collagen matrix.
- System II (Synthetic-Based Combination): A formulation of phenolic syntan (10%) and white syntan (15%) was employed to execute the synthetic organic tanning trials.

- System III (Chrome-Focused Combination): A combination of standard basic chromium sulphate (7%) and phenolic syntan (10%) was applied to establish the mineral-synthetic tanning matrix.

All other auxiliary post-tanning chemicals—including sodium format and sodium bicarbonate for basification/ neutralization, specialized fatliquoring agents (neat's-foot oil, lecithin, sulfated oil, sulfosuccinate, and combined oil matrices) and formic acid (HCOOH) for fixation—were of commercial grade and applied directly according to standard industrial leather manufacturing protocols.

Tanning Protocols and Mechanical Operations

The processed bovine hides were split into sides and transferred into experimental tanning drums. The samples were separate-batched and subjected to three independent tanning formulations: System I (vegetable combination), System II (synthetic combination), and System III (chrome-focused combination) (Figure 1). Following the completion of the respective tanning and fixation processes, all experimental leathers were drained, aged on horses, hooked for air-drying, and subjected to identical mechanical softening (setting out and staking) operations.

	TANNING SYSTEM 1	TANNING SYSTEM 2	TANNING SYSTEM 3
DE-PICKLING	• %80 Wator (7-8 Be°) • %1 Sodium Formate, 15' • %1 Sodium Bicarbonate, 60'	• %80 Water (7-8 Be°)	• %80 Water (7-8 Be°)
TANNING	• %10 Mimosa • %10 Quebracho • %2 Penetrating agent, 60' • %1 Sulfite oil, 360', **pH: 4**	• %10 Phenolic Syntan • %5 White Syntan, 60' • %1 Sulfite oil, 30' • %10 White Syntan, 180'	• %10 Phenolic Syntan • %3 Chromium Sulfate, 60' • %1 Sulfite oil, 30' • %4 Chromium Sulfate, 240'
BASIFICATION	-	• %150 Water • %1 Sodium Formate • %1 Sodium Bicarbonate, 180', **pH: 4**	• %100 Water • %1 Sodium Formate • %1 Sodium Bicarbonate, 180', **pH: 4**
WASHING	• %200 Water, 15'	• %200 Water, 15'	• %200 Water, 15'
NOTRALIZATION	• %100 Water • %1.5 Sodium Formiate, 20' • %1 Sodium Bicarbonate, 60', **pH: 5**	• %100 Water • %1.5 Sodium Formiate, 20' • %1 Sodium Bicarbonate, 60', **pH: 5**	• %100 Water • %1.5 Sodium Formiate, 20' • %1 Sodium Bicarbonate, 60', **pH: 5**
FATLIQUORING	• %2 Tallow oil • %2 Lesitin oil • %2 Sulfite oil • %2 Sulfosuccinate • %2 Combine oil, 60' • %1.5 HCOOH, 20'	• %2 Tallow oil • %2 Lesitin oil • %2 Sulfite oil • %2 Sulfosuccinate • %2 Combine oil, 60' • %1.5 HCOOH, 20'	• %2 Tallow oil • %2 Lesitin oil • %2 Suifite oil • %2 Sulfosuccinate • %2 Combine oil, 60' • %1.5 HCOOH, 20'
WASHING	• %300 Water, 15'	• %300 Water, 15'	• %300 Water, 15'

Figure 1. Leather tanning recipes

Sampling and Conditioning

To execute the physical and mechanical characterizations, test specimens were sampled systematically from the designated structural locations of the processed sides in strict compliance with the TS EN ISO 2418 standard. Prior to any mechanical testing, all specimens were kept in a standard controlled atmosphere at 20 ± 2°C and 65 ± 2% relative humidity for at least 48 hours to ensure complete moisture equilibrium according to TS EN ISO 2419.

Mechanical Characterization

The mechanical behavior of the belt leathers was quantified using multi-axial physical tests performed via standardized equipment and specialized templates:

Determination of Thickness: The thickness of the conditioned leather samples

was measured in accordance with the TS EN ISO 2589 standard using a specialized thickness gauge (SATRA, model STD 483). The measurements were executed across designated structural locations to establish the structural baseline for subsequent mechanical evaluations.

Tensile Strength and Elongation (%): The ultimate tensile strength (N/mm^2) and percentage elongation at break of the leather samples were determined using a universal testing machine (Shimadzu, model AG-IS) equipped with a 5 kN load cell and managed via Trapezium-2 software in accordance with the TS EN ISO 3376 standard. The testing machine was operated under continuous structural loading to evaluate the directional resistance of the collagen matrices.

Single Edge Tear Load: The single-edge tear load of the samples was evaluated in accordance with the TS EN ISO 3377-1 standard. The trouser-shaped leather specimens were cut using specialized dies and positioned firmly between the jaws of the Shimadzu AG-IS testing machine with a 5 kN load cell to record the maximum force (N) required to propagate the tear line.

Double Edge Tear Load: The evaluation of multi-directional tear strength was carried out in accordance with the TS EN ISO 3377-2 standard. The rectangular leather samples featuring standard internal slots were positioned between the jaws of the Shimadzu AG-IS testing machine equipped with a 5 kN load cell. The machine was operated until complete structural rupture occurred, and the peak force exerted during the tearing process was recorded in Newtons (N).

Determination of Extension Set: The evaluation of permanent linear deformation profiles was carried out in accordance with the TS EN ISO 17236 standard. Flawless leather specimens were cut to dimensions of 250 x 10 mm using specialized cutting dies. The samples were mounted between the jaws of the universal testing machine (Shimadzu, model AG-IS) with a 5 kN load cell. The testing machine was operated via Trapezium-2 software to subject each specimen to a cyclical mechanical loading up to a force of 20 N for a total of 5 consecutive times. Following the completion of the loading cycles, the leather specimens were removed from the device grips and placed flat on a smooth, horizontal surface, where the final linear dimensions were precisely measured to calculate the percentage of structural extension set.

Determination of Distension and Strength of Surface (Ball Burst Method): The conditioned leather samples were tested according to the principles described in the TS EN ISO 3379 standard using a lastometer. Each leather sample was secured under a standardized compression ring ensuring the central grain area remained clear. While the lastometer advanced a steel ball towards the sample at a constant velocity of 12 mm/min, the force (kgf) and linear distension (mm) at the exact moment of grain cracking were recorded. The device continued to operate until absolute structural bursting occurred, where the ultimate burst force (kgf) and corresponding burst distension (mm) were systematically noted.

Stitch Tear Resistance: Performed using flawless rectangular specimens measuring 50 x 20 mm in accordance with the TS EN ISO 23910 standard. Structural slits were formed on the samples using specialized cutting dies. The test setup was initiated by clamping the upper end of a metal specimen holder into the top grip of a universal tensile testing machine (Shimadzu AG-IS). The perforated end of the leather specimen was positioned between the arms of the holder, and a specialized steel mandrel was locked through both the holder hole and the leather slit. The free lower end of the leather sample was clamped firmly by the bottom grip of the machine. The tensile device was operated at a constant speed of 100 ± 20 mm/min until complete structural rupture occurred. The maximum force at the exact moment of tearing was recorded in Newtons (N) via specialized computer software (Trapezium-2), and comparative analyses were evaluated alongside the pre-measured leather thickness (mm) values.

Statistical Analysis

The experimental data obtained from the physical and mechanical tests were statistically evaluated using one-way analysis

of variance (ANOVA) to determine the effect of tanning system on the measured properties. Prior to the analysis, the data were checked for normal distribution and homogeneity of variances. When significant differences were detected among the tanning systems, Tukey's multiple comparison test was applied to identify differences between group means. Statistical significance was considered at a confidence level of 95% ($p < 0.05$). All results are presented as mean ± standard deviation.

RESULTS AND DISCUSSIONS

The mechanical properties of belt leathers produced using different tanning systems are presented in Table 1. Statistical analysis revealed that the tanning system significantly affected most of the investigated properties ($p < 0.05$).

Table 1: Dependence of physical and mechanical properties of belt leathers on tanning system

Property	Tanning Systems		
	System I	System II	System III
Thickness (mm)	2.32 ±0.07	2.34 ±0.14	3.80 ±0.06
Tensile strength (N/mm²)	20.75 ± 6.67^{b}	20.69 ± 6.77^{b}	25.34 ± 3.64^{a}
Elongation at break (%)	57.33 ± 16.73^{a}	69.74 ± 16.34^{a}	36.92 ± 5.13^{b}
Double-edge tear strength (N)	168.39 ± 21.89^{b}	153.87 ± 33.09^{b}	361.57 ± 34.08^{a}
Single-edge tear strength (N)	89.39 ± 13.41^{b}	90.42 ± 15.09^{b}	156.27 ± 27.94^{a}
Stitch tear strength (N)	242.47 ± 31.70^{b}	243.74 ± 31.80^{b}	509.61 ± 80.54^{a}
Extension set (%)	2.22 ± 1.53^{a}	1.30 ± 0.42^{b}	0.00 ± 0.00^{c}
Crack length (mm)	12.71 ± 0.57^{a}	12.58 ± 0.54^{a}	8.69 ± 0.65^{b}
Crack force (kgf)	45.67 ± 5.51^{b}	43.00 ± 5.57^{b}	65.00 ± 15.00^{a}
Burst length (mm)	15.41 ± 0.34^{a}	14.65 ± 0.19^{a}	11.96 ± 1.31^{b}
Burst force (kgf)	61.33 ± 3.51^{b}	50.67 ± 2.89^{b}	100.00 ± 7.21^{a}

^{a,b,c} Different superscript letters within the same row indicate statistically significant differences according to Tukey's multiple comparison test ($p < 0.05$).

The tensile strength and elongation at break of the leathers are presented in Figure 2. Leathers tanned with System III exhibited the highest tensile strength (25.34 N/mm^2), followed by System I (20.75 N/mm^2) and System II leathers (20.69 N/mm^2). While the difference between System III and System II leathers was statistically significant, System I leathers demonstrated a tensile strength profile that was statistically similar to the synthetic-tanned group. In contrast, the highest elongation at break was observed for synthetic-tanned leathers (69.74%), followed by System I (57.33%) and System II leathers (36.92%). System II and System I leathers demonstrated statistically similar elongation behavior, whereas System III leathers exhibited a significantly lower ultimate elongation capacity.

The results obtained in terms of force-based mechanical properties were generally similar to the findings reported in the literature for upper leathers [2, 10–12]. However, a distinctly different trend was observed particularly regarding the extension set values. While certain levels of permanent elongation are commonly reported for shoe upper leathers, dimensional stability—a critical performance criterion for belt leathers—was revealed more prominently in this study. Notably, the absence of any permanent deformation in System III leathers indicates that this specific tanning system provides a vital technical advantage for high-performance belt applications.

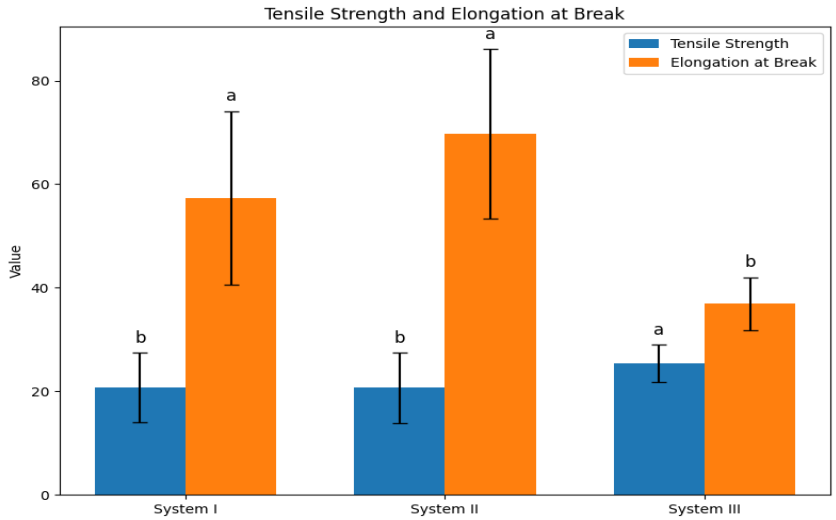


Figure 2. Tanning system influence on tensile strength and elongation of belt leathers

The tear resistance behavior is illustrated in Figure 3, including single-edge, double-edge, and stitch tear strength. A similar trend was observed for tear resistance. System III leathers demonstrated significantly higher double-edge tear strength (361.57 N) than System I (168.39 N) and System II leathers (153.87 N) ($p < 0.05$). For single-edge tear strength, System III leathers also exhibited the highest value (156.27 N), whereas System I and System II leathers showed statistically similar results, averaging 89.39 N and 90.42 N, respectively. The tanning system had a pronounced effect on stitch tear resistance. System III leathers yielded the highest stitch tear strength (509.61 N) and differed significantly from System I (242.47 N) and synthetic tanned focused leathers (243.74 N), which were statistically similar ($p < 0.05$). The superior tear and stitch resistance observed for System III may be associated with the combined effects of chromium complexes and phenolic syntan within the applied tanning formulation.

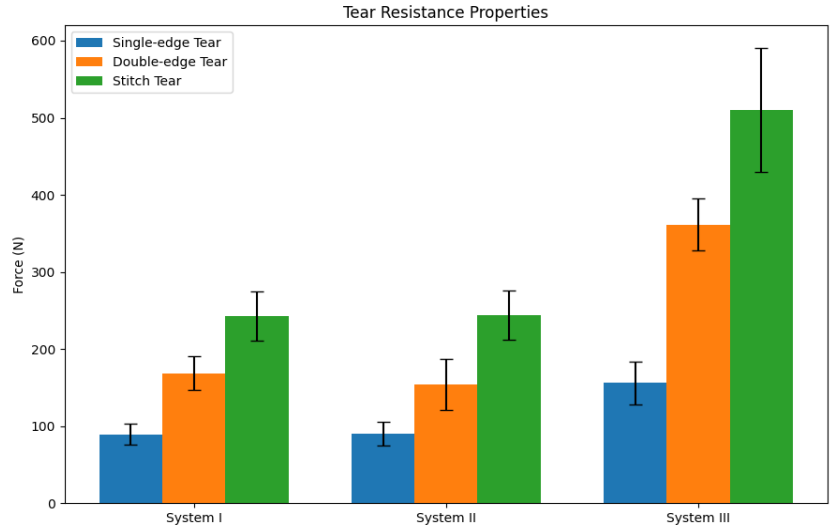


Figure 3. Effect of different tanning systems on tear resistance (single edge, double edge, and stitch tear) of belt leathers

Extension set values are presented in Figure 4, representing permanent deformation behavior. Extension set values showed the opposite tendency. System III leathers exhibited no measurable permanent elongation (0.00%), whereas System II and System I leathers showed values of 1.30% and 2.22%, respectively. Statistical analysis

indicated significant differences among all tanning systems ($p < 0.05$), suggesting that System III provides superior dimensional stability for belt applications where permanent deformation is undesirable.

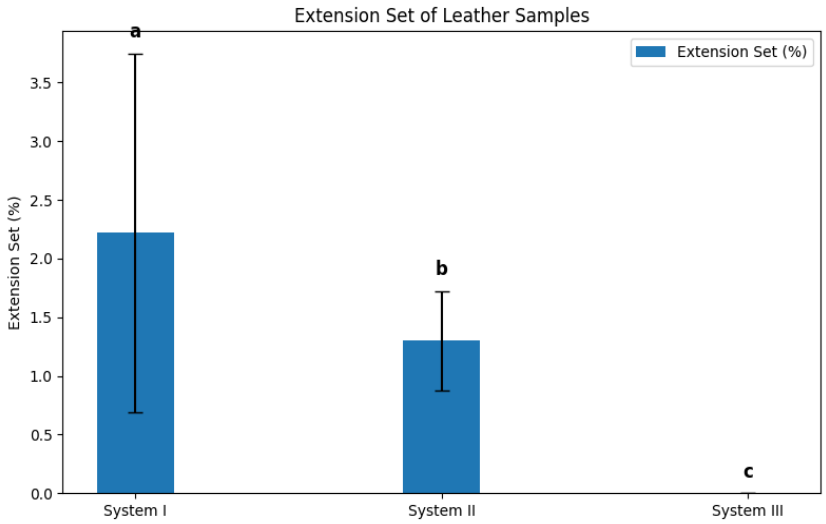


Figure 4. Extension set (permanent structural deformation) profile of belt leathers according to tanning system

Grain surface resistance properties are presented in Figure 5. Grain crack and grain burst properties were also significantly influenced by tanning type. The highest crack length values were obtained for System I (12.71 mm) and System II leathers (12.58 mm), whereas System III leathers showed significantly lower values (8.69 mm). Similarly, burst length values were significantly higher for System I leathers (15.41 mm) and System II leathers (14.65 mm) than for System III leathers (11.96 mm). These results indicate greater extensibility of vegetable- and synthetic-tanned focused leathers. However, System III leathers required significantly higher forces for both grain crack (65.00 kgf) and grain burst (100.00 kgf), demonstrating superior resistance against grain damage.

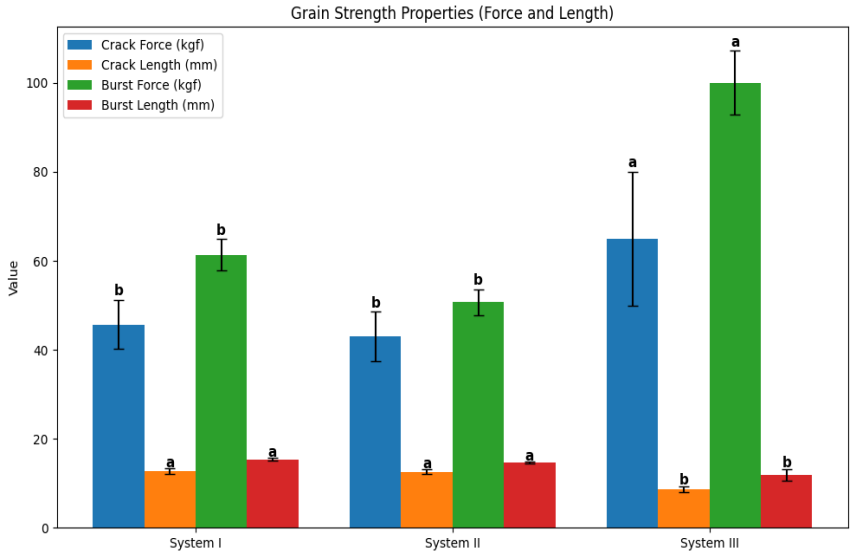


Figure 5. Influence of tanning system on grain crack and burst strength/distension of belt leathers

From a mechanical performance perspective, System III, which combined 7% basic chromium sulphate with 10% phenolic syntan, exhibited higher tensile strength, tear resistance, stitch tear strength, grain strength, and dimensional stability than Systems I and II

under the conditions investigated. These findings should be attributed to the specific tanning formulation used in System III rather than to chrome tanning in general. Similar trends have been reported in previous studies comparing chrome-tanned and alternative-tanned leathers, where chrome tanning was associated with higher tensile and tear strength values [13–15]. However, the present findings concern the specific combined formulation used in System III and should not be interpreted as evidence for pure chrome tanning. For belt applications, mechanical strength alone is not sufficient; dimensional stability and resistance to permanent deformation are also important performance criteria. The extension set results obtained in the present study demonstrated that System III leathers exhibited the highest dimensional stability, indicating their suitability for heavy-duty belt production. System II leathers showed the highest elongation at break, suggesting a more extensible and flexible collagen structure. Although their tensile and tear strength values were lower than those of System III leathers, their increased flexibility may be advantageous for applications requiring greater adaptability and comfort. In contrast, System I leathers exhibited the highest grain crack and grain burst distension values, indicating a greater capacity for deformation before structural failure. This behavior may be associated with the structural characteristics induced by the specific vegetable tanning formulation used in System I [13].

Overall, System III provided the highest mechanical resistance, particularly in terms of tensile strength, tear strength, stitch tear resistance, and grain strength. Conversely, System II enhanced extensibility and elongation properties, while System I generally exhibited intermediate behavior with lower mechanical performance but higher deformability.

CONCLUSIONS

In this study, three commercial tanning systems were comparatively evaluated using bovine hides. System I consisted of 10% mimosa and 10% quebracho, System II consisted of 10% phenolic syntan and 15% white syntan, and System III consisted of 7% basic chromium sulphate and 10% phenolic syntan. Therefore, the results obtained in this study should be interpreted specifically in relation to these formulations rather than as general characteristics of vegetable, synthetic, or chrome tanning systems.

Among the tanning methods investigated, System III leathers exhibited superior tensile strength, tear resistance, stitch tear strength, grain strength and dimensional stability. In particular, the absence of measurable extension set in System III indicates that this specific formulation may be well suited to belt applications where shape retention and resistance to deformation are critical requirements.

System II leathers showed the highest elongation at break, indicating a more elastic structure compared to the other tanning systems. Although their strength properties were lower than those of System III, they exhibited comparable performance in several mechanical tests and may be considered as an alternative for applications requiring greater flexibility.

System I leathers generally displayed lower mechanical strength values but provided the highest grain crack and burst distension values, reflecting their greater deformability. In addition, the use of plant-derived tannins in System I may also be of interest for applications where renewable tanning materials are prioritized.

Overall, the findings indicate that the selection of the tanning system should be based on the intended end-use requirements of the leather product. Under the conditions investigated, System III—the combination of 7% basic chromium sulphate and 10% phenolic syntan—provided the most favorable overall mechanical performance for belt leather production, particularly in terms of strength and dimensional stability. However, synthetic and vegetable tanning focused systems may offer viable alternatives when flexibility, sustainability or specific aesthetic characteristics are prioritized. Future studies may focus on the environmental performance and long-term durability of these tanning

systems to provide a more comprehensive evaluation of their suitability for leather goods production.

Acknowledgements

The authors gratefully acknowledge Koyuncuoğlu Invest (Bolu, Türkiye) for providing the raw hides utilized in this study, and Arifoğulları Group (Bolu, Türkiye) along with Pak Asya Leather (Bolu, Türkiye) for supply of the necessary commercial leather processing chemicals.

REFERENCES

1. Bielak, E., Zielinska, G., Comparison and Assessment of Selected Parameters of Chrome-Free and Chrome-Tanned Leather, *Leather and Footwear Journal,* **2022**, 22, 1, https://doi.org/10.24264/lfj.22.1.1.
2. Afsar, A., Ozgunay, H., Yilmaz, O., Zengin, A.C.A., Zengin, G., Applicability of Lubricating Acrylic Syntans in Vegetable Tanned Saddlery Leathers, *Journal of Textiles and Engineer*, **2013**, 20, 89, 21–27, https://doi.org/10.7216/130075992013208903.
3. Onem, E., Gulumser, G., Renner, M., Yesil Celiktas, O., High Pressure Vegetable Tanning of Sheepskins Using Supercritical Carbon Dioxide, *J Supercrit Fluids*, **2015**, 104, 259-264, https://doi.org/10.1016/j.supflu.2015.07.002.
4. Lee, W., The Production of Good Quality Leathergoods, *Satra Bulletin,* **2019**, 36-42, https://www.satra.com/bulletin/article_lock.php?id=2400.
5. Mihai, A., Seul, A., Curteza, A., Costea, M., Mechanical Parameters of Leather in Relation to Technological Processing of the Footwear Uppers, *Materials*, **2022**, 15, 5107, https://doi.org/10.3390/ma15155107.
6. Dilek, Y., Basaran B., Sancakli, A., Bitlisli B.O., Yorgancioglu, A., Evaluation of Collagen Hydrolysate on the Performance Properties of Different Wet-White Tanned Leathers, *J Soc Leather Technol Chem*, **2019**, 103, 3,129-134.
7. Srinivasan, P., Sundaramoorthy, S., Sathish, M., Jayakumar, G.C., Rathinam, A., Madhan, B., Saravanan, P., Rao, J.R., Chromium-free and Waterless Vegetable-Aluminium Tanning System for Sustainable Leather Manufacture, *Chem Eng J Adv*, **2021**, 7, 100108, https://doi.org/10.1016/j.ceja.2021.100108.
8. Ferraris, S., Gamna, F., Luxbacher, T., Maculotti, G., Giorio, L., Kholkhujaev, J., Genta, G., Galetto, M., Sarnataro, A., Nogarole, M., Florio, C., Comparative Characterization of Leather from Different Tanning Processes as a Contribution for a Sustainable Development of the Leather Industry, *Sci Rep*, **2025**, 15, 10608, https://doi.org/10.1038/s41598-025-94531-y.
9. Ork, N., Ozgunay, H., Mutlu, M.M., Ondogan, Z., Comparative Determination of Physical and Fastness Properties of Garment Leathers Tanned with Various Tanning Materials for Leather Skirt Production, *Textile and Apparel*, **2014**, 24, 4, 413–418.
10. Ali, F., Kamal, M., Islam, M.S., Comparative Study on Physical Properties of Different Types of Leather in Bangladesh, *Int J Eng Res Appl*, **2020,** 10, 2, 55-63, https://doi.org/10.9790/9622-1002035563.
11. Meyer, M., Dietrich, S., Schulz, H., Mondschein, A., Comparison of the Technical Performance of Leather, Artificial Leather, and Trendy Alternatives, *Coatings*, **2021**, 11, 2, 226, https://doi.org/10.3390/coatings11020226.
12. Hossain, M.D., Azam, F.A.B., Chowdhury, M., Quality Assessment of Shoe Leather Based on the Properties of Strength and Comfort, Collected from Different Footwear and Leather Industries in Bangladesh, *Text Leather Rev*, **2021**, 4, 1, 30-37, https://doi.org/10.31881/TLR.2020.20.
13. Lakic, S., Botić, T., Borković, A., Novak, B., Janjić, S., Comparison of Physical and Mechanical Properties of Chrome and Vegetable Tanned Leather, VII International Scientific Conference, "Contemporary Trends and Innovations in the Textile Industry", 19th-20th September, **2024**, Belgrade, Serbia, https://doi.org/10.5937/CT_ITI24030L.
14. Rosiati, N.M., Rachmawati, L., Udkhiyati, M., Characteristic of Chrome-Tanned and Vegetable-Tanned Goat Garment Leathers, *Jurnal Peternakan*, **2024**, 21, 2, 284-294, https://doi.org/10.24014/jupet.v21i2:28919.
15. Nashy, E.H.A., Osman, O., Mahmoud, A.A., Ibrahim, M., Molecular Spectroscopic Study for Suggested Mechanism of Chrome Tanned Leather, *Spectrochim Acta A*, **2012**, 88, 171–176, https://doi.org/10.1016/j.saa.2011.12.024.

© 2026 by the author(s). Published by INCDTP-ICPI, Bucharest, RO. This is an open access article distributed under the terms and conditions of the Creative Commons Attribution license (http://creativecommons.org/licenses/by/4.0/).

CONDUCTIVE TEXTILES FOR ELECTROMAGNETIC SHIELDING: A SHORT REVIEW

Cornel Adrian MARIN*, Raluca Maria AILENI

The National Research & Development Institute for Textiles and Leather, 030508, Bucharest, Romania, email: adrian.marin@incdtp.ro

Received: 15.04.2025 Accepted: 28.09.2026 https://doi.org/10.24264/lfj.26.3.6

CONDUCTIVE TEXTILES FOR ELECTROMAGNETIC SHIELDING: A SHORT REVIEW

ABSTRACT. The increasing use of electronic devices and wireless communications has generated growing demand for efficient electromagnetic interference (EMI) shielding materials. Traditional metallic enclosures, while effective, are heavy and rigid, limiting their use in modern wearable and flexible applications. Functionalized textiles have emerged as a versatile alternative, combining flexibility, low weight, and adaptability to complex geometries with effective EMI attenuation. This review provides a comprehensive, up-to-date analysis of conductive textile systems for EMI shielding, with explicit treatment of the underlying shielding mechanisms – reflection loss (SE_r), absorption loss (SE_a), and multiple internal reflections (SE_{MIR}). Major material categories are systematically discussed: metallic fiber fabrics, metal-coated textiles, intrinsically conducting polymer coatings, carbon-based nanomaterial systems, MXenes, and hybrid multi-layer architectures. Consolidated comparative tables of material performance and fabrication methods are provided as practical references. Practical challenges of washability, scalable manufacturing, standardization, and biocompatibility are discussed. Reported shielding effectiveness (SE) values range from ~5 dB for simple conductive-polymer coatings to over 100 dB for advanced hybrid multi-layer composites.

KEYWORDS: conductive polymers, metal-coated fabrics, flexible shielding, nanomaterials, MXene, EMI shielding effectiveness, wearable textiles

TEXTILE CONDUCTOARE PENTRU ECRANARE ELECTROMAGNETICĂ: O SCURTĂ ANALIZĂ

REZUMAT. Utilizarea tot mai frecventă a dispozitivelor electronice și a comunicațiilor fără fir a generat o cerere din ce în ce mai mare de materiale eficiente pentru ecranarea împotriva interferențelor electromagnetice (EMI). Carcasele metalice tradiționale, deși eficiente, sunt grele și rigide, ceea ce le limitează utilizarea în aplicații moderne, flexibile sau de tip dispozitiv purtabil. Textilele funcționalizate au apărut ca o alternativă versatilă, combinând flexibilitatea, greutatea redusă și adaptabilitatea la geometrii complexe cu o atenuare eficientă a interferențelor electromagnetice. Sinteza de față oferă o analiză cuprinzătoare și actualizată a sistemelor textile conductoare destinate ecranării EMI, abordând în mod explicit mecanismele fundamentale de ecranare: pierderile prin reflexie (SE_r), pierderile prin absorbție (SE_a) și reflexiile interne multiple (SE_{MIR}). Sunt analizate sistematic principalele categorii de materiale: țesături din fibre metalice, textile acoperite cu metal, straturi din polimeri intrinsec conductori, sisteme bazate pe nanomateriale pe bază de carbon, MXene și arhitecturi hibride multistrat. Sunt incluse tabele comparative sintetice privind performanța materialelor și metodele de fabricație, servind drept referințe practice. De asemenea, sunt discutate provocările practice legate de lavabilitate, producția la scară largă, standardizare și biocompatibilitate. Valorile raportate pentru eficacitatea ecranării (SE) variază de la aproximativ 5 dB, în cazul straturilor simple de polimeri conductori, până la peste 100 dB, în cazul compozitelor hibride multistrat avansate.

CUVINTE CHEIE: polimeri conductori, țesături acoperite cu metal, ecranare flexibilă, nanomateriale, MXene, eficacitatea ecranării EMI, textile purtabile

TEXTILES CONDUCTEURS POUR LE BLINDAGE ÉLECTROMAGNÉTIQUE : UNE BRÈVE SYNTHÈSE

RÉSUMÉ. L'utilisation croissante des appareils électroniques et des communications sans fil a engendré une demande accrue pour des matériaux efficaces de blindage contre les interférences électromagnétiques (IEM). Les enceintes métalliques traditionnelles, bien qu'efficaces, sont lourdes et rigides, ce qui limite leur usage dans les applications modernes, notamment les dispositifs souples et portables. Les textiles fonctionnalisés s'imposent comme une alternative polyvalente, alliant flexibilité, légèreté et adaptabilité à des géométries complexes, tout en assurant une atténuation efficace des IEM. Cette synthèse propose une analyse complète et actualisée des systèmes textiles conducteurs destinés au blindage électromagnétique, en examinant en détail les mécanismes sous-jacents : les pertes par réflexion (SE_r), les pertes par absorption (SE_a) et les réflexions internes multiples (SE_{MIR}). Les principales catégories de matériaux sont passées en revue : tissus à base de fibres métalliques, textiles revêtus de métal, revêtements en polymères intrinsèquement conducteurs, systèmes à base de nanomatériaux carbonés, MXènes et architectures hybrides multicouches. Des tableaux comparatifs synthétiques, portant sur les performances des matériaux et les méthodes de fabrication, sont fournis en guise de référence pratique. Les défis concrets — tels que la lavabilité, la montée en échelle de la production, la normalisation et la biocompatibilité — sont également abordés. Les valeurs d'efficacité de blindage (SE) rapportées dans la littérature s'échelonnent d'environ 5 dB pour des revêtements simples en polymères conducteurs à plus de 100 dB pour des composites hybrides multicouches avancés.

MOTS-CLÉS : polymères conducteurs, tissus revêtus de métal, blindage souple, nanomatériaux, MXène, efficacité de blindage électromagnétique, textiles portables

* *Correspondence to: Cornel Adrian MARIN, The National Research & Development Institute for Textiles and Leather, 030508, Bucharest, Romania, email: adrian.marin@incdtp.ro*

INTRODUCTION

Electromagnetic pollution has become a major global concern with the proliferation of electronic devices, recognized as the fourth environmental pollutant after noise, water, and air. Excessive exposure to electromagnetic fields can negatively impact human health, with documented biological effects on the nervous system, reproductive function, and sleep quality, while sensitive electronic equipment can malfunction due to electromagnetic interference (EMI) [1]. The rapid expansion of 5G telecommunications, the Internet of Things (IoT), autonomous vehicles, and wearable health-monitoring devices has dramatically increased both the density of EMI sources and the stringency of electromagnetic compatibility (EMC) requirements in critical sectors [2]. International directives such as the EU EMC Directive (2014/30/EU) and FCC regulations in the United States impose increasingly strict limits on electromagnetic emissions, driving demand for efficient, lightweight, and cost-effective shielding solutions.

Traditional EMI shielding is achieved through rigid metallic enclosures of aluminum, copper, or steel, which, despite excellent conductivity and shielding performance, present well-documented drawbacks: high density, mechanical rigidity, susceptibility to corrosion, and high fabrication cost [3]. These limitations are especially problematic in the context of modern portable, miniaturized, or body-worn devices, where metal enclosures are impractical and incompatible with ergonomic requirements. Conductive polymer-matrix composites have emerged as a partial alternative, but they too cannot replicate the flexibility of a textile substrate [3, 4]. Textile substrates offer a compelling alternative: flexible, breathable, lightweight, and moldable into complex three-dimensional shapes, with well-established industrial manufacturing processes. However, conventional textile fibers are dielectric insulators; the electrical conductivity necessary for EMI shielding must be imparted through a subsequent functionalization process [4].

The concept of electrically conductive textiles is not new, metallic threads have been woven into fabrics for centuries, but the rigorous exploitation of their electromagnetic properties is a more recent development, gaining momentum in the 1980s and accelerating dramatically with nanotechnology and surface engineering advances in the 2000-2020s [5-7]. The global market for electronic and smart textiles was valued at over $1.5 billion in 2022 and is estimated to exceed $5 billion by 2030, with EMI shielding as one of the principal application segments [2].

THEORETICAL BACKGROUND OF EMI SHIELDING

Shielding Effectiveness (SE)

Shielding effectiveness (SE) is the fundamental figure of merit for EMI shielding materials, defined as the ratio of the incident electromagnetic field intensity to the transmitted field intensity, expressed in decibels (dB) [8]:

$$SE\ (dB) = 20\ \log_{10}(E_0/E_1) = 20\ \log_{10}(H_0/H_1) = 10\ \log_{10}(P_0/P_1) \quad (1)$$

where E, H, and P are the electric field strength, magnetic field strength, and power of the electromagnetic wave, respectively; subscripts 0 and 1 denote values before and after the shield. SE of 0 dB corresponds to complete transmission; 20 dB means only 10% of the incident field is transmitted; 40 dB means 1%; 80 dB means 0.01%. Values above 20 dB are considered commercially adequate for civilian electronics; 40-60 dB are required for sensitive computing and communications equipment; critical military and medical applications typically demand SE > 80 dB [9]. SE is a frequency-dependent quantity and material performance can vary significantly across different frequency bands, making full-band characterization essential [8, 9].

Shielding Mechanisms

The total shielding effectiveness (SE_t) of an EMI shielding material is the sum of three components: shielding effectiveness due to absorption (SE_a), reflection (SE_r), and multiple internal reflections (SE_{Mir}), as illustrated in Figure 1:

$$SET = SE_r + SE_a + SE_{mir} \quad (2)$$

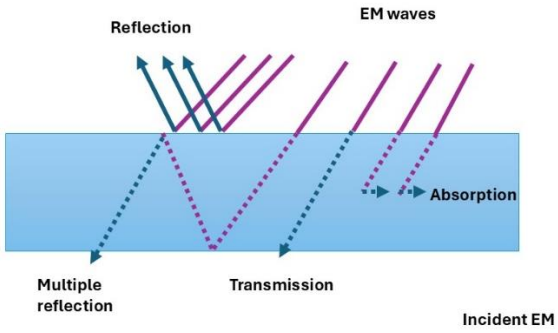


Figure 1. Schematic representation of the fundamental mechanisms in EMI shielding materials

Reflection Loss (SE_r)

Reflection at the shield surface arises from the impedance mismatch between the incident wave in free space (impedance $\eta_0 \approx 377\ \Omega$) and the much lower intrinsic impedance of a conductive material. For a conductor with conductivity σ (S/m), relative permeability μ_r, at frequency f (Hz), the reflection loss is [8, 10]:

$$SE_r\ (dB) \approx 168 + 10 \log_{10}(\sigma / (f \times \mu_r)) \quad (3)$$

High-conductivity, low-permeability materials provide very large reflection losses even at relatively low frequencies. Copper (σ ≈ 5.8x107 S/m) and silver (σ ≈ 6.3x107 S/m) offer SE_r of 100-150 dB at GHz frequencies, while stainless steel (σ ≈ 1.4x106 S/m) offers somewhat lower values, partially offset by its higher magnetic permeability. Reflection is a surface phenomenon, essentially independent of shield thickness, which is why even extremely thin metallic layers (a few nm) can provide significant reflection [10, 11].

Absorption (SE_a)

The second primary EMI shielding mechanism is absorption (SE_a), which depends entirely on the intrinsic physical properties of the shielding material and is not influenced by the nature of the electromagnetic field source. Unlike reflection, which occurs at the material's surface, absorption involves the propagation of the electromagnetic wave into the bulk of the material, where its amplitude progressively decreases following an exponential decay law. This attenuation arises from induction currents generated within the material, which lead to energy dissipation through the Joule effect and its subsequent conversion into thermal energy. The main factors governing the magnitude of these losses are the ohmic resistance encountered by the induced currents and the dissipation associated with cyclic electric and magnetic polarization phenomena within the material's structure. To achieve effective absorption across the frequency range of interest, a shielding material must simultaneously exhibit high electrical conductivity, significant magnetic permeability, and adequate thickness.

Multiple Internal Reflections (SE_{MIR})

When the shield is thinner than the skin depth, electromagnetic energy reaching the second surface is not completely absorbed and a significant fraction is reflected back toward the first surface. These multiple internal reflections reduce the effective SE below the simple sum $SE_r + SE_a$. This correction term is negative and is given by [8]:

$$SE_{mir}\ (dB) = 20 \log_{10}|1 - e^{-2t}/\delta| \quad (4)$$

For thick shields (t >> δ), the exponential term approaches zero and $SE_{MIR} \approx 0$, so it is neglected in practice. However, the condition t < δ is frequently encountered for thin coatings of moderately conductive materials: graphene or rGO films, MXene layers, conducting polymer coatings, and vapor-deposited metals – where typical thickness is 1-100 µm. In these cases, the SE_{MIR} correction can reduce total SE by 5-15 dB compared to the simple $SE_r + SE_a$ estimate, especially at lower frequencies where δ is larger [11, 12]. Porous or multilayer textile architectures are engineered to exploit internal interfaces as additional absorption mechanisms, converting SE_{MIR} from a negative penalty into a structural advantage [12].

Key Material Parameters

The primary intrinsic material parameters governing SE are: electrical conductivity (σ), magnetic permeability (µ), and dielectric permittivity (ε). High σ enhances both reflection (SE_r) and absorption (SE_a); high µ increases SE_a and reduces δ but contributes negatively to SE_r by reducing input impedance;

high ε broadens dielectric loss mechanisms. At the textile structural level, weave or knit pattern, yarn twist, fabric porosity, and layer count control the effective conductivity of the composite and the electromagnetic transparency of open apertures. Theoretical studies based on equivalent electrical network modeling of textile structures have shown that the critical aperture size below which electromagnetic leakage becomes negligible is approximately λ/100 at the frequency of interest [12, 7].

TYPES OF TEXTILE STRUCTURES

Woven Textiles

Woven textiles are produced by interlacing warp and weft yarns in perpendicular directions, yielding dimensionally stable structures with controllable aperture geometry, good mechanical strength, and uniformity of conductivity distribution. Conductive yarns – pure metallic wires or hybrid yarns blending metallic fibers with synthetic or natural fibers – can be incorporated directly into the fabric in the warp, weft, or both directions. Their spatial distribution determines the density of the conductive network and hence the SE. Wang *et al*. [13] developed a multifunctional stretchable woven fabric incorporating tri-component elastic-conductive composite yarns containing stainless steel wire. The fabric exhibited effective electromagnetic shielding in the X-band (8.2–12.4 GHz), with no degradation of shielding effectiveness after 15 stretching cycles at 20% extension, while maintaining excellent stretchability (>40% elongation) and structural stability.

Knitted Textiles

Knitted fabrics are produced by forming interconnected loops of yarn, yielding highly elastic and three-dimensionally conformable structures particularly suited for body-worn applications where the shape and motion of the human body must be accommodated without loss of functional performance. Their inherently higher porosity compared to woven structures reduces SE for a given metal content; however, superior flexibility and higher body coverage compensate in many practical applications. Mikolajczyk *et al*. [14] investigated ten knitted fabric variants differing in stitch pattern, structural parameters, and conductive yarn type. The results demonstrated that electromagnetic shielding effectiveness depends strongly on the fabric structure, stitch pattern, and yarn composition, with measurements performed in the 2–4 GHz and 4–7 GHz frequency ranges. Perumalraj and Dasaradan [15] investigated the electromagnetic shielding effectiveness of knitted fabrics incorporating copper core yarns in the 20 MHz–18 GHz frequency range. The study demonstrated that shielding effectiveness increased with the fabric tightness factor, wale density, and course density. Furthermore, interlock knitted fabrics exhibited superior shielding performance compared with rib and plain knitted structures, while increasing the copper wire diameter resulted in reduced shielding effectiveness.

Nonwoven Textiles

Nonwoven fabrics – including electrospun fiber mats, needle-felted batts, wet-laid sheets, and thermally or chemically bonded materials – are assembled from individual fibers bonded together without weaving or knitting processes. Their high porosity, large specific surface area, and controllable thickness make them excellent substrates for coating techniques, as conductive solutions can penetrate through the material thickness and form a continuous three-dimensional conductive network. Electrospun nonwovens, composed of fibers with diameters of 100 nm-10 µm, offer particularly large specific surface areas (tens of m^2/g), facilitating highly uniform coating with minimal conductive material quantities. Duan *et al*. [16] fabricated a $Ti_3C_2T_x$ MXene/carbon fiber fabric/ thermoplastic polyurethane (TPU) composite through electrohydrodynamic atomization deposition, layer-by-layer stacking, and hot pressing. The composite achieved an EMI shielding effectiveness of up to 40.4 dB, while exhibiting excellent mechanical strength, flexibility, durability, and stable shielding performance after repeated bending cycles. The enhanced shielding was attributed to the

dielectric loss provided by the conductive MXene fillers and the increased absorption within the sandwich structure. Liang *et al*. [17] fabricated porous $Ti_3C_2T_x$ MXene nanosheets sandwiched between electrospun polyimide fiber mats, achieving an EMI shielding effectiveness of 48.8 dB in the X-band (8.2–12.4 GHz). The porous nonwoven architecture provided high flexibility, low weight, and enhanced electromagnetic wave attenuation through multiple internal reflections.

CONDUCTIVE MATERIALS AND FABRICATION METHODS

Metallic Fiber Integration

The most direct and industrially mature route to conductive textiles involves mechanically integrating metallic fibers or wires into the textile structure at the yarn spinning or fabric formation stage. Stainless steel fibers with diameters of 4-12 µm, known in industry as ultra-fine stainless steel fibers, are the most commonly used material, produced by intimate blending with polyester or polyamide fibers at concentrations of 10-30 wt%. The electrical conductivity of the resulting hybrid yarn follows the percolation of the metallic network and reaches values sufficient for shielding at concentrations above ~15 wt%. Gupta *et al*. [18] demonstrated that the electromagnetic shielding performance of hybrid woven fabrics strongly depends on the conductive yarn content and fabric structure. A cell-structured fabric containing 32.58 wt% stainless steel achieved shielding effectiveness of approximately 31–35 dB in the 8.2–18 GHz frequency range while maintaining good breathability. Copper and silver fibers confer higher conductivity than stainless steel but are more expensive and more prone to corrosion; they are used in niche applications where maximum conductivity is a priority [7, 18]. The primary trade-off is between metal content – which increases SE but adds weight and stiffness – and textile comfort characteristics: bending stiffness, air permeability, and long-term skin compatibility.

Metallic Coatings

Applying a continuous and conformal metallic layer on the surface or through the bulk of the textile is among the most effective strategies for achieving high SE while preserving substrate flexibility and low weight. Electroless plating deposits a metal (typically copper, nickel, or silver) through chemical reduction onto a catalytically activated textile surface without external current. The method provides conformal coverage of complex fiber geometries, scalable batch processing, and good adhesion. Hu *et al*. [19] investigated copper-coated nonwoven textile materials (MEFTEX) fabricated via electroless copper plating for electromagnetic interference shielding applications. The results showed that shielding effectiveness increases with the areal density of the material, reaching values of approximately 56–63 dB in the frequency range of 30 MHz–1.5 GHz for single-layer samples. Furthermore, multilayer structures significantly improved shielding performance due to increased thickness and reduced electrical resistivity, with up to 83% enhancement compared to single-layer configurations [19]. Electroplating enables the formation of relatively thick metallic coatings on textile substrates, resulting in high electrical conductivity and enhanced electromagnetic shielding effectiveness. However, the process often leads to increased fabric stiffness and reduced breathability due to the continuous metallic layer covering the textile structure. Magnetron sputtering enables the deposition of thin metallic coatings onto textile substrates to improve their electrical conductivity and electromagnetic shielding properties. Surdu *et al*. [21] investigated copper coatings with thicknesses of 200, 400, 800, and 1200 nm deposited on woven textile structures, including cotton, polyester, and fabrics containing conductive yarns. The authors reported electromagnetic attenuation values of 20–34 dB for copper-coated fabrics incorporating conductive yarns, while fabrics coated with copper on one side exhibited lower attenuation values of 3–8.5 dB. These findings highlight the potential of magnetron sputtering for developing textile-based electromagnetic shielding materials.

Conductive ink printing with silver nanoparticles or carbon-based inks enables spatially patterned conductive structures on textile surfaces, opening the way to integrating shielding with antennas and electrodes in multifunctional smart garments [22].

Conducting Polymer Coatings

Intrinsically conducting polymers (ICPs) – polypyrrole (PPy), polyaniline (PANI), polythiophene (PTh), and poly(3,4-ethylenedioxythiophene) (PEDOT) – can be chemically synthesized directly on textile fiber surfaces through in-situ oxidative polymerization, providing a conformal conductive coating without metallic components. *In-situ* polymerization involves immersing the textile in a monomer solution followed by addition of an oxidizing agent, initiating polymerization preferentially at fiber surfaces. Rybicki *et al*. [23] investigated conductive polymer coatings on polyacrylonitrile (PAN) fabrics using reactive inkjet printing of polyaniline (PANI) and polypyrrole (PPy). The electromagnetic shielding effectiveness was evaluated in the frequency range of 2.5–18 GHz using the waveguide method. The results showed that both PAN/PANI and PAN/PPy composites exhibit good EMI shielding performance, with PAN/PANI demonstrating higher effectiveness. This difference was attributed to the higher electrical conductivity of doped polyaniline compared to polypyrrole. Bashir *et al*. [24] synthesized and characterized conductive fibers based on PEDOT and polypyrrole (PPy) for smart textile applications. The study focused on the preparation and evaluation of electrically conductive polymer-based fibers, highlighting their potential for wearable electronic and textile applications.

Zou *et al*. [25] developed a durable EMI shielding fabric based on a polypyrrole (PPy)-modified textile coated with a hydrophobic 1H,1H,2H,2H-perfluorooctyltriethoxysilane (POTS) layer. The system exhibited strong resistance to water, salt, and corrosive environments. Additionally, the protective layer could be rapidly self-healed via microwave-induced heating within approximately 4 seconds, due to the thermal response of PPy under electromagnetic irradiation. The self-healing process was repeatable even after severe damage, demonstrating high potential for durable EMI shielding applications.

Carbon-Based Nanomaterials

Carbon nanomaterials – single-walled (SWCNT) and multi-walled carbon nanotubes (MWCNT), graphene, reduced graphene oxide (rGO), and carbon black – are widely used in EMI shielding textiles due to their unique combination of high electrical conductivity (σ up to 104-105 S/m for MWCNT networks), low density, very high aspect ratio (>103 for MWCNT), chemical stability, and processability from aqueous suspension. MWCNT-coated fabrics show SE of 15-40 dB in the GHz range, with superior values obtained for covalently functionalized MWCNTs that form denser networks due to improved dispersion [26]. Pande *et al*. [26] demonstrated that multilayer MWCNT/PMMA structures prepared by stacking thin composite films exhibit significantly improved electromagnetic interference shielding effectiveness compared to bulk composites. Shielding effectiveness up to ~40 dB was achieved for a seven-layer configuration, compared to ~30 dB for thicker multilayer structures. The results highlight that multilayer architecture enhances shielding performance, primarily through absorption-dominated mechanisms. Song *et al*. [27] fabricated multilayer graphene/polymer sandwich composite films and investigated their electromagnetic interference shielding performance. The results showed that shielding effectiveness is strongly influenced by the electrical conductivity of the composites. Both experimental and theoretical analyses indicated that reflection is the dominant shielding mechanism, while absorption can be enhanced by optimizing thickness and electrical properties. An optimized shielding effectiveness of up to approximately 27 dB was reported for the fabricated structures.

MXenes and 2D Nanomaterials

MXenes – a large and expanding class of two-dimensional nanomaterials comprising

transition metal carbides, nitrides, and carbonitrides, with the general formula:

$$M_{n+1}X_nT_x \quad (5)$$

where M is an early transition metal such as Ti, V, Nb, Mo, or Cr; X is C and/or N; n = 1, 2, or 3; and T_x represents surface functional groups -OH, =O, -F, which have emerged since 2016 as the most promising class of two-dimensional nanomaterials for EMI shielding, becoming one of the fastest-growing areas in conductive textile literature [29]. MXene synthesis involves selective etching of the A layers (typically Al) from MAX phase precursors (Mn+1AXn) in hydrofluoric acid solutions or inorganic fluoride mixtures, followed by delamination and exfoliation into mono- or few-layer nanosheets. $Ti_3C_2T_x$, the most extensively studied MXene, exhibits metallic electrical conductivity in films (σ up to 10,000 S/cm), excellent processability from stable aqueous colloidal dispersions, and rich surface chemistry that promotes adhesion to cellulosic fiber surfaces through electrostatic interactions and hydrogen bonding [29, 30]. Shahzad *et al*. [29] first reported SE of freestanding MXene of 92 dB in the X-band for a 45 µm thick film, establishing MXene as the most efficient shielding material per unit thickness among all reported materials at that time. Duan *et al*. [16] fabricated a MXene/carbon fiber fabric/TPU nonwoven composite achieving ~38 dB SE in the X-band with a density below 0.5 g/cm³. Yin *et al*. [30] fabricated a lightweight and flexible PANI/MXene/carbon fiber fabric using a layer-by-layer assembly approach, in which MXene nanosheets and polyaniline were alternately deposited onto carbon fiber substrates. The resulting composite (0.55 mm thickness, five cycles) achieved an EMI shielding effectiveness of 26.0 dB in the X-band (8–12 GHz), together with good electrical conductivity and a high specific shielding effectiveness of 135.5 dB·cm³/g. The material also exhibited excellent Joule heating performance, air permeability, and structural stability. The shielding mechanism was reported to be absorption-dominated. Han *et al*. [31] investigated the EMI shielding performance of 16 different MXenes, including single-metal, ordered double-metal, and solid-solution compositions. Thin films prepared via spin coating, spray coating, and vacuum filtration exhibited effective EMI shielding above 20 dB. Ultrathin $Ti_3C_2T_x$ films (~40 nm) achieved about 21 dB, and the study showed that shielding performance can be tuned through elemental composition and structure, highlighting the potential of MXenes for ultrathin and flexible EMI shielding applications [31].

Hybrid and Multilayer Architectures

The highest SE values reported in conductive textile literature are achieved by hybrid architectures that synergistically combine multiple conductive components, exploiting the complementarity of physical mechanisms: metallic components with high conductivity maximize reflection (SE_r), while magnetic or carbon-based inclusions enhance absorption (SE_a), and hierarchical interface structuring increases the effective path length of the wave through the material. Jia *et al*. [32] demonstrated a robust superhydrophobic electromagnetic interference (EMI) shielding textile based on a silver nanowire (AgNW) network deposited onto a commercial cotton fabric, combined with a surface modification strategy to achieve both water repellency and electromagnetic shielding performance. The resulting textile exhibited a high water contact angle of 160.8° and a low sliding angle of 2.9°, confirming excellent superhydrophobic behavior.

In terms of electromagnetic performance, the developed material achieved a shielding effectiveness of approximately 51.5 dB in the X-band (8–12 GHz). Importantly, the multifunctional textile maintained both its superhydrophobic properties and a significant EMI shielding effectiveness of 42.6 dB even after 5000 stretching–releasing cycles, demonstrating outstanding mechanical durability.

Additional tests confirmed strong resistance to harsh environmental conditions, including ultrasonic treatment, repeated peeling cycles, acidic and alkaline solutions, and exposure to various organic solvents. This exceptional durability is attributed to the synergistic effect of the AgNW conductive network together with carbon nanotubes, polytetrafluoroethylene (PTFE) nanoparticles,

and a fluoroacrylic polymer coating, which together provide robust mechanical stability, chemical resistance, and sustained electrical conductivity [30, 32].

COMPARATIVE PERFORMANCE

Table 1 consolidates representative performance metric values for the main categories of conductive textile EMI shielding systems based on peer-reviewed literature data.

Table 1: Comparative performance values of conductive textile EMI shielding materials

Material	Conductivity (S/m)	SE (dB)	Frequency Range	Flexibility	Wash Resistance	Ref.
Stainless steel fiber fabric	1.4×10^{6}	30–60	1–18 GHz	Moderate	Good	[7,17]
Silver-coated fabric (Ag)	4×10^{5}	40–70	30MHz–40 GHz	High	Moderate	[18]
Copper-coated fabric (Cu)	5×10^{7}	42–80	30 MHz–30 GHz	Moderate	Moderate	[18, 20]
Metal film fabric (Ag/Cu sputtering)	1×10^{7}	40–60	1–40 GHz	High	Low	[21]
Conductive polymer-coated fabric (PANI / PPy)	10^{2}–10^{3}	5–22	0.1–18 GHz	Very high	Low–Moderate	[23, 25]
Carbon nanotube-coated fabric (MWCNT)	10^{3}	15–40	0.1–18 GHz	Very high	Low–Moderate	[26, 28]
Graphene / reduced graphene oxide (rGO) coated fabric	5×10^{3}	20–65	1–18 GHz	Very high	Low–Moderate	[27]
MXene-coated fabric ($Ti_3C_2T_x$)	1×10^{4}	38–75	8–12 GHz	High	Moderate	[15, 30, 31]
Hybrid multilayer fabric AgNW + Fe_3O_4	~10^{6}	60–100	8–12 GHz	High	Good	[32]

Table 2 provides a fabrication-oriented comparative summary, designed as a practical tool for selecting material and fabrication method depending on the specific application requirements.

Table 2: Comparative overview of fabrication methods for conductive textile EMI shielding systems

Fabrication Method	Typical SE (dB)	Scalability	Cost	Key Advantages	Key Limitations
Metal fiber integration	20-45	High	Moderate	Durable; no post-processing	Reduced comfort; heavy
Electroless plating	40-70	High	Low-Moderate	Conformal; uniform	Wastewater treatment
Electroplating	60-80	Medium	Moderate	Thick coatings; high sigma	Stiff; less breathable
Magnetron sputtering	40-60	Low-Med.	High	Uniform thin films; pure	Vacuum equipment needed
Dip/spray (CNT, graphene, MXene)	20-75	High	Moderate	Flexible; solution process	Wash durability; aggregation
In-situ polymerization	5-25	High	Low	Biocompatible; low cost	Lower sigma; aging sensitivity
Conductive ink printing	10-40	High	Low-Moderate	Patternable; multifunctional	Crack formation on flex
Layer-by-layer assembly	40-100	Medium	Moderate	Nanoscale control; high SE	Time-consuming

PRACTICAL APPLICATIONS

Conductive textiles for EMI shielding have found practical applications across diverse sectors with distinct performance and comfort requirements. In the sector of personal protection and occupational safety, military uniforms and technical coveralls for operators working in proximity to intense EMI sources (radar stations, high-power transmitters, industrial electrical installations) have incorporated stainless steel or copper wire fabrics to reduce operator exposure below the

limits recommended by ICNIRP (International Commission on Non-Ionizing Radiation Protection) [1, 5]. European standard EN 50490-1 specifies minimum SE requirements for EMF protective clothing, mandating SE > 20 dB across relevant frequency bands.

In the medical sector, conductive textiles are used in: (i) isolation garments for patients with sensitive electronic implants (cardiac pacemakers, neurostimulators) that must be protected from ambient EM fields; (ii) shielding blankets and curtains for magnetic resonance imaging (MRI) and electroencephalography (EEG) enclosures, where external radiofrequency fields degrade image quality; and (iii) wearable devices for monitoring bioelectric signals (ECG, EMG, EEG) in high-EMI environments, where shielding integrated into the garment suppresses interference without requiring rigid external cabling [4, 5]. Biocompatibility requirements are strict in these applications, limiting materials to silver (used clinically as an antimicrobial agent) and to conducting polymers with documented biocompatibility.

The consumer electronics industry employs conductive textiles as flexible shields integrated into laptop, tablet, and smartphone cases – replacing rigid metallic shields with lightweight flexible textile foils. The aerospace and aeronautics industry has adopted conductive textile materials for shielding cabling and electronic modules in civil and military aircraft, where weight reduction compared to conventional metallic shields generates direct fuel savings [3].

CHALLENGES AND FUTURE DIRECTIONS

Performance-Comfort Trade-Off

There is a fundamental trade-off between electromagnetic shielding performance and textile comfort properties: higher SE and conductivity generally come at the cost of reduced breathability (lower air and water vapor permeability), increased weight, and higher bending stiffness. Engineering solutions that partially decouple these properties include: (i) patterned metal meshes that maintain significant open area for air permeability; (ii) auxetic textile geometries with negative Poisson's ratio that distribute strain more uniformly; (iii) ultra-thin MXene or graphene coatings (~10-100 nm) applied only to critical garment regions, minimizing mass addition; and (iv) integration of micro-structured conductors (micro-grids, micro-coils) that are nearly invisible and do not disturb the textile texture [32]. Multidisciplinary research integrating materials science, textile engineering, and applied ergonomics is essential for achieving the optimal performance-comfort trade-off in commercial products.

Scalable and Sustainable Manufacturing

The vast majority of high-performance conductive textile systems reported in the literature rely on laboratory-scale fabrication processes that cannot be directly transferred to continuous industrial processing (roll-to-roll, large batch). Key technical barriers include: (i) formulation of stable dispersions of nanomaterials at high concentrations without agglomeration, compatible with industrial coating machines; (ii) optimization of line speeds and drying/heat treatment conditions to achieve uniform coating thicknesses at scale; (iii) management of waste streams from metallic plating processes in compliance with environmental requirements; and (iv) quality control and inline SE inspection at production speed, where standard measurement methods cannot be applied inline [36]. The transition from laboratory to industry requires close collaboration between materials scientists, textile process engineers, and production engineers.

Biocompatibility and Safety

For textiles intended for direct prolonged skin contact or medical applications, systematic evaluation of the biocompatibility of conductive coatings is an essential and regulated requirement (EU MDR 2017/745, ISO 10993 standards). Silver nanoparticles have demonstrated useful antibacterial activity but also cytotoxicity at high concentrations for human skin cells; nanoparticle migration studies indicate that conventional silver-coated textiles can release significant amounts of Ag+ ions under normal use conditions [36]. High-aspect-ratio carbon nanotubes have been associated with asbestos-like biological effects at high doses, and long-term biocompatibility data for MXenes remain insufficient. Research

in the biocompatibility of conductive textiles represents a major barrier to the certification and commercialization of products for medical and personal protection applications.

CONCLUSIONS

This review has summarized the fundamental principles, materials, fabrication strategies, and application domains of conductive textile-based electromagnetic interference (EMI) shielding systems. The analysis shows that EMI shielding in textiles is governed primarily by a combination of reflection, absorption, and multiple internal reflection mechanisms, which are strongly dependent on intrinsic material properties such as electrical conductivity, magnetic permeability, and dielectric permittivity, as well as on textile architecture and structural design.

A clear hierarchy of material performance emerges across the reviewed systems. Metallic-based solutions, particularly silver- and copper-coated textiles, still provide the highest shielding effectiveness (SE), often exceeding 70–80 dB, due to their superior electrical conductivity. However, these materials suffer from limitations related to cost, rigidity, and reduced durability under mechanical deformation or washing cycles. Carbon-based materials, including carbon nanotubes and graphene derivatives, offer a favorable balance between flexibility and moderate-to-high SE (up to ~65 dB), while enabling lightweight and mechanically robust structures. MXenes, particularly $Ti_3C_2T_x$, represent the most promising emerging class of materials, combining metallic-level conductivity with solution processability and enabling SE values exceeding 70 dB in thin-film configurations. Conductive polymers, although limited in intrinsic conductivity, provide advantages in terms of low cost, lightweight nature, and potential biocompatibility, especially when combined with carbon nanostructures.

From a structural perspective, textile architecture plays a critical role in determining shielding performance. Woven structures generally provide higher SE due to lower porosity and more controlled conductive pathways, while knitted and nonwoven structures offer superior flexibility, breathability, and conformability, making them more suitable for wearable applications despite their lower baseline shielding performance. Hybrid and multilayer architectures consistently demonstrate superior performance by synergistically combining reflection-dominant metallic components with absorption-enhancing carbon- or magnetic-based materials, often achieving SE improvements beyond the additive contributions of individual components.

In terms of fabrication methods, no single approach is universally optimal. Metallic fiber integration remains the most industrially scalable solution, while electroless plating offers an effective compromise between performance, cost, and scalability. Advanced techniques such as magnetron sputtering, conductive ink printing, and layer-by-layer assembly enable high-performance or multifunctional systems but are currently limited by cost, complexity, or scalability constraints. Solution-based approaches, particularly dip-coating and spray-coating with nanomaterials, are attractive for large-scale production but require further improvements in dispersion stability and long-term wash durability.

Despite significant progress, several key challenges remain unresolved. The most critical issue is the intrinsic trade-off between electromagnetic shielding effectiveness and textile comfort properties, including breathability, flexibility, and weight. In addition, scalable and environmentally sustainable manufacturing routes are still under development, particularly for nanomaterial-based coatings. Biocompatibility and long-term safety also remain essential concerns, especially for applications involving direct skin contact or medical use, where potential cytotoxicity and nanoparticle migration must be carefully controlled.

Future research is expected to focus on the development of hierarchical hybrid systems, self-healing conductive networks, and stimuli-responsive or frequency-selective shielding textiles. Furthermore, the integration of artificial intelligence and data-driven materials design is likely to accelerate the optimization of textile architectures and compositions. Overall, conductive textile EMI shielding represents a rapidly evolving interdisciplinary field at the intersection of materials science, textile engineering, and applied electromagnetics, with

strong potential for scalable deployment in next-generation wearable electronics, healthcare systems, and advanced communication technologies.

Acknowledgements

This work was carried out through the Core Programme within the National Research Development and Innovation Plan 2022-2027, with the support of MCID, project no. 6N/2023, PN 23 26 01 03, project title: Materiale electroconductive pe bază de metalizări multistrat pentru sisteme termoelectrice, ecranare electromagnetică și senzori biomedicali integrați în sisteme IoT (3D-WearIoT) / Electrically conductive materials based on multilayer metallizations for thermoelectric systems, electromagnetic shielding, and biomedical sensors integrated into IoT systems (3D-WearIoT).

REFERENCES

1. Rubeziene, V., Varnaite-Zuravliova, S., EMI Shielding Textile Materials, in: Joseph, K., Wilson, R., George, G. (eds.), *Materials for Potential EMI Shielding Applications*, Elsevier, **2020**, 357-378, https://doi.org/10.1016/B978-0-12-817590-3.00022-1.
2. Xiao, H., Shi, M.W., Wang, Q., Liu, Q., The Electromagnetic Shielding and Reflective Properties of Electromagnetic Textiles with Pores, Planar Periodic Units and Space Structures, *Text Res J*, **2014**, 84, 16, 1679-1691, https://doi.org/10.1177/0040517514527371.
3. Geetha, S., Kumar, K.K.S., Rao, C.R., Vijayan, M., Trivedi, D.C., EMI Shielding: Methods and Materials – A Review, *J Appl Polym Sci*, **2009**, 112, 4, 2073-2086, https://doi.org/10.1002/app.29812.
4. Stoppa, M., Chiolerio, A., Wearable Electronics and Smart Textiles: A Critical Review, *Sensors*, **2014**, 14, 7, 11957-11992, https://doi.org/10.3390/s140711957.
5. Akram, S., Ashraf, M., Javid, A., Abid, H.A., Ahmad, S., Nawab, Y., Rasheed, A., Xue, Z., Nosheen, A., Recent Advances in Electromagnetic Interference (EMI) Shielding Textiles: A Comprehensive Review, *Synth Met*, **2023**, 294, 117305, https://doi.org/10.1016/j.synthmet.2023.117305.
6. Yin, J., Ma, W., Gao, Z., Lei, X., Jia, C., A Review of Electromagnetic Shielding Fabric, Wave-Absorbing Fabric and Wave-Transparent Fabric, *Polymers*, **2022**, 14, 3, 377, https://doi.org/10.3390/polym14030377.
7. Blachowicz, T., Wojcik, D., Surma, M., Magnuski, M., Ehrmann, G., Ehrmann, A., Textile Fabrics as Electromagnetic Shielding Materials – A Review of Preparation and Performance, *Fibers*, **2023**, 11, 3, 29, https://doi.org/10.3390/fib11030029.
8. Simon, R.M., EMI Shielding through Conductive Plastics, *Polym-Plast Technol Eng*, **1981**, 17, 1, 1-28, https://doi.org/10.1080/03602558108070126.
9. Liang, C., Gu, Z., Zhang, Y., Ma, Z., Qiu, H., Gu, J., Structural Design Strategies of Polymer Matrix Composites for Electromagnetic Interference Shielding: A Review, *Nano-Micro Lett*, **2021**, 13, https://doi.org/10.1007/s40820-021-00707-2.
10. Ott, H.W., *Electromagnetic Compatibility Engineering*, John Wiley & Sons, Hoboken, NJ, USA, **2009**, https://doi.org/10.1002/9780470508510.
11. Sankaran, S., Deshmukh, K., Ahamed, M.B., Pasha, S.K.K., Recent Advances in Electromagnetic Interference Shielding Properties of Metal and Carbon Filler Reinforced Flexible Polymer Composites: A Review, *Compos Part A-Appl S*, **2018**, 114, 49-71, https://doi.org/10.1016/j.compositesa.2018.08.006.
12. Shyr, T.W., Shie, J.W., Electromagnetic Shielding Mechanisms Using Soft Magnetic Stainless Steel Fiber Enabled Polyester Textiles, *J Magn Magn Mater*, **2012**, 324, 23, 4127-4132, https://doi.org/10.1016/j.jmmm.2012.07.037.
13. Wang, Y., Gordon, S., Baum, T., Xu, Z., Multifunctional Stretchable Conductive Woven Fabric Containing Metal Wire with Durable Structural Stability and Electromagnetic Shielding in the X-Band, *Polymers*, **2020**, 12, 2, 399, https://doi.org/10.3390/polym12020399.
14. Mikolajczyk, Z., Nowak, I., Januszkiewicz, L., Szewczyk, M., Junak, J., Modern Electromagnetic-Radiation-Shielding Materials Made Using Different Knitting Techniques, *Materials*, **2024**, 17, 13, 3052, https://doi.org/10.3390/ma17133052.
15. Perumalraj, R., Dasaradan, B.S., Electromagnetic Shielding Effectiveness of Copper Core Yarn Knitted Fabrics, *Indian J Fibre Text Res*, **2009**, 34, 2, 149-154.
16. Duan, N., Shi, Z., Wang, Z., Zou, B., Zhang, C., Wang, J., Xi, J., Zhang, X., Zhang, X., Wang, G.,, Mechanically Robust $Ti_3C_2T_x$ MXene/Carbon Fiber Fabric/Thermoplastic Polyurethane Composite for Efficient Electromagnetic Interference Shielding Applications, *Mater Des*, **2022**, 214, 110382, https://doi.org/10.1016/j.matdes.2022.110382.
17. Liang, W., Wu, J., Zhang, S., Zhao, P.-Y., Cong, Y., Guo, Y., Wang, G.-S., Porous $Ti_3C_2T_x$ MXene Nanosheets Sandwiched Between Polyimide Fiber Mats for Electromagnetic Interference Shielding, *Nano Res*, 2024, 17, 2070-2078, https://doi.org/10.1007/s12274-023-6405-4.

18. Gupta, K.K., Abbas, S.M., Abhyankar, A.C., Effect of Yarn Composition and Fabric Weave Design on Microwave and EMI Shielding Properties of Hybrid Woven Fabrics, *J Text Inst*, **2022**, 113, 9, 1862-1877, https://doi.org/10.1080/00405000.2021.1954427.
19. Hu, S., Wang, D., Periyasamy, A.P., Kremenakova, D., Militky, J., Tunak, M., Ultrathin Multilayer Textile Structure with Enhanced EMI Shielding and Air-Permeable Properties, *Polymers*, **2021**, 13, 23, 4176, https://doi.org/10.3390/polym13234176.
20. Chandra, R.B.J., Prabhu, N.N., Suresha, R., Rao, A., Babu, P.D., Shivamurthy, B., Morphology, Conductivity, Thermal Stability and Electromagnetic Radiation Shielding Study on Cu, Cu-Ni Coated Polyester Fabric and Polyester Mesh, *Cogent Eng*, **2024**, 11, 1, 2356175, https://doi.org/10.1080/23311916.2024.2356175.
21. Surdu, L., Aileni, R.M., Chiriac, L., Rădulescu, R.I., Mitu, B., Fabrics with Electromagnetic Shielding Properties Achieved by Magnetron Sputtering Deposition, *Buletinul AGIR*, **2019**, 4, 23-27.
22. Maity, S., Chatterjee, A., Conductive Polymer-Based Electro-Conductive Textile Composites for Electromagnetic Interference Shielding: A Review, *J Ind Text*, **2018**, 47, 8, 2228-2252, https://doi.org/10.1177/1528083716670310.
23. Rybicki, T., Stempien, Z., Karbownik, I., EMI Shielding and Absorption of Electroconductive Textiles with PANI and PPy Conductive Polymers and Numerical Model Approach, *Energies*, **2021**, 14, 22, 7746, https://doi.org/10.3390/en14227746.
24. Bashir, T., Skrifvars, M., Persson, N.-K., Synthesis of High Performance, Conductive PEDOT-Coated Polyester Yarns by OCVD Technique, *Polym Adv Technol*, **2012**, 23, 3, 611-617, https://doi.org/10.1002/pat.1932.
25. Zou, L., Lan, C., Zhang, X., Xu, Z., Li, C., Yang, L., Ruan, F., Tan, S.C., Near-Instantaneously Self-Healing Coating toward Stable and Durable Electromagnetic Interference Shielding, *Nano-Micro Lett*, **2021**, 13, 1, 190, https://doi.org/10.1007/s40820-021-00709-0.
26. Pande, S., Singh, B.P., Mathur, R.B., Dhami, T.L., Saini, P., Dhawan, S.K., Improved Electromagnetic Interference Shielding Properties of MWCNT-PMMA Composites Using Layered Structures, *Nanoscale Res Lett*, **2009**, 4, 11, 1305-1312, https://doi.org/10.1007/s11671-008-9246-x.
27. Song, W.-L., Cao, M.-S., Lu, M.-M., Bi, S., Wang, C.-Y., Liu, J., Yuan, J., Fan, L.-Z., Flexible Graphene/Polymer Composite Films in Sandwich Structures for Effective Electromagnetic Shielding, *Carbon*, **2014**, 66, 67-76, https://doi.org/10.1016/j.carbon.2013.08.043.
28. Bonaldi, R.R., Siores, E., Shah, T., Characterization of Electromagnetic Shielding Fabrics Obtained from Carbon Nanotube Composite Coatings, *Synth Met*, **2014**, 187, 1, 1–8, https://doi.org/10.1016/j.synthmet.2013.10.003.
29. Shahzad, F., Alhabeb, M., Hatter, C.B., Anasori, B., Hong, S.M., Koo, C.M., Gogotsi, Y., Electromagnetic Interference Shielding with 2D Transition Metal Carbides (MXenes), *Science*, **2016**, 353, 6304, 1137-1140, https://doi.org/10.1126/science.aag2421.
30. Yin, G., Wang, Y., Wang, W., Yu, D., Multilayer Structured PANI/MXene/CF Fabric for EMI Shielding, *Colloids Surf A*, **2020**, 601, 125047, https://doi.org/10.1016/j.colsurfa.2020.125047.
31. Han, M., Shuck, C.E., Rakhmanov, R., Parchment, D., Anasori, B., Koo, C.M., Friedman, G., Gogotsi, Y., Beyond $Ti_3C_2T_x$: MXenes for Electromagnetic Interference Shielding, *ACS Nano*, **2020**, 14, 4, 5008-5016, https://doi.org/10.1021/acsnano.0c01312.
32. Jia, L.-C., Zhang, G., Xu, L., Sun, W.J., Zhong, G.J., Lei, J., Yan, D.X., Li, Z.M., Robustly Superhydrophobic Conductive Textile for Efficient Electromagnetic Interference Shielding, *ACS Appl Mater Interfaces*, **2019**, 11, 1, 1680-1688, https://doi.org/10.1021/acsami.8b18459.
33. Daniel, S., Thomas, S., Shielding Efficiency Measuring Methods and Systems, in: Jaroszewski, M., Thomas, S., Rane, A.V. (eds.), *Advanced Materials for Electromagnetic Shielding: Fundamentals, Properties, and Applications*, Wiley, **2018**, https://doi.org/10.1002/9781119128625.ch4.
34. IEEE Std. 299-2006, IEEE Standard Method for Measuring the Effectiveness of Electromagnetic Shielding Enclosures, IEEE, **2006**.
35. ASTM D4935-18, Standard Test Method for Measuring the Electromagnetic Shielding Effectiveness of Planar Materials, ASTM International, **2018**.
36. Aschberger, K., Johnston, H.J., Stone, V., Aitken, R.J., Tran, C.L. Hankin, S.M., Peters, S.A.K., Christensen, F.M., Review of Fullerene Toxicity and Exposure - Appraisal of a Human Health Risk Assessment based on Open Literature, *Regul Toxicol Pharmacol*, **2010**, 58, 3, 455-473, https://doi.org/10.1016/j.yrtph.2010.08.017.

© 2026 by the author(s). Published by INCDTP-ICPI, Bucharest, RO. This is an open access article distributed under the terms and conditions of the Creative Commons Attribution license (http://creativecommons.org/licenses/by/4.0/).

COMPACT THERMOPLASTIC POLYMER BIOCOMPOSITE BASED ON PE/PE-G-MA/EPDM/CF AND DYNAMICALLY VULCANIZED WITH DICUMYL PEROXIDE

Laurenția ALEXANDRESCU*, Mihai GEORGESCU, Maria SÖNMEZ

Rubber Research Department, National Research and Development Institute for Textiles and Leather – Division: Leather and Footwear Research Institute, 93 Ion Minulescu st., district 3, Bucharest, Romania, laurentia.alexandrescu@icpi.ro

Received: 03.07.2026 Accepted: 29.09.2026 https://doi.org/10.24264/lfj.26.3.7

COMPACT THERMOPLASTIC POLYMER BIOCOMPOSITE BASED ON PE/PE-G-MA/EPDM/CF AND DYNAMICALLY VULCANIZED WITH DICUMYL PEROXIDE

ABSTRACT. Polymer biocomposites are considered a way to stimulate the creation of a new type of material with much improved properties, which economically and efficiently combines the properties of at least two polymers (elastomer and plastomer) and natural reinforcing materials, which are component elements of composite materials, intended to improve their mechanical, thermal or chemical properties. This paper presents the development of dynamically vulcanized thermoplastic biocomposites, with anti-thermal and antimicrobial characteristics, using circular economy concepts for the development of "green" polymer composites, with market demand in niche areas of significant economic activity for the industry, while respecting the requirements of the economic and social environment. Dynamically vulcanized multiphase elasto-plastic polymer biocomposites are reinforced with natural calcium carbonate waste for products used in the food and pharmaceutical fields, based on elastomer (ethylene propylene terpolymer rubber – EPDM) and calcium carbonate waste dispersed in a plastomer matrix (high-density polyethylene – HDPE). The natural calcium carbonate waste was obtained from seashells, cryogenically ground to a particle size of 200-300nm and functionalized with polydimethylsiloxane (PDMS). The elastomers and calcium carbonate waste, through their micrometric dispersion in the plastomer matrix, led to the obtaining of a high-performance polymeric material with multifunctional characteristics (rubber and thermoplastic) and processing properties specific to plastics. The new material can be recycled for at least 5 cycles, without modifying its physical and mechanical properties. The experimental composites were characterized physically and mechanically by standardized methods specific to plastics.
KEYWORDS: biocomposites, dynamically vulcanized thermoplastic polymer, calcium carbonate waste, eco-design

BIOCOMPOZIT POLIMERIC TERMOPLAST COMPACT, PE BAZĂ DE PE/PE-G-MA/EPDM/CF, VULCANIZAT DINAMIC CU PEROXID DE DICUMIL

REZUMAT. Biocompozitele polimerice sunt considerate ca fiind o cale de stimulare pentru crearea unui nou tip de material cu proprietăți mult îmbunătățite, care combină în mod economic și performant proprietățile a cel puțin doi polimeri (elastomer și plastomer) și materiale de ranforsare naturale. Materialele de ranforsare naturale sunt elemente componente ale materialelor compozite, care au menirea să îmbunătățească proprietățile mecanice, termice sau chimice ale acestora. Această lucrare prezintă realizarea de biocompozite termoplaste vulcanizate dinamic, cu caracteristici antitermice și antimicrobiene, utilizând concepte ale economiei circulare pentru realizarea de compozite polimerice „verzi", cu cerere de piață în domeniile de nișă ale unor activități economice semnificative pentru industrie, cu respectarea cerințelor mediului economic și social. Biocompozitele polimerice elasto-plaste multifazice vulcanizate dinamic sunt ranforsate cu deșeu de carbonat de calciu natural pentru produse utilizate în domeniul alimentar și farmaceutic, pe baza de elastomer (cauciuc etilen-propilen-terpolimer – EPDM) și deșeu de carbonat de calciu dispersate în matrice de plastomer (polietilenă de înaltă densitate – HDPE). Deșeul de carbonat de calciu natural a fost obținut din cochilii de scoici măcinate criogenic, cu dimensiunea particulei de 200-300nm și funcționalizat cu polidimetilsiloxan. Elastomerii și deșeul de carbonat de calciu, prin dispersarea lor de ordin micrometric în matrice de plastomer, au condus la obținerea unui material polimeric performant cu caracteristici multifuncționale (de cauciuc și termoplast) și proprietăți de prelucrare specifice maselor plastice. Noul material poate fi recirculat cel puțin 5 cicluri, fără să-și modifice proprietățile fizico-mecanice. Compozitele experimentate au fost caracterizate fizico-mecanic prin metode standardizate specifice maselor plastice.
CUVINTE CHEIE: biocompozite, termoplast vulcanizat dinamic, deșeu de carbonat de calciu, eco-design

BIOCOMPOSITE POLYMÈRE THERMOPLASTIQUE COMPACT, À BASE DE PE/PE-G-MA/EPDM/CF, À VULCANISATION DYNAMIQUE AVEC PEROXYDE DE DICUMYLE

RÉSUMÉ. Les biocomposites polymères représentent une voie prometteuse pour la création de nouveaux matériaux aux propriétés nettement améliorées. Ils combinent de manière économique et efficace les propriétés d'au moins deux polymères (élastomère et plastomère) et de matériaux de renforcement naturels. Ces derniers, constituants des matériaux composites, visent à améliorer leurs propriétés mécaniques, thermiques ou chimiques. Cet article présente la création de biocomposites thermoplastiques à vulcanisation dynamique, dotés de propriétés antithermiques et antimicrobiennes. Cette approche s'appuie sur les principes de l'économie circulaire pour la production de composites polymères « verts », répondant à la demande du marché dans des secteurs de niche à forte activité économique pour l'industrie, tout en respectant les exigences environnementales et sociales. Des biocomposites polymères élasto-plastiques multiphasiques vulcanisés dynamiquement sont renforcés par des déchets de carbonate de calcium naturel. Ces biocomposites, destinés aux secteurs agroalimentaire et pharmaceutique, sont composés d'un élastomère (caoutchouc terpolymère éthylène-propylène – EPDM) et de déchets de carbonate de calcium dispersés dans une matrice plastomère (polyéthylène haute densité – PEHD). Les déchets de carbonate de calcium naturel, issus de coquilles de palourdes, sont broyés cryogéniquement jusqu'à une granulométrie de 200 à 300 nm, puis fonctionnalisés avec des polydiméthylsiloxanes. La dispersion micrométrique des élastomères et des déchets de carbonate de calcium dans la matrice plastomère permet d'obtenir un matériau polymère haute performance aux caractéristiques multifonctionnelles

* *Correspondence to: Laurenția ALEXANDRESCU, Rubber Research Department, National Research and Development Institute for Textiles and Leather – Division: Leather and Footwear Research Institute, 93 Ion Minulescu st., district 3, Bucharest, Romania, laurentia.alexandrescu@icpi.ro*

(caoutchouc et thermoplastique) et aux propriétés de mise en œuvre spécifiques aux plastiques. Ce nouveau matériau est recyclable au moins cinq fois sans altération de ses propriétés physiques et mécaniques. Les composites expérimentaux ont été caractérisés physico-mécaniquement par des méthodes normalisées spécifiques aux plastiques.
MOTS-CLÉS : biocomposites, thermoplastique vulcanisé dynamiquement, déchets de carbonate de calcium, écoconception

INTRODUCTION

Globally, the market for biodegradable polymeric materials has grown from $3.7 billion in 2022 to $9.5 billion in 2026, representing a compound annual growth rate (CAGR) of 20.6% for the 2022–2026 period [1]. In recent years, driven by increasing environmental concerns and the demand for sustainable materials, research has focused on replacing synthetic fibers with natural ones in various composites intended for engineering applications [2]. Furthermore, thermoplastic elastomers (TPEs) have gained attention as potential replacements for vulcanized rubber in sealing systems, owing to their recyclability and processability [3]. Currently, two types of TPE are frequently used: styrenic block copolymer TPEs (TPE-S) and vulcanized TPEs (TPE-V).

Dynamically vulcanized thermoplastics (TPE-Vs) constitute a special class of engineering materials consisting of a cross-linked rubber phase dispersed within a thermoplastic matrix [4]. Finished products processed from TPE-Vs exhibit physical-mechanical properties similar to those of vulcanized rubber. Moreover, TPE-Vs can be melted and reshaped using conventional processes specific to thermoplastic materials [5]. It has been established that the process of dynamic vulcanization of thermoplastic and rubber blends yields polymer composites with superior mechanical properties, as well as greater impact and thermal resistance, compared to samples prepared by simple blending without crosslinking agents. It has been demonstrated that TPE-Vs are utilized in the automotive industry. Among the types of rubber and thermoplastic materials used to produce TPE-Vs, natural rubber (NR) and polypropylene (PP) are frequently employed [6]. Historically, Ethylene Propylene Diene Monomer (EPDM) has remained the most widely used material for the production of sealing systems (weatherstripping/gaskets). The TPE-Vs typically selected for the manufacture of such seals consist of a blend of polypropylene and small particles of EPDM rubber. Polypropylene is a popular thermoplastic material used in a wide range of applications; it is characterized by unique properties, such as a high melting point and resistance to both high temperatures and chemical substances. Furthermore, it exhibits good processability, a hallmark of thermoplastic materials [7-8]. Previous studies indicate that the properties of TPE-Vs depend on their phase morphology [9-11]. Polymer composites are considered a promising avenue for creating new types of materials with significantly enhanced properties, combining the advantages of polymers with the characteristics of reinforcing materials [12]. Reinforcing materials are, therefore, components of composite materials designed to improve their mechanical properties. They appear in various forms and orientations, depending on the required properties: 1. enhancement of mechanical characteristics; 2. improvement of thermal resistance; 3. compatibility with the composite matrix; 4. good adaptability to processing methods; 5. low weight; 6. low cost, etc. [13].

In this study, natural calcium carbonate was selected as a reinforcing agent. Seashells are marine organic remains that possess good mechanical properties; their structure consists of approximately 95% calcium carbonate and less than 5% organic and inorganic compounds [14]. Shells contain various polymorphic forms of $CaCO_3$—prismatic, lamellar, lenticular, foliated, crossed-lamellar (including complex crossed-lamellar), and homogeneous—which result in a diverse range of structural configurations [15]. The antimicrobial effect is achieved by functionalizing the reinforcing agent (based on calcium carbonate) through silanization or the adsorption of long-chain alkyl compounds, to which an ammonium-type group can be

grafted [16]. While research exists demonstrating the feasibility of functionalizing carbonates (including calcium carbonate) [17], there are no known publications describing such functionalization—particularly in the context of composite materials. This paper presents the development of a hybrid polymeric biocomposite—based on PE, PE-g-MA, EPDM, and functionalized natural calcium carbonate—that is compact, possesses antimicrobial properties, is resistant to high temperatures, and exhibits a biodegradation effect, due to the use of calcium carbonate waste.

EXPERIMENTAL

Materials and Methods

Materials

All composites contain the same two polymers: the EPDM elastomer (Nordell IP 3745P-DuPont) and the low-density polyethylene (LDPE-SIDPEC, Egyptene), in 50:50 and 25:75 ratios. EPDM is plasticized with paraffinic oil in 100% percentage.

In addition to the polymers, other additives were used, as follows: compatibilizer: polyethylene graft maleic anhydride (PE-g-MA, Sigma Aldrich); crosslinking agent: dicumyl peroxide, powder – Perkadox F40, AkzoNobel, Germany; activators: zinc oxide and stearic acid – Bayer, Germany; antioxidants: Dilauryl Thiodipropionate (Irganox 1010) and 2,2,4-Trimethyl-1,2-Dihydroquinoline polymer (Flectol TMQ), R.E.Carroll Inc. New Jersey, USA; seashell waste.

Functionalization of Seashell Waste

Functionalization of seashell waste was achieved by mixing with a stirrer with helical paddles, for 2h at a temperature of 80°C with slow dripping of polydimethylsiloxane (PDMS) and a speed of 40 rpm. Different percentages of functionalizing agent relative to the amount of waste were experimented, but the percentage of 7% was selected, being considered optimal due to the degree of absorption, the elimination of particles agglomeration, work method and the favorable influence on the physical-mechanical characteristics of the composite.

Table 1: Formulations for peroxide-crosslinked polymer biocomposites, filled with functionalized $CaCO_3$ waste (20% and 40%) and plasticized (100 parts by weight of paraffinic oil per 100 parts by weight of elastomer – EPDM). EPDM/HDPE ratios: 50/50 and 25/75.

Biocomposites	S0-Control	PP2A20	PP2A40	VP2A20	VP2A40
EPDM-Nordel IP 3745P	50	50	50	25	25
Paraffinic oil, premix (EPDM with paraffinic oil, 50:50)	-	50	50	25	25
LDPE	50	50	50	75	75
PE-g-MA	-	7	7	7	7
Zinc oxide	5	5	5	5	5
Stearic acid	0.4	0.4	0.4	0.4	0.4
Flectol TMQ	1	1	1	1	1
Irganox 1010	1	1	1	1	1
$CaCO_3$ waste from seashells, functionalized	-	20	40	20	40
Perkadox F40	3	4	4	3.5	3.5

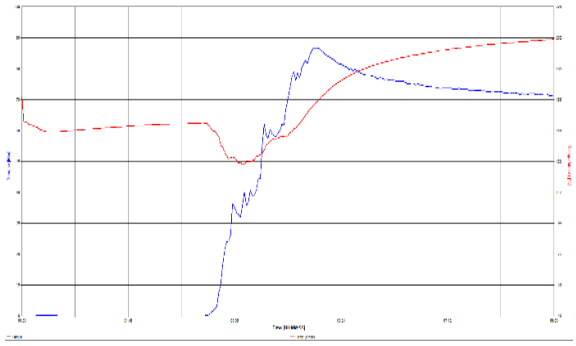
The formulations presented in Table 1 were prepared using a Plasti-Corder Brabender Mixer 350 E (Figure 1), which features the following specifications: 3 heating/cooling zones (using compressed air), a heating temperature range of 0–300°C, a capacity of 350 cm^3, a maximum rotational speed of 300 RPM, and a pressure of 600 bar.



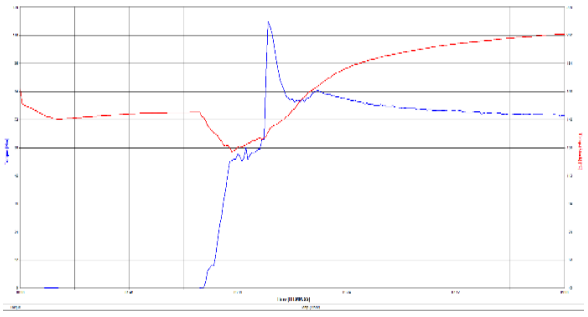
Figure 1. Plasti-Corder Brabender Mixer 350 E

The operating procedure and parameters for the Brabender Plasticorder mixer are as follows:

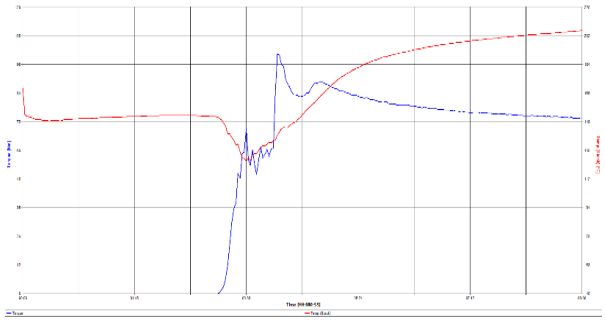
- At a temperature of 150–175°C, the polyethylene is added; once it has softened and plasticized, the EPDM is introduced, and the mixture is blended for 2 minutes at a mixing speed of 350–370 rpm. Following homogenization, the calcium carbonate waste—derived from processed and functionalized seashell fragments—is added, along with antioxidants, compatibilizing agents, zinc oxide, and stearic acid. Mixing continues at a speed of 250–280 rpm until all ingredients are incorporated and the mixture is uniform;
- The temperature is lowered to approximately 80°C, and the vulcanizing agent—dicumyl peroxide—is introduced;
- The mixture is removed from the mixer and processed using molds—specifically those designed for the test specimens required for physico-mechanical and chemical characterization—or it is granulated for subsequent extrusion or injection molding. Finally, the material undergoes physico-mechanical and morpho-structural characterization.



S0



PP2A40



VP2A40

Figure 2. Torque and temperature variations over time, recorded using the Brabender Plasticorder, for the samples S0, PP2A40 and VP2A40

From the Brabender plastograms specific to each mixture—partially shown in Figure 2—the vulcanization parameters (induction time, vulcanization time, and maximum torque) were determined. Based on the rheological data presented in Table 2, the following observations can be made:

- The reference sample (S0)—which contains no calcium carbonate waste or plasticizer—exhibits the shortest induction times (T_i) and vulcanization times (T_v) compared to the filled and plasticized samples;
- Peroxide-based vulcanization results in the lowest values for the vulcanization parameters across all polymer structures (reference, filled, and plasticized);
- The presence of the waste material, regardless of the amount of plasticizer used, influences T_i and T_v by increasing the vulcanization parameters in proportion to the quantity of waste present.

Table 2: Rheological characteristics of thermoplastic polymer biocomposites dynamically vulcanized with dicumyl peroxide, consisting of plasticized polymeric materials filled with functionalized calcium carbonate waste

Rheological indices	S0 - Control	PP2A20	PP2A40	VP2A20	VP2A40
Induction time*, min.	0.2	3.5	3.6	2.5	3.0
Optimal vulcanization time**, min.	0.8	4	5.5	3.5	4.0
Maximum shear torque, N/m	960	940	940	180	340

*Induction time = T_i = time required for crosslinking initiation

**Optimal vulcanization time = T_v = T_i + time taken to reach the maximum shear

The optimal technological parameters for a functional process tailored to the microstructure are as follows:

- For the mixer:

- The chamber fill level is as follows:
  - 1 for an EPDM/HDPE ratio of 50/50;
  - 1.1 for an EPDM/HDPE ratio of 25/75;
- Temperature: 180 ± 20°C;
- Rotor speed: 80 ± 1 rpm;
- Processing time: 8 minutes;

- For the electric press:

a) Preheating: 4 min × 190 ± 20°C × 1 atm;
b) Pressing: 5 min × 190 ± 20°C × 190 atm;
c) Cooling: approx. 10 min × 23 ± 20°C × 190 atm.

Testing Methods

Tensile tests of the samples were carried out according to SR ISO 37:2020 using a Schopper Tensile Testing machine 1445, at a constant crosshead speed of 500 ± 5 mm/min.

Hardness of the samples was measured by Shore “A” Durometer according to SR ISO 48-4:2022.

Abrasion resistance was carried out according to ISO 4649/2024, the cylinder method, using a pressure of 10 N. Abrasion resistance was expressed by relative volume loss in relation to calibrated abrasive paper. A wearing tester with abrasive cloth having granulation of 212–80 mm (PE 80). The samples used were obtained from rolled blends and pressed into sheets, then cutting with a rotating die and have cylindrical shape, with a diameter of 16 mm and height of min. 6 mm.

RESULTS AND DISCUSSIONS

Table 3: Physical-mechanical properties of reference polymer structures, filled and plasticized with 100 parts by weight of oil. EPDM/HDPE ratio: 50/50. Peroxide crosslinking system.

Properties	S0 Control	PP2A20	PP2A40	VP2A20	VP2A40
Normal state					
Hardness, °Sh A	96	95	97	95	96
Elasticity, %	28	22	26	22	23
300% modulus, N/mm^2	-	-	-	-	-
500% modulus, N/mm^2	-	-	-	-	-
Tensile strength, N/mm^2	6.8	13	9.3	8.4	10
Elongation at break, %	280	190	173	280	180
Residual elongation, %	25	93	65	93	63
Tear strength, N/mm	63	87	81	99	78
Density, g/cm^3	0.95	1.10	1.13	1.09	1.14
Wear, mm^3	107	202	204	210	212
Accelerated ageing – 168h /100°C					
Hardness, °Sh A		96	98	95	96
Elasticity, %		26	24	24	26
300% modulus, N/mm^2		-	-	-	-
Tensile strength, N/mm^2		16.1	11.3	10.2	13.1
Elongation at break, %		80	153	160	120
Residual elongation, %		23	36	73	64
Tear strength, N/mm		98	88.2	88	105
Accelerated ageing – 336h /100°C					
Hardness, °Sh A		97	96	96	97
Elasticity, %		22	20	24	24
300% modulus, N/mm^2		-	-	-	-
Tensile strength, N/mm^2		16.2	11	9.7	12.7
Elongation at break, %		40	160	200	120
Residual elongation, %		16	20	72	51
Tear strength, N/mm		91	92	86.5	92

Based on the data presented, the following observations can be made:

Normal State:

- *Hardness* is high (95–97 °ShA), regardless of the amount of calcium carbonate waste or oil, due to the morphology of the composite;

- *Elasticity* is lower (22–26%) compared to the control sample, due to plasticization with paraffinic oil; the amount of carbonate waste has very little influence on elasticity;

- *Tensile strength* exhibits the following characteristics:

  - It is superior to that of the reference mixture, showing an increase of approximately 20%;
  - The highest value (13 N/mm²) is obtained for the structure (PP2A20) loaded with PDMS-functionalized calcium carbonate waste and plasticized with 100 parts of oil (relative to the amount of EPDM);
  - The value decreases in proportion to the amount of waste used in the mixture;

- *Elongation at break* is lower than that of the control sample, due to peroxide crosslinks that offer greater resistance to stretching. It is observed that loading and plasticization—compared to an unloaded and unplasticized mixture—result in lower values for this parameter; these values decrease as the amounts of oil and filler increase;

- *Residual elongation* is lower than that of the control sample, which will result in low compression set for the peroxide-cured structures. In general, compared to the control structure, loading and plasticization lead to higher permanent set values; furthermore, as the amounts of filler and plasticizer increase, the value of this parameter generally increases as well.

- *Tear resistance* shows significantly better values compared to the reference compound (unfilled and unplasticized)

crosslinked with peroxide. For this type of crosslinking, the addition of fillers and plasticizers results in values approximately 25–32% higher, regardless of the amount of oil and filler used.

- *Regarding wear*: although it is about 50% higher than in structures crosslinked with sulfur and accelerators, it is 100% better than that of conventional elastomeric compounds. As the amount of oil and filler increases, wear resistance improves by approximately 25–40%, with the best results achieved when using active silica.

Thermo-oxidative Aging:

Following thermo-oxidative aging (for 7 and 14 days at 100°C), the following observations are made:

- *Hardness* remains nearly constant after both 7 and 14 days, maintaining the same value.

- *Elasticity* is unaffected by the aging process.

- *Tensile strength* increases by 10–15% after 7 days, indicating that the elastomeric crosslinking process is continuing. After 14 days, this parameter stabilizes, signifying that the composite is fully crosslinked. This behavior is observed across all structures, regardless of the filler content.

- *Tear resistance*, for the same reasons, shows higher values after 7 days, while remaining nearly constant thereafter (after 14 days).

- *Elongation at break* and residual elongation tend to decrease by approximately 5% and 10%, respectively, after 7 days of aging; by 14 days, these values become very low.

Therefore, following thermo-oxidative aging (7 and 14 days at 100°C), an improvement in technical parameters is observed—attributed to continued elastomer crosslinking—which is more pronounced in peroxide-crosslinked composites. Very minor variations are noted in the physical-mechanical properties (hardness, elasticity, elongation, strength), indicating good long-term resistance at elevated temperatures.

CONCLUSIONS

The overall results can be considered important. The optimum values of the main physico-mechanical parameters, characteristic for thermoplastic vulcanizates (high values of °Shore A hardness, 300% modulus, stress at break, tear strength and low values of strain at break, elasticity), were obtained in the case of vulcanized with dicumyl peroxide. This was confirmed by the physico-mechanical tests. Furthermore, resistance to high temperatures through the use of calcium carbonate waste has been demonstrated via accelerated aging tests, with the values of the physical-mechanical characteristics after 336 hours at 100°C being similar to those in the initial (normal) state.

Acknowledgements

This study was funded by the National Research Authority through the Nucleu Program, project PN 23 26 03 01 – Advanced and Sustainable Polymer Biocomposites for the Footwear Industry and Niche Areas Made According to the Principles of the Circular Economy (AVANS-COMP-POLYMER).

REFERENCES

1. Biodegradable Polymers: Global Markets and Technologies, BCC Publishing, **2024**, https://www.bccresearch.com/market-research/plastics/biodegradable-polymers-global-markets-and-technologies.html.
2. Yan, L., Chouw, N., Yuan, X., Improving the Mechanical Properties of Natural Fibre Fabric Reinforced Epoxy Composites by Alkali Treatment, *J Reinf Plast Comp*, **2012**, 31, 6, 425–37, https://doi.org/10.1177/0731684412439494.
3. Harper, C., *Handbook of Plastics, Elastomers & Composites*, McGraw-Hill Professional, **2002**.
4. Goharpey, F., Katbab, A., Nazockdast, H., Formation of Rubber Particle Agglomerates During Morphology Development in Dynamically Crosslinked EPDM/PP Thermoplastic Elastomers. Part 1: Effects of Processing and Polymer Structural Parameters, *Rubber Chem Technol*, **2003**, 76, 1, 239-252, https://doi.org/10.5254/1.3547737.
5. l'Abee, R., Goossens, H., van Duin, M., Spoelstra, A., Sub-Micrometer Thermoplastic Vulcanizates Obtained by Reaction-Induced Phase Separation of Miscible Mixtures of Poly(ethylene) and Alkyl

Methacrylates, *Eur Polym J*, **2009**, 45, 2, 503-514, https://doi.org/10.1016/j.eurpolymj.2008.11.002.
6. Whelan, A., Lee, K., *Developments in Rubber Technology—2: Synthetic Rubbers*, Springer Science & Business Media, **2013**, https://doi.org/10.1007/978-94-009-8108-9.
7. Mohamad, N., Interaction of Mixing Factors with Mechanical Properties of PP/ENR Blend via Response Surface Methodology, *J Mech Eng*, **2014**, 11, 1, 1-13.
8. Jaziri, M., Mnif, N., Massardier-Nageotte, V., Perier-Camby, H., Rheological, Thermal, and Morphological Properties of Blends Based on Poly(propylene), Ethylene Propylene Rubber, and Ethylene-1-Octene Copolymer that Could Result from End of Life Vehicles: Effect of Maleic Anhydride Grafted Poly(propylene), *Polym Eng Sci*, **2007**, 47, 7, 1009-1015, https://doi.org/10.1002/pen.20758.
9. Naskar, K., Noordermeer, J.W., Thermoplastic Elastomers by Dynamic Vulcanization, *Prog Rubber Plast Recycl Technol*, **2005**, 21, 1, 1-26, https://doi.org/10.1177/147776060502100101.
10. Wu, H., Tian, M., Zhang, L., Tian, H., Wu, Y., Ning, N., Hu, G.-H., Effect of Rubber Nanoparticle Agglomeration on Properties of Thermoplastic Vulcanizates during Dynamic Vulcanization, *Polymers*, **2016**, 8, 4, 127, https://doi.org/10.3390/polym8040127.
11. Chatterjee, T., Basu, D., Das, A., Wiessner, S., Naskar, K., Heinrich, G., Super Thermoplastic Vulcanizates Based on Carboxylated Acrylonitrile Butadiene Rubber (XNBR) and Polyamide (PA12), *Eur Polym J*, **2016**, 78, 235-252, https://doi.org/10.1016/j.eurpolymj.2016.03.027.
12. Bose, S., Bhattacharyya, A.R., Kulkarni, A.R., Pötschke, P., Electrical, Rheological and Morphological Studies in Co-continuous Blends of Polyamide 6 and Acrylonitrile–Butadiene–Styrene with Multiwall Carbon Nanotubes Prepared by Melt Blending, *Compos Sci Technol*, **2009**, 69, 3-4, 365–372, https://doi.org/10.1016/j.compscitech.2008.10.024.
13. Kumar, M., Jena, H., Sea Shell: A Marine Waste to Filler in Polymer Composite, International Conference on Artificial Intelligence in Manufacturing & Renewable Energy, **2019**.
14. Barthelat, F., Rabiei, R., Toughness Amplification in Natural Composites, *J Mech Phys Solids*, **2011**, 59, 4, 829-840, https://doi.org/10.1016/j.jmps.2011.01.001.
15. Pal, P., Banerjee, A., Soren, K., Chakraborty, P., Pandey, J.P., Sen, G., Bandopadhyay, R., Novel Biocide Based on Cationic Derivative of Psyllium: Surface Modification and Antibacterial Activity, *J Polym Environ*, **2019**, 27, 6, 1178-1190, https://doi.org/10.1007/s10924-019-01419-w.
16. Shahbakhsh, S., Tohidlou, E., Khosravi, H., Influence of Modified Carbonate Calcium Nanoparticles on the Mechanical Properties of Carbon Fiber/Epoxy Composites, *J Text I*, **2019**, 111, 4, 550-554, https://doi.org/10.1080/00405000.2019.1651155.
17. Ramos, M., Dominici, F., Luzi, F., Jimenez, A., Garrigos, M.C., Torre, L., Puglia, D., Effect of Almond Shell Waste on Physicochemical Properties of Polyester-Based Biocomposites, *Polymers*, **2020**, 12, 4, 835, https://doi.org/10.3390/polym12040835.

© 2026 by the author(s). Published by INCDTP-ICPI, Bucharest, RO. This is an open access article distributed under the terms and conditions of the Creative Commons Attribution license (http://creativecommons.org/licenses/by/4.0/).

EUROPEAN RESEARCH AREA

COTANCE NEWSLETTERS

Starting with January 2019, the COTANCE Council has issued a monthly ***COTANCE Newsletter*** with the purpose of **promoting an improved image of leather** to relevant decision makers and domestic stakeholders including Members of the European and National Parliament, Governmental authorities, Ministerial officers, Customers of the leather industry, Brands, Retail chains, Relevant NGOs, Designers, etc. The monthly newsletters present topics that tell the truth about a controversial aspect or a fact that is not well known by the general public to bring about a better understanding of leather and the European leather industry, as well as a positive predisposition to legislate in favor of the leather industry. The newsletters are available in seven languages at https://www.euroleather.com/leather/newsletter, and were also published in the 2019-2025 issues of *Leather and Footwear Journal*.



NEWS 4/2026



Three European Regions Empowered to Deliver Training for the Tanneries

Somewhere in a tannery in Tuscany, a worker is watching a short video about waste recovery filmed in that same tannery, in their own language, on their own phone. In Baden-Württemberg, a 19-year-old apprentice is navigating a virtual tannery, guided by an AI avatar named Paul, learning the full production process step by step before they set foot on the tannery floor. In Campania, up to 205 people - tannery workers, researchers, students and technicians - have already gathered for some knowledge sharing opportunities, passing craftsmanship from masters to the apprentices.

These are the real stories already taking place in those European regions that chose to act and establish their TCLF Regional Partnerships for Skills.

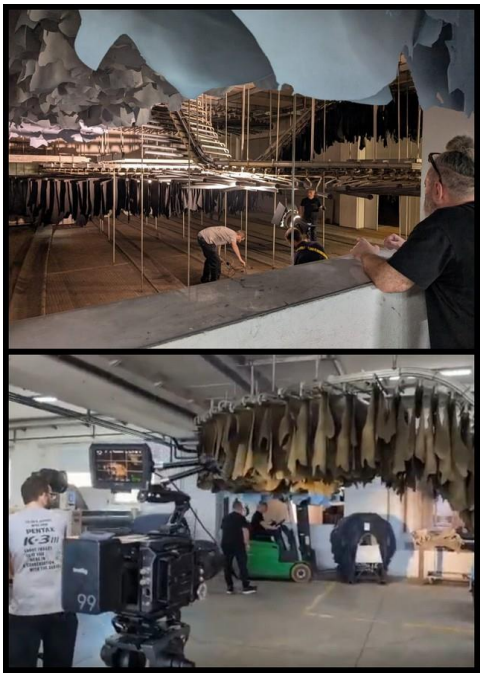
How and Why is this happening?

The initiatives mentioned above are part of the **TCLF SkillBridge project**, funded by the European Commission's **DG GROW** under the Single Market Programme and coordinated by **EURATEX** (EU Textiles and Clothing association), **CEC** (EU footwear association) and **COTANCE**, which supports the creation of Regional Skills Partnerships (RSPs) across Europe's Textile, Clothing, Leather and Footwear sectors. Within the project, ten partnerships received funding to deliver tailored training services for SMEs, including for leather-only in *Tuscany, Baden-Württemberg* and *Campania*.

Find out what each leather region has achieved so far!

Toscana is Building the Toolkit the Sector has always needed

Led by UNIC-Concerie Italiane, together with Consorzio Conciatori and Polo Tecnologico Conciario, the Tuscany RSP is modernising the way tanneries train their people.



The team spent the first months visiting seven tanneries, filming approximately 60 videos of real production processes. These videos will feed into 3 training modules - now in the development stage - one dedicated for new hires, two for upskilling existing staff, covering circularity, sustainability compliance and the EU regulatory landscape. A dedicated Toscana Leather SME Onboarding Toolkit will be ready by autumn 2026, designed to remain with SMEs as a lasting resource long after the project ends.

16 tanneries have already engaged. The broader target is 50 companies and 100 employees directly trained by the end of the year.

Baden-Württemberg becomes the Region where Leather Training meets the AI Era

Led by VDL - the German Leather Federation - the Baden-Württemberg RSP is building something that did not exist before: a virtual tannery, accessible in three languages, that lets any worker or any young person considering a career in leather explore the full production process at their own pace, from any device, and at any time.

The platform that is being developed has two parts: a video framework guided by an AI avatar named Paul, where workers can navigate every step of the production process on demand, and a gamified training tool where they apply what they have learned and track their own progress.

What contributes to such impressive results is cooperation. The video material filmed in Tuscany's tanneries is now being used by the Baden-Württemberg team across the border. It wasn't planned but happened because the TCLF SkillBridge project facilitated the work between these regions, beyond borders.

Click on Paul for a short video showcasing the results

Campania leads on the Intergenerational Knowledge Transfer



In the Solofra district, the Regional Skills partnership for leather in the Campania region - MedLeather I-HUB - led by Time Vision together with SSIP and UNIC, already delivered four trainings bringing together 205 participants: 38 SMEs, 26 students from Higher Technical Institutes, and 141 researchers, technicians and supply-chain professionals. The standout moment was in Pozzuoli in April, where 26 students sat alongside master technicians for a direct, hands-on knowledge transfer.

A digital learning platform - the LMS - is fully operational and already accessible to regional SMEs, updated with materials after each event. With six more training sessions planned before the end of 2026, the programme is on track to exceed its target of 400 total participants.



What this means for the European Leather Industry

These three leather regions are demonstrating something important: that although every region has its own industrial identity and its own starting point, the skills challenge faced by the European leather industry is shared between regions; and the most effective way to address it is through structured, permanent cooperation.

EU-driven TCLF Regional Skills Partnerships as part of the Pact for Skills initiative - bringing together industry associations, training providers, social partners and regional authorities - is the answer.

European Leather, Footwear, Textiles or Clothing Regions: When do you Join ?

COTANCE is here to assist you. Whether you represent a tannery, a training provider, a trade association or a regional authority, we can connect you with the right stakeholders, the right projects, and the right opportunities.

Contact us at EUprojects@euroleather.com
Learn more at www.euroleather.com

edited by

COTANCE

In Collaboration with

VDL Verband der Deutschen Lederindustrie e.V. | UNIC CONCERIE ITALIANE

VDL- Verband der Deutschen Lederindustrie UNIC - Concerie Italiane

IULTCS NEWSLETTER

Newsleather

Stay curious, informed and connected

Edition 15

Welcome

This is the fifteenth edition of our scientific newsletter, dedicated to providing the latest updates on research, regulatory developments, technology, and standard methods in the leather industry..

NOTE: This newsletter is in English, Italian, Spanish, Portuguese and Turkish. One version after the other. [LFJ Editor's note: For other language versions please visit www.iultcs.org].

In this issue, we feature an interview with Mr. Burak Uyguner in Tuzla, Türkiye.

Few voices carry as much weight in the global tanning community as that of Mr. Burak Uyguner. As President of the International Council of Tanners (ICT), he represents tanners across the world; closer to home, he leads Uyguner Tannery and Gelner Gıda as Chairman of the Board of Directors, continuing a family tradition now three generations deep. He is also a steady presence behind DETEK (Turkish Leather Chemists Association) and IULTCS alike, lending his support wherever the industry needs it.

For this edition, we're especially thankful — Mr. Uyguner's candor and the depth of insight he shared made for an interview well worth reading.

Please share your comments and suggestions to secretary@iultcs.org

Subscribe to the Newsleather here: https://bit.ly/3NsXNeL

Kind regards,
Dr. Luis A. Zugno, editor

IULTCS INTERVIEW

Lifeline: Mr. Burak Uyguner
Chairman of the Board of Directors for Gelner Gıda in Gönen, Türkiye



Mr. Burak Uyguner is a 3rd generation tanner born in 1971, in Istanbul, Turkey. He received his higher education at the American College of Switzerland in Switzerland. He grew up in a family that was passionate about Leather, which sparked his interest in the leather industry from a young age.

After completing his education, Uyguner began his career in the Leather industry as a tanner in their family-owned tannery which has been operating since 1935. His company exports leather to more than 30 countries. Uyguner Deri also founded Gelner Gıda in Turkey to produce powder and leaf gelatine from cowhide.

Despite his busy schedule, Uyguner is actively involved in NGO's. He is the President of the Turkish Leather Industrialists Association (TDSD), and the President of the International Council of Tanners (ICT).

IULTCS Question 1: CT has its roots going back to 1926. What were the original circumstances and motivations that led to its founding, and how much has its core mission evolved since then?

ICT was established in 1926, at a time when international trade in hides, skins and leather was growing rapidly, but there were very few common commercial rules. So, one of the main reasons for establishing ICT was actually quite practical: to create a uniform international contract for the buying and selling of hides, skins and leather. The aim was to make international trade more predictable and give both buyers and sellers greater confidence. That is still an important part of our heritage. Website: https://leather-council.org/

The fundamental purpose of ICT has not really changed. It exists to protect, represent and promote the leather-producing industry globally. What has changed dramatically is the environment in which we operate.

Today, we are dealing with much more than trade and technical standards. Sustainability, chemical regulations, traceability, climate policy, animal welfare, environmental claims and the public perception of leather have all become important parts of the discussion. ICT's objectives today also explicitly include promoting sustainable leather manufacturing and supporting free and fair trade.

So, I would say the mission is fundamentally the same, but the agenda has become much broader.

In 1926, the priority was to create some basic rules for international trade. Today, we still have that responsibility, but we also have to explain and defend the position of leather in a much more complex regulatory and consumer environment.

IULTCS Question 2:How much of ICT's work now goes into regulatory and trade defense, and what are the current battles member associations should watch?

Regulatory work has become one of the most important parts of what ICT does. I would hesitate to put a precise percentage on it because ICT is a relatively lean organization, and many of the issues are now closely connected. Sustainability, technical standards, communication and regulation often overlap.

The EUDR is a good example. We consistently argued that hides and skins should be treated correctly as by-products of livestock production, rather than being seen as economic drivers of cattle farming or deforestation. The European Commission announced in July 2026 the removal of cattle hides and leather from the scope of the regulation. For our industry, that is a very significant outcome.

But obviously, the regulatory work does not stop there.

Chemical regulation remains extremely important. Chromium VI in leather articles has been restricted under REACH for many years, and the industry increasingly has to follow developments concerning chemicals throughout the whole manufacturing chain. On the trade side, we are also operating in a period of greater protectionism and tariff uncertainty. For ICT, the principle is quite straightforward: leather is an internationally traded material, and our industry needs predictable, science-based regulations and free and fair-trading conditions.

The real challenge is to engage early. Once a regulation has been developed without properly understanding how leather is produced, it becomes much harder to correct it afterwards.

IULTCS Question 3: What share of global leather production does ICT represent, and where are the gaps?

Today, ICT represents the leather industries of 23 countries and at least 50% of global leather production, including some of the world's largest producing countries.

But I don't think the percentage tells the whole story.

Our active membership includes major national associations from countries such as China, Brazil, Italy, Turkey, the United States, France, Germany, Spain and Japan, among others. We also have regional participation through COTANCE in Europe.

There are still important gaps, though.

The geography of leather production has changed significantly over the last several decades, particularly with the growth of production in Asia and other emerging regions. ICT needs to reflect that change.

For me, the objective is not simply to add more associations to a membership list. We need meaningful participation from the countries that are actually producing leather today.

Greater involvement from Asia, Africa and Latin America would make ICT more representative. More importantly, it would give the global leather industry a stronger common voice.

Regulation is global. Sustainability is global. The image of leather is global. Our representation needs to be global as well.



Figure 1: Leather being finished at Uyguner tannery in Bursa

IULTCS Question 4:Would ICT consider committing resources to a coordinated global campaign to promote leather?

I think the leather industry definitely needs to speak with a stronger and more coordinated voice.

At the same time, we should recognize that good work is already being done. Leather Naturally, for example, is specifically focused on communicating the value of responsibly produced leather to consumers, designers and brands. The 2026 Make It Leather initiative around World Leather Day is also a good example of a more coordinated global approach.

I don't think ICT needs to become a consumer marketing agency. That would simply duplicate the work of organizations that already have expertise in communication.

But ICT can certainly play a role in bringing the industry together, providing institutional support, encouraging national associations to participate and helping to establish consistent messages.

For a long time, parts of our industry assumed that the qualities of leather were so obvious that the product would speak for itself.

Today, I don't think that is enough.

We need to explain why leather is valuable. It is durable, repairable and long-lasting. We also need to explain that hides are a by-product of the food system and that they can either be transformed into a valuable, long-lasting material or become part of a waste stream.

Our competitors are very good at communicating their messages. Leather needs to do the same.

But we should do it based on facts, science and transparency rather than relying on slogans.

IULTCS Question 5: How reliable is current global production and environmental data, and what would it take to establish better benchmarking?

This is one area where I think the global leather industry still has quite a lot of work to do.

We have a significant amount of data. The problem is that much out of date or is in private hands and is not always comparable.

A tannery producing automotive leather in Europe cannot simply be compared with a tannery producing wet blue or footwear leather somewhere else in the world. The raw materials, process stages, energy sources, water availability and final product specifications can all be very different.

Even the denominator matters.

Are we measuring impact per hide, per kilogram, per square meter of finished leather, or using an economic allocation approach? These choices can have a significant effect on the result.

ICT already has a long history of helping the industry establish common methodologies. International contracts, terminology, measurement standards and statistics are all examples of this coordinating role.

I believe the next step should be to develop a more harmonized global environmental database, working together with organizations such as the Institute for Data Integrity, IULTCS and relevant technical institutes.

We need credible benchmarks for water, energy, carbon footprint, chemical efficiency and waste recovery.

But the methodology has to be scientifically robust. It also needs to properly recognize the fact that hides and skins are by-products.

Good data is no longer just a technical issue. It has become essential to maintaining the credibility of industry.

IULTCS Question 6: Looking ten years ahead, how do you see leather evolving, and should ICT's mandate expand?

I expect the leather industry ten years from now to be smaller in some areas, but more technologically sophisticated, more transparent and increasingly circular.

Production will continue to be influenced by the availability of raw materials, cost competitiveness and access to markets. At the same time, environmental regulation is going to become stricter in almost every part of the world.

Tanners that cannot demonstrate responsible water use, proper chemical management, energy efficiency, traceability and effective utilization of by-products will find it increasingly difficult to compete.

I do think ICT's voice needs to extend further into the climate and sustainability debate. The leather sector has already participated in successive COP initiatives through the Leather Manifesto, so we have a foundation to build on.

But I would not turn ICT into a certification body. I think its real strength is bringing national industries together, developing common positions and representing the global tanning sector internationally.

The basic model is still valid.

What needs to change is our level of ambition.

ICT needs to be involved before policies are written, rather than simply responding after the fact. We should be at the table when policymakers are discussing circularity, natural materials, product environmental footprints and the future of sustainable manufacturing.

That, in my view, is where ICT can have the greatest impact in the coming years.

IULTCS Question 7: What were the biggest challenges of moving Uyguner Tannery operations from Tuzla to Bursa, and has the move delivered the expected benefits?

From my own experience, relocating a tannery is much more complicated than simply moving machinery from one building to another.

A tannery is really an ecosystem. You have wastewater treatment, chemical storage, energy systems, logistics, laboratory control, skilled operators, maintenance teams and a supply chain that has developed around the factory over many years. When you move, you have to rebuild that whole system in a new location. That creates both technical and human challenges.

The workforce issue is particularly important. You can move a machine, but you cannot move years of experience that easily. Many skilled tannery workers have decades of practical knowledge and replacing that experience is very difficult.

On the other hand, being part of a modern organized industrial structure has clear advantages, especially when it comes to environmental infrastructure and wastewater management. It also creates better opportunities to invest in newer technologies and improve the way the tannery operates.

In our own case, the relocation also made us rethink the way the tannery should operate. We were not simply trying to reproduce the old factory in a new location. We had an opportunity to look at the whole operation again and ask what could be done better.

Overall, I believe the direction is right. Modern leather production needs proper industrial-scale environmental infrastructure. But relocation by itself does not make a tannery sustainable or competitive. It must be supported by investment in technology, people, efficiency and better utilization of by-products.



Figure 2. Overview of one of the finishing lines at Uyguner tannery

IULTCS Question 8:What is driving the decline of Turkey's sheepskin tanning sector, and can it be reversed?

I think it is the result of several factors rather than one single problem.

Turkey has historically had a very strong position in sheepskin, particularly in garment leather and double-face products. We have developed a lot of know-how in this area. But it is also a sector that is very sensitive to fashion trends, labor costs and changes in consumer demand.

At the same time, international competition has become much stronger. When demand is weak, countries with higher manufacturing costs naturally feel the pressure first. Raw material availability, quality and pricing also create additional uncertainty.

So I would be cautious about expecting the sector simply to return to the size it had in the past.

I think the future is more about specialization than volume. Turkish producers have know-how, flexibility and the ability to produce sophisticated articles. We should build on these strengths rather than trying to compete purely on manufacturing cost.

There will always be a market for high-quality sheepskins and specialty leather. The important thing is to make sure Turkey is competing in the part of the market where craftsmanship, innovation, speed and quality are valued and can command a premium.



Figure 3. Overview of the Gelner Gida collagen factory in Gönen

IULTCS Question 9:Is the growth of collagen and gelatin becoming a competitor for leather-grade hides, or is it complementary?

I see it mainly as complementary, although naturally there will be some competition at the margins.

This is an area I know particularly well because we are involved in both leather and gelatin production. When you work in both industries, you quickly realize that a bovine hide should not be looked at as single-purpose raw material.

Different parts of the hide have different potential values.

For good-quality hides, leather should normally remain the highest-value application. It gives the material a very long useful life and creates significant economic value.

But there are also trimmings, headpieces, splits, fleshings and other materials that may not be suitable for high-quality leather. These materials can still have considerable value for gelatin, collagen, protein, fat and other applications.

I therefore see an opportunity to build a cascading value chain that minimizes waste from animal-derived raw materials.

Demand for collagen will continue to grow, particularly in food, pharmaceutical, nutraceutical and biomedical applications. I don't see this as a threat to leather as long as we manage the raw material properly.

In fact, closer integration of the two industries could make the entire leather value chain more sustainable and economically resilient.



Figure 4. Gelner Gida collagen ready for shipment

IULTCS Question 10: Where will the Turkish leather industry be in five to ten years, and how will the collagen industry evolve?

I don't think Turkey's future is to become the world's lowest-cost leather producer. I don't believe that is the right competition for us.

Our strengths are elsewhere: flexibility, technical knowledge, our geographical position, fast delivery to European markets and the ability to manufacture higher-value products. Turkey has a very deep leather culture and an industrial infrastructure that has been built over decades. But we also have to accept that the industry may become more concentrated. The companies that remain will probably be larger, more efficient, more automated and much stronger in terms of environmental performance.

For me, one of the biggest opportunities is to stop thinking only about tanning. We need to think about the total value of the hide.

Leather will remain the highest-value application for material that is suitable for it. But around the leather process there is a much larger bioeconomy: gelatin, collagen, proteins, fats, keratin, fertilizers and other products can all potentially be recovered from materials that were historically considered waste.

I expect collagen and gelatin production in Turkey to grow significantly. Turkey has access to bovine raw materials, an established meat and leather industry, proximity to Europe and significant processing experience. These are real competitive advantages.

So, I think the successful Turkish tannery of the future may look quite different from the tannery we knew twenty years ago. It will still produce leather, but it may increasingly operate as part of an integrated biorefinery, where almost every component of the raw material is recovered and used for its highest possible value.

For me, that is not only the future of the Turkish leather industry. I believe it is increasingly the direction of the global leather industry as well.

***Disclaimer: ** The content presented in this interview is the responsibility of the author alone. Any copyrighted material included in the interview is used at the author's discretion, and IULTCS assumes no liability for any infringements that may occur. IULTCS disclaims all responsibility for the content and use of the information provided in this interview.*

INSTRUCTIONS FOR AUTHORS

Publication Ethics and Malpractice Statement

Leather and Footwear Journal publishes articles reviewed by two independent reviewers selected by the Editorial Board. The Publication Ethics and Malpractice Statement for *Leather and Footwear Journal*, based on COPE's Best Practice Guidelines for Journal Editors, clearly outlines standards of expected ethical behavior for all parties involved in the act of publishing (the author, the journal editor(s), the peer reviewer and the publisher) and is available on the journal's website, https://www.revistapielarieincaltaminte.ro.

Open Access Statement

Leather and Footwear Journal is a peer reviewed, open access journal. All articles published open access will be immediately and permanently free for everyone to read, download, copy and distribute, under the provisions of a Creative Commons Attribution (CC BY) which lets others distribute and copy the article, create extracts, abstracts, and other revised versions, adaptations or derivative works of or from an article (such as a translation), include in a collective work (such as an anthology), text or data mine the article, even for commercial purposes, as long as they credit the author(s), do not represent the author as endorsing their adaptation of the article, and do not modify the article in such a way as to damage the author's honor or reputation.

Open Access Publication Fee

Leather and Footwear Journal requires article processing charges of 200 EURO per article, for accepted manuscripts, payable by the author to cover the costs associated with publication. There are no submission charges.

Author Rights

The copyright for all articles published in *Leather and Footwear Journal* shall remain the property of the author(s). The copyright on the layout and final design of the articles published in *Leather and Footwear Journal* belongs to INCDTP – Division: Leather and Footwear Research Institute and cannot be used in other publications.

Presentation of Papers

The scientific papers should be presented for publishing in English only. The text of the article should be clear and precise, as short as possible to make it understandable. As a rule, the paper should not exceed fifteen pages, including figures, drawings and tables. The paper should be divided into heads and chapters in a logical sequence. Manuscripts must meet high scientific and technical standards. All manuscripts must be typewritten using MS Office facilities, single spaced on white A4 standard paper (210 x 297 mm) in 11-point Times New Roman (TNR) font.

Paper Format

Title. Title (Centered, 12 pt. TNR font) should be short and informative. It should describe the contents fully but concisely without the use of abbreviations.
Authors. The complete, unabbreviated names should be given (Centered, 10 pt. TNR font), along with the affiliation (institution), city, country and email address (Centered, 9 pt. TNR font). The author to whom the correspondence should be addressed should be indicated, as well as email and full postal address.
Abstract. A short abstract in a single paragraph of no more than 200-250 words must accompany each manuscript (8 pt. TNR font). The abstract should briefly describe the content and results of the paper and should not contain any references.
Keywords. Authors should give 3-5 keywords.

Text

Introduction. Should include the aims of the study and results from previous notable studies.
Materials and Methods. Experimental methods should be described clearly and briefly.
Results and Discussions. This section may be separated into two parts. Unnecessary repetition should be avoided.
Conclusions. The general results of the research are discussed in this section.
Acknowledgements. Should be as short as possible.
References. Must be numbered in the paper, and listed in the order in which they appear.

Diagrams, Figures and Photographs should be constructed so as to be easy to understand and should be named "Figures"; their titles should be given below the Figure itself. The figures should be placed immediately near (after or before) the reference that is being made to them in the text. Figures should be referred to by numbers, and not by the expressions “below” or “above”. The number of figures should be kept to minimum (maximum 10 figures per paper).
Tables. Should be numbered consecutively throughout the paper. Their titles must be centered at the top of the tables (10 pt. TNR font). The tables text should be 9 pt. TNR font. Their dimensions should correspond to the format of the Journal page. Tables will hold only the horizontal lines defining the row heading and the final table line. The tables should be placed immediately near (after or before) the reference that is being made to them in the text. Tables should be referred to by numbers, and not by the expressions “below” or “above”. The measure units (expressed in International Measuring Systems) must be explicitly presented.
Formulas, Equations and Chemical Reactions should be numbered by Arabic numbers in round brackets, in order of appearance, and should be aligned left. The literal part of formulas should be in Italics. Formulas should be referred to by Arabic numbers in round brackets.
Nomenclature. Should be adequate and consistent throughout the paper, should conform as much as possible to the rules for Chemistry nomenclature. It is preferable to use the name of the substances instead of the chemical formulas in the text.
References should be numbered consecutively throughout the paper in order of citation in square brackets; the references should list recent literature also. Footnotes are not allowed. If the cited literature is in other language than English, the English translation of the title should be provided, followed by the original language in round brackets. Example: Handbook of Chemical Engineer (in Romanian), vol. 2, Technical Press, Bucharest, **1951**, 87.
We strongly recommend that authors cite references using DOIs where possible. DOIs are persistent links to an object/entity and can be used to cite and link to any article existing online, even if full citation information is not yet available. DOIs should always be displayed as full links. Example: Onem, E., Cin, G., Alankus, A., Pehlivan, H., Mutlu, M.M., Utilization of Chestnut Shell Wastes as a Dyeing Agent for Leather Industry, *Leather and Footwear Journal*, **2016**, 16, 4, 257-264, https://doi.org/10.24264/lfj.16.4.1.
Citation of Journal Articles: all authors' names (surname, name initials), abbreviated journal title, year, volume number, issue number, full page reference, e.g.: Helissey, P., Giorgi–Renault, S., Renault, J., *Chem Pharm Bull*, **1989**, 37, 9, 2413-2425.
In case the reference is not cited in original, the author(s) should also list the original paper that has been consulted.
Citation of Books: authors' full name and name (initials), title of the book, issue number in Arabic numbers, publishing house, editors' names (if present), city where the book has been published, year of publication, the page(s) containing the text that has been cited.
Citation of Patents: all authors' names (surname, name initials), or company's name, country and patent number, date of issuance.

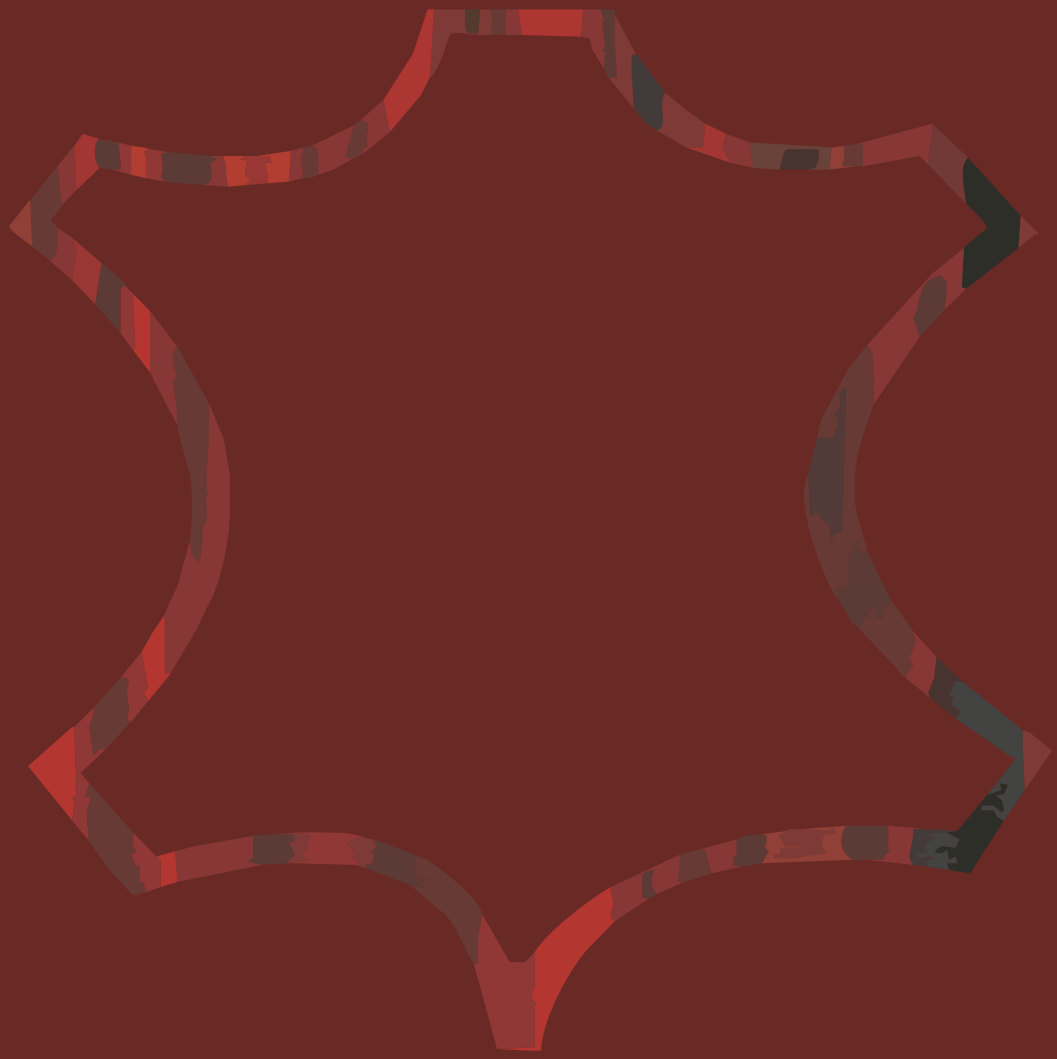
Paper template is available for download on the journal's website, https://www.revistapielarieincaltaminte.ro.

Manuscript Submission

By submitting your manuscript to be considered for publishing in *Leather and Footwear Journal* you are giving consent to processing personal data for administration and publication purposes. Our Privacy Policy is available on the journal's website.
Manuscripts should be submitted in electronic format by email to the following address:

Dana Gurău, Editor-in-chief
INCDTP - Leather and Footwear Research Institute (ICPI)
93 Ion Minulescu St., code 030215, Bucharest, Romania
Phone: +4021-323.50.60; Fax: +4021-323.52.80.
E-mail: jlfjournal@gmail.com

INCDTP - SUCURSALA INSTITUTUL DE CERCETĂRI PIELĂRIE ÎNCĂLŢĂMINTE



ISSN 1583-4433